

INFORMATION TO USERS

This manuscript has been reproduced from the microfilm master. UMI films the text directly from the original or copy submitted. Thus, some thesis and dissertation copies are in typewriter face, while others may be from any type of computer printer.

The quality of this reproduction is dependent upon the quality of the copy submitted. Broken or indistinct print, colored or poor quality illustrations and photographs, print bleedthrough, substandard margins, and improper alignment can adversely affect reproduction.

In the unlikely event that the author did not send UMI a complete manuscript and there are missing pages, these will be noted. Also, if unauthorized copyright material had to be removed, a note will indicate the deletion.

Oversize materials (e.g., maps, drawings, charts) are reproduced by sectioning the original, beginning at the upper left-hand corner and continuing from left to right in equal sections with small overlaps. Each original is also photographed in one exposure and is included in reduced form at the back of the book.

Photographs included in the original manuscript have been reproduced xerographically in this copy. Higher quality 6" x 9" black and white photographic prints are available for any photographs or illustrations appearing in this copy for an additional charge. Contact UMI directly to order.

UMI

A Bell & Howell Information Company
300 North Zeeb Road, Ann Arbor MI 48106-1346 USA
313/761-4700 800/521-0600

UNIVERSITY OF OKLAHOMA

GRADUATE COLLEGE

CONFORMATIONAL DYNAMICS AND STRUCTURE OF FEPA, A LIGAND-
GATED CHANNEL IN THE BACTERIAL OUTER MEMBRANE

A Dissertation

SUBMITTED TO THE GRADUATE FACULTY

in partial fulfillment of the requirements for the

degree of

Doctor of Philosophy

By

Xunqing Jiang

Norman, Oklahoma

1998

UMI Number: 9826291

UMI Microform 9826291
Copyright 1998, by UMI Company. All rights reserved.

**This microform edition is protected against unauthorized
copying under Title 17, United States Code.**

UMI
300 North Zeeb Road
Ann Arbor, MI 48103

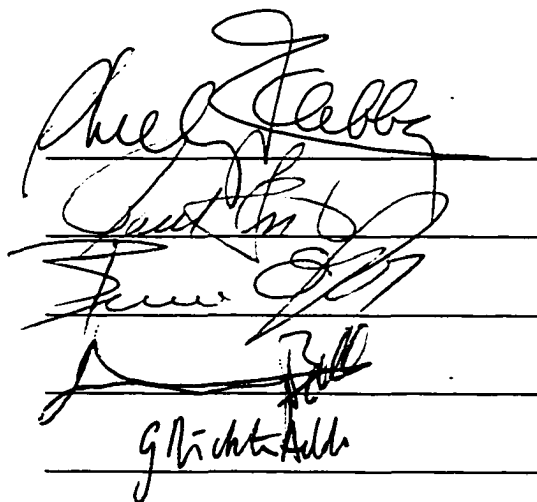
©Copyright by Xunqing Jiang 1998

All Rights Reserved

CONFORMATIONAL DYNAMICS AND STRUCTURE OF FEPA, A LIGAND-
GATED CHANNEL IN THE BACTERIAL OUTER MEMBRANE

A Dissertation APPROVED FOR THE
DEPARTMENT OF CHEMISTRY AND BIOCHEMISTRY

BY



The image shows four handwritten signatures on a background of horizontal lines. The signatures are written in black ink. The first signature is the most prominent and appears to be 'Paul J. Feby'. The second signature is partially obscured by the first. The third signature is also partially obscured. The fourth signature is 'G. Lichtner-Adda'.

In memory of my father.

ACKNOWLEDGMENTS

I would like to express my deepest appreciation to my major advisor, Dr. Phillip E. Klebba, for his guidance and training during my graduate studies. I am thankful for his confidence and enthusiasm. His pursuit of excellence helped inspire me in my search for knowledge.

My gratitude is also extended to my advisory committee, Professors Paul Cook, Bruce Roe, George Richter-Addo and Jimmy Ballard for their advice and encouragement during my graduate work.

Innumerable thanks go to Dr. Sally Newton. I am indebted to her for her scientific input and invaluable support in my dissertation work.

Innumerable thanks also go to Dr. Jimmy Feix and Dr. Yashige Kotake for their helpful instruction and cooperation, to Dr. Marvin Payne for helping me analyze some experimental data.

I also appreciate the financial support from Department of Chemistry & Biochemistry and Graduate College at University of Oklahoma, and the research assistantship funded by the National Science Foundation (NSF) and National Institutes of Health (NIH).

I am also grateful to all members in our research group. I would like to thank Zengbiao Qi, Zhenghua Cao, Jennifer Allen, Cathy Sprencel, John Igo, Padma Thulasiraman, Matthew Bauler, Danny Scott, Glen Abel, Sam Foster, Todd Robeson, and Nora Ivanoff who shared many enjoyable events and conversations with me over these years. I am particularly grateful to Marjorie Montague for her excellent technical assistance.

Finally, genuine appreciation is expressed to my parents for initiating this journey so many years ago, for their love, confidence, and perseverance. I also wish to thank my wife and my daughter for the enormous sacrifices they have made to further my career, for their love and encouragement.

Table of Contents

	Page
List of Tables	x
List of Figures	xi
Chapter	
Chapter I. Introduction	
<i>Bacterial Outer Membrane</i>	1
Bacterial Outer Membrane Bilayer	1
Porin Channels in Bacterial Outer Membrane	3
<i>Iron Transport in Enteric Bacteria</i>	7
Iron Transport in Enteric Bacteria	7
TonB	10
<i>The Study of Ferric Enterobactin Receptor, FepA</i>	14
Historical Background of FepA Study	14
Significance	18
<i>Site-Directed Spin Labeling of Membrane Proteins</i>	20
General Structural Difference between Water-Soluble Proteins and Membrane Proteins	20
Experimental Approaches for the Study of Membrane Protein	21

Structure	
Electron Spin Resonance (ESR) Spin Labeling	26
Chapter II. Methods	
<i>Media, Bacterial Strains, Plasmids, and Bacterophage</i>	36
<i>Experimental Procedures</i>	38
Chapter III. Results	
<i>ESR Analysis of Conformational Changes of FepA in vivo</i>	58
Introduction	58
Generation and Characterization of Rabbit anti-Nitroxide Sera	59
Specific Labeling of FepA in Live Bacteria	65
Structural Changes in FepA during Ligand Transport in Live Bacteria	73
Effect of CROX to the Mobility of MTSL Attached to FepAE280C in Live Bacteria	86
Comparison of Spin-Label Probes Used for <i>in vivo</i> Spin Labeling	88
Accessibility of Engineered FepA Cys Residues to Spin- Label Probe	91
<i>Location of the TonB-Box Domain of FepA</i>	93
Introduction	93
M13 Site-Directed Mutagenesis	94
Siderophore Nutrition Assays of FepA Mutants	96

Colicin B Killing Assay	98
Western Blot	100
Affinity Purification of FepA	102
<i>In vitro</i> and <i>in vivo</i> Spin Labeling of Receptors	102
Power Saturation Experiment	118
Chapter IV. Discussion	
<i>ESR Analysis of Conformational Changes of FepA in vivo</i>	125
<i>Determine the Location of the TonB-Box Domain of FepA</i>	134
Chapter V. General Conclusions and Discussion	142
References	145

List of Tables

Table 1.	Bacterial strains, plasmids, and phages	37
Table 2.	TonB-box mutant oligonucleotides used for mutagenesis	38
Table 3.	The effects of single Cys mutation on ferricenterobactin growth halo diameters and colicin B killing	98
Table 4.	$\Delta P_{1/2}$ Parameters for MTSL-labeled FepA cysteine mutants in liposomes	104

List of Figures

Figure 1. Separation of BSA-MAL6 (G-50).	61
Figure 2. ESR spectra of MAL6 and BSA-MAL6.	62
Figure 3. ELISA (anti-BSA-MAL6 Serum, 4°C).	63
Figure 4. Immunoblot to detect the specificity of anti-MAL6 serum.	64
Figure 5. ESR spectra of IASL, BSA-IASL, and OVA-IASL.	66
Figure 6. SDS-PAGE and Immunoblot analysis of IASL-labeled proteins.	67
Figure 7. Western blot of spin labeled FepAE280C proteins which were reconstituted into liposomes	69
Figure 8. ESR spectra of MAL6, FepA-MAL6 in TTE, and FepA-MAL6 in liposome.	70
Figure 9. Bacterial growth curves.	72
Figure 10. ESR analyses of MTSL-labeled bacteria expressing FepAE280C.	74
Figure 11. [¹²⁵ I]-labeled protein A western blots with anti-MAL6 sera.	75
Figure 12. ESR spectra of OM (top) and IM (bottom) of MTSL-labeled KDF541/pFepAE280C cells.	76
Figure 13. Concentration dependence of colicin B binding by MAL6-spin labeled cells.	77
Figure 14. Effect of ferric enterobactin on the mobility of MTSL attached to FepAE280C in live bacteria.	79
Figure 15. Effect of colicin B on the mobility of MTSL attached to FepAE280C in live bacteria.	80
Figure 16. ESR spectra of MTSL-E280C in liposomes with colicin B at different temperature.	82

Figure 17. Statistical analysis of ferric enterobactin- and colicin B-induced variations in FepAE280C-MTSL motion.	83
Figure 18.	85
(a). TonB and energy dependence of conformational changes in FepAE280C.	
(b). Time-course ESR for <i>fepA</i> , <i>tonB</i> ⁺ bacteria (KDF541) expressing FepAE280C under glucose starvation condition.	
(c). Time-course ESR for <i>fepA</i> , <i>tonB</i> bacteria (KDF570) expressing FepAE280C.	
Figure 19. Conformational changes in FepAE280C at different temperature.	87
Figure 20. Effect of CROX to the mobility of MTSL attached to FepAE280C in live bacteria.	89
Figure 21. Comparison of spin-label probes used for <i>in vivo</i> spin labeling.	90
Figure 22. Accessibility of engineered FepA Cys residues to spin-label probe.	92
Figure 23. Western blot of FepA receptors.	101
Figure 24. Purification of FepA using ColB-Sepharose affinity chromatography.	103
Figure 25. ESR spectra of D12C in TTE, liposomes, and live cells.	106
Figure 26. ESR spectra of T13C in TTE, liposomes, and live cells.	107
Figure 27. ESR spectra of I14C in TTE, liposomes, and live cells.	108
Figure 28. ESR spectra of V15C in TTE, liposomes, and live cells.	109
Figure 29. ESR spectra of V16C in TTE, liposomes, and live cells.	110
Figure 30. ESR spectra of T17C in TTE, liposomes, and live cells.	111
Figure 31. ESR spectra of A18C in TTE, liposomes, and live cells.	112
Figure 32. ESR spectra of A19C in TTE, liposomes, and live cells.	113

Figure 33. ESR spectra of E20C in TTE, liposomes, and live cells.	114
Figure 34. ESR spectra of spin-labeled TonB-box mutants in liposomes.	115
Figure 35. ESR spectra of D12C/E20C in TTE and in liposomes.	117
Figure 36. Continuous wave power saturation curves.	121
Figure 37. The CROX and O ₂ accessibility of the nitroxide side chains on MTSL-labeled FepA TonB-box mutants.	123

Chapter I

Introduction

Part I. Bacterial Outer Membrane

Bacterial Outer Membrane Bilayer

Biological membranes are sheetlike structures that are composed of proteins and lipid molecules held together by noncovalent interactions. The functions carried out by membranes are indispensable for life.

As early as 1884, Christian Gram found that some prokaryotic cells could retain a crystal violet-iodine dye complex after washing with alcohol (Gram-positive), and some could not (Gram-negative). The different results of this Gram stain reaction are due to the fundamental difference in the cell structure of different bacteria. Unlike Gram-positive cells, which have a cytoplasmic membrane and a thick cell wall of peptidoglycan (PG), Gram-negative cells are surrounded by cytoplasmic membrane, a much thinner layer of PG, and an outer

membrane. The aqueous compartment between the two membranes is known as periplasmic space.

The inner or cytoplasmic membrane of Gram-negative bacteria is a phospholipid bilayer that provides the hydrophobic barrier needed to allow the differential accumulation of small molecules and ions relative to the growth medium. The inner membrane contains proteins necessary to generate and maintain a proton motive force (pmf), as well as proteins that use pmf to obtain nutrients via active transport. In the periplasmic space lies a peptidoglycan or murein network that imparts shape and rigidity to the cell. Proteins localized in this periplasmic region fulfill important functions in the transport of essential nutrients into the cell, and in the biogenesis of the cell envelope. The outer membrane of Gram-negative bacteria protects the cell from harmful agents such as detergents, antibiotics, toxins, phages, and proteases, and against drastic changes in osmotic pressure (Nikaido & Nakae, 1979). It also contains proteins that promote the uptake of most nutrients needed for growth.

The outer membrane of Gram-negative bacteria is an asymmetric bilayer (Decad & Nikaido, 1976; Nikaido & Vaara, 1985). The lipopolysaccharide (LPS) molecules are located in the outer leaflet of the bilayer. Most of the inner leaflet is occupied by phospholipids phosphatidyl ethanolamine and phosphatidyl glycerol (Goldfine, 1982). LPS consists of a proximal hydrophobic lipid A region embedded in the bilayer and two peripheral structures: the oligosaccharide core, which is rich in charged groups, and the distal O-antigenic side chain. The lipid A

region contains six or seven saturated fatty acid chains; the hydrocarbon interior of the monolayer is much less fluid than that of an usual phospholipid membrane. X-ray diffraction experiments revealed the very rigid, nearly crystalline nature of the outer leaflet of the outer membrane. In the presence of divalent cations that neutralize and bridge the electrostatic repulsion between polyanionic LPS molecules, the interaction between LPS molecules is very strong. A relatively invariant group of the specialized sugar, 2-keto-3-deoxy-*D*-mannoic acid (KDO), forms the inner oligosaccharide core, that links to lipid A (Nikaido, 1973). Other more variable sugars form the outer core. O-antigen contains highly variable, repeating unit of sugars. These last two saccharide domains, oligosaccharide and O-antigen, give the cell surface its hydrophilic character (Kastowsky, et al., 1992). Because of the extreme hydrophilicity of the LPS core and O-antigen sugars, it is difficult for hydrophobic small molecules to penetrate. Gram-negative bacteria protect themselves from hostile environments by their outer membranes. Loss of part of the peripheral LPS domains, as in the “deep rough” mutants, makes the strains exceptionally sensitive to a wide range of hydrophobic compounds, including dyes, antibiotics, bile salts, other detergents, and mutagens.

Porin Channels in Bacterial Outer Membrane

Gram-negative enteric bacteria live in a hostile environment. Their outer membranes act as a molecular sieve that allow the passage of small hydrophilic

molecules (Nakae, 1975; Nakae & Nikaido, 1975; Decad & Nikaido, 1976; Nikaido *et al.*, 1991). This diffusion-mediated transport occurs mainly through the channels made by porin proteins (Nikaido & Rosenberg, 1981; Nikaido & Vaara, 1985).

Porins are transmembrane proteins with large pores. They facilitate and regulate the entry of small molecules into Gram-negative bacteria. Three types of porins have been identified.

a. Non-specific, open channels like general diffusion porin OmpF, or OmpC

Expression of matrix porin (OmpF) and osmoporin (OmpC), encoded by the genes *ompF* and *ompC* respectively, is regulated by osmotic pressure and temperature. The properties of general porins are well defined. The channel-forming motif of both porins is a 16-stranded, amphiphilic β -barrel that traverses the outer membrane bilayer. Short β -hairpin turns define one end of the barrel (the smooth end) and a series of long irregular hydrophilic antigenic loops protrude to the cell surface (the rough end). In OmpF, the amino and carboxyl termini are linked by a salt bridge within the 16th β strand, thus forming a pseudo-cyclic structure (Weiss *et al.*, 1990, 1991; Cowan *et al.*, 1992).

General porins are trimers. The major contribution of this trimer formation is hydrophobic force. The surface loops of this trimer form a large vestibule on the cell surface. This vestibule, akin to a funnel, collects solutes and deflects them to three underlying, open, non-specific, hydrophilic channels that traverse the outer membrane bilayer to the periplasm. In general porins, there is

an atypical loop, L3 loop, which folds into the barrel and constricts the size of the pore at about half the height of the barrel, narrowing the effective diameter from 20 Å at the exterior to 10 Å at the constriction (Weiss *et al.*, 1990, 1991; Lou *et al.*, 1996).

The majority of nutrients in *E. coli* diffuse through the general porins. General porins behave as passive pores, through which small molecules enter by diffusion down their concentration gradients (Nikaido & Rosenberg, 1981, 1983).

b. Substrate-specific, open channels, like maltoporin LamB

LamB was initially identified as bacterial virus receptor, for bacteriophage λ. It was also involved in allowing the passage of maltose and maltodextrins through the outer membrane. LamB resembles general porins in many ways. It forms tightly associated trimers. Each monomer contains an independent channel. The connections between successive strands toward the cell surface are long loops, whereas the periplasmic connections are short turns. Its third surface loop, L3, is entirely folded into the barrel, while L1 and L6 from the same monomer and L2 from an adjacent one fold inward to different extents, forming a constriction toward the middle of the channel. However, LamB has about 100 more residues than general porins, so LamB monomer contains 18 strands, rather than 16. Among its surface loops, L9 is of particular interest, because along with L4 and L6, it folds over each LamB monomer to form an “umbrella” that physically shields the underlying pore (Schirmer *et al.*, 1995; Hofnung, 1995).

LamB facilitates the specific diffusion of maltodextrin across the outer membrane. It seems likely that maltoporin initially binds its substrates at the rim of the channel (Klebba *et al.*, 1994, 1997). Localization of sugars at this site within the narrow channel vestibule favors their subsequent interaction with a second, stronger binding region at the constriction of the pore. A series of aromatic residues arrange along the channel lining. They form a “greasy slide” (Schirmer *et al.*, 1995) and extend from the constriction to the periplasmic outlet. The sugar probably then moves to the aromatic residues of the greasy slide and enters the periplasm by diffusion (Schirmer *et al.*, 1995; Meyer *et al.*, 1997).

c. Ligand-gated, energy-dependent, TonB-dependent channels like FepA

The ferric enterobactin receptor, FepA, is a TonB-dependent gated porin that transports the siderophore ferric enterobactin across the outer membrane of Gram-negative bacteria (Pugsley & Reeves, 1975; Neilands, 1981; Klebba *et al.*, 1982). FepA also serves as the surface receptor for colicin B and D (Timmis, 1972; Pugsley & Reeves, 1976; Timmis, 1981; Mende & Braun, 1989). FepA has been crystallized (Jalal & van der Helm, 1989), but its structure is not yet known. It is predicted that FepA consists of 29 β -strands, 7-12 residues in length, that circumscribe a large pore with a minimum diameter of 20 Å (Murphy *et al.*, 1990). Unlike either general or specific porins, FepA does not contain an open channel. Its surface loops physically close the underlying channel (Liu *et al.*, 1993). In the natural environment, siderophore concentrations are too low to drive diffusion-mediated accumulation at rates sufficient to support growth: FepA

cannot function by simple facilitation diffusion. For ferric enterobactin, FepA has at least two transport stages. First, it has a surface region that recognizes and binds ferric enterobactin. Deletion of the cell-surface ligand binding peptides of FepA from residues 258-339 generates mutant proteins that are incapable of high-affinity uptake, but they instead form nonspecific channels in the outer membrane (Rutz *et al.*, 1992). Secondly, FepA has a transmembrane channel that opens in response to interaction with TonB, to internalize ligands bound on the cell surface. Due to the tight binding of ferric enterobactin by FepA, it is envisioned that conformational changes in its surface loops may internalize bound ligands across the outer membrane, and release them into periplasmic space. Energy is needed during transport to dislodge the ligand from surface loops into the channel (Rutz *et al.*, 1992). It is believed that the release of ligands from the periplasmic face of the outer membrane receptor is an active process. The mechanism by which TonB catalyzes movements of ligands through their outer membrane receptors remains unknown.

Part II. Iron Transport in Enteric Bacteria

Iron Transport in Enteric Bacteria

Iron is an essential nutrient for all living cells. It is required not only for the cytochrome-containing electron transport chain in the inner membrane of aerobes, but also for ferredoxins (protein factor of low redox potential) in anaerobes. Also, it is used as a cofactor for reduction of ribonucleotides (RNA) to

deoxyribonucleotides (DNA) in most organisms. Iron is involved in so many essential processes inside cells because it has an electronic structure that undergoes reversible changes in its oxidation states.

Many bacteria require a free iron concentration of 1 μM for optimum growth (Wang, 1969a, b). Fe^{2+} is highly soluble. However, under aerobic conditions, iron Fe^{2+} oxidizes to Fe^{3+} , which is not accessible to cells because it forms insoluble polymers $[\text{Fe}(\text{OH})_n]$ at neutral pH, results in a free ferric iron concentration on the order of 10^{-12} μM (Neilands, 1981; Klebba *et al.*, 1982). Under these conditions of iron deficiency, *E. coli* derepresses the synthesis of a multi-enzyme system that produce enterobactin. The bacteria release this high-affinity iron chelator, also known as a siderophore (Greek “iron carrier”), which releases Fe^{3+} from its hydroxide complexes in the extracellular milieu. Siderophores are low-molecular-weight (500-1000 daltons), virtually ferric-specific ligands (Neilands, 1981). Their biosynthesis is carefully regulated by iron, and they function to supply iron to the cell. The components of siderophore biosynthesis and transport systems are derepressed in iron-deficient environment. Fur, the product of the *ferric uptake regulation* gene, binds a consensus sequence of operator DNA, called the “iron box” or “fur box”, and control the expression of siderophore and its transport system by negative transcriptional regulation (Neilands, 1982; Guerinot, 1994; Harle *et al.*, 1995).

E. coli produces the phenolate-type siderophore enterobactin and the hydroxamate-type siderophore aerobactin (Neilands, 1981; Neilands *et al.*, 1981;

Neilands, 1995). Fe(III), a “hard” acid ion, is linked to “hard” base atoms, which accounts for its preference of oxygen ligands. Siderophores bind Fe(III) by wrapping six ligating atoms around the ferric ion in either a right-handed (Δ) or left-handed (Λ) coordination propeller (Neilands, 1995). For example, ferrichrome, a hydroxamate type siderophore derived from *L*-ornithine, binds iron with the Λ form, while enterobactin, a catechol type siderophore derived from 2, 3-dihydroxybenzoyl-*L*-serine, forms a Δ chelate. After siderophores chelate and solubilize iron, ferric siderophores enter cells through iron-regulated outer membrane proteins (IROMPs). *E. coli* can also utilize siderophores synthesized and secreted by other microorganisms.

In *Escherichia coli*, at least five ferric iron systems that use enterobactin, aerobactin, citrate, ferrichrome, and coprogen have been identified. FepA is the OM receptor for ferric enterobactin, IutA for ferric aerobactin, FecA for ferric citrate, FhuA for ferrichrome (which is produced by fungi and utilized widely by *E. coli*), and FhuE for coprogen (Zimmermann *et al.*, 1984; Guerinot, 1994). FepA is the OM protein that binds and transports the native *E. coli* siderophore, ferric enterobactin. Ferric enterobactin, with a molecular weight of 719, is too large to pass through porin channels of the bacterial outer membrane (Neilands, 1981). FepA is a specialized receptor for ferric enterobactin. It binds the siderophore in a cell surface-exposed site which is centrally located in FepA primary structure. In a TonB-dependent, energy-dependent step, FepA releases ferric enterobactin into an underlying channel, formed by amphiphilic β -strands

within its structure, that is open to the periplasm (Rutz *et al.*, 1992). FepB, a periplasmic protein, binds ferric enterobactin and delivers it to the FepA permease in the cytoplasmic membrane (Pierce & Earhart, 1986). The Fep permease complex, of FepC, FepD, FepG, and P43 (Shea & McIntosh, 1991), passes ferric enterobactin to the cytoplasm by an energy-dependent mechanism. Fe(III)-enterobactin is reduced in the cytoplasm. The relatively weak complexing of Fe(II) affords an efficient means of release inside the cell. The macrocyclic ester backbone of enterobactin is cleaved by Fes, releasing Fe(II) to Fur, which represses transcription of enterobactin biosynthetic and transport genes (Neilands, 1982; de Lorenzo *et al.*, 1988). These genes occur in the order *entD fepA fes entF fepC fepB ent EBGFCA*, and are located in a cluster between minute 13.3 and 13.8 on the *E. coli* chromosome. Seven genes (*entA-G*) participate in enterobactin biosynthesis, three (*fepA-C*) code for transport proteins, and the *fes* product is necessary for the release of iron from the siderophore. Unlike ferrichrome, which is allowed to recycle, enterobactin is hydrolyzed within the cell, so each molecule functions only once (Neilands, 1982).

TonB

The TonB protein is required for a variety of energy-dependent outer membrane processes including the uptake of all iron-siderophore complexes, vitamin B₁₂ transport, the action of many colicins, and the irreversible step in binding of bacteriophages such as T1 and ϕ 80 (Davies & Reeves, 1975; Bradbeer

& Woodrow, 1976; Bassford et al., 1976; Pugsley et al., 1976, 1977; Benedetti et al., 1995; Lathrop et al., 1995). The transport systems for iron-siderophore complexes and vitamin B₁₂ into *E. coli* and related bacteria each entail different outer membrane receptors and inner membrane transport components, yet all share a common requirement for TonB. TonB is also required for the action of many colicins and phages that use these same outer membrane receptors. Without TonB, there is no active transport of nutrients across the outer membrane (Wookey, 1982; Rutz et al., 1992).

The *tonB* gene maps at 27 minute on the *E. coli* chromosome. The *tonB* gene has been cloned and sequenced: it codes for 239 amino acids with a calculated molecular weight of 26.1 kD. However, in SDS-PAGE, TonB protein appears as 36 kD. This unusual electrophoretic mobility occurs because it is comprised of 17% Pro, a very unusual overall amino acid composition. Deletion of amino acids 66-100 restores TonB protein to a predicted molecular mass of 23 kD on SDS gels, confirms that this proline-rich region appears to be entirely responsible for the anomalous behavior of TonB on SDS-PAGE.

In summary, TonB contains unusual structural features, including with 17% proline in its amino acid sequence, TonB contains few recognizable β -turns. Hydrophobicity analysis suggests that two hydrophobic regions exist within the primary amino acid sequence, one at each terminal, while the central region is hydrophilic. Distinct structural features of each domain are summarized below.

a. The N-terminus

The first 32 amino acids of TonB have characteristics of signal peptides that promote protein export: a positively charged N-terminus followed by a hydrophobic segment that may span a membrane bilayer as a hydrophobic helix. The N-terminal of TonB serves as an export signal, but is not cleaved following its export from the cytoplasm. By analogy to other proteins whose signal sequences are not cleaved following export, the hydrophobic amino-terminus of TonB probably serves to anchor the protein to the cytoplasmic membrane. TonB also interacts with ExbB and ExbD which are both anchored in the inner membrane (Plastow & Holland, 1979; Roof *et al.*, 1991; Jaskula *et al.*, 1994).

b. The central, elongated core region

This region comprises amino acids 75-107 of the opening frame, with the sequence (Glu-Pro)₄-Ile-Pro-Glu-Pro-Pro-Lys-Glu-Ala-Pro-Val-Val-Ile-Glu-(Lys-Pro)₆. A short peptide segment of TonB with this 33 residues has been studied by ¹H and ¹³C nuclear magnetic resonance spectroscopy. The sequence of this peptide segment contains multiple Glu-Pro and Lys-Pro dipeptide repeats that is thought to maintain rigid, elongated structures and a flank short connecting segment that adopts a β -strand configuration. NMR results suggested this rigid elongated central domain spans the periplasm between the inner and outer membranes of the Gram-negative bacteria (Evans *et al.*, 1986; Brewer *et al.*, 1990; Klebba *et al.*, 1993).

c. The C-terminus

The intermediate hydrophobicity of the carboxy-terminal domain has made prediction of its localization uncertain. It consists of three amphiphilic, potentially transmembrane structures (β -strand- α -helix- β -strand), separated from each other by strongly predicted β -turns (Klebba *et al.*, 1993). All fusions of periplasmic proteins alkaline phosphatase or β -lactamase to various regions of TonB carboxyl terminus are active, suggesting that the carboxy-terminus is periplasmically localized. However, the use of alkaline phosphatase or β -lactamase fusions as probes of membrane topology cannot rule out the possibility that the carboxyl terminal of TonB could be localized in the outer membrane (Klebba *et al.*, 1993).

It had long been thought that expression of TonB is not regulated by iron. However, some evidence suggests that *tonB* is transcriptionally regulated by iron availability and *fur* gene (Neilands, 1982; Guerinot, 1994).

TonB is thought to provide a functional link between the inner and outer membranes of Gram-negative bacteria (Konisky, 1978; Tatsumi *et al.*, 1995; Letain & Postle, 1997). The potential energy generated by proton gradients across the inner membrane may be transformed into mechanical force or a chemical action by TonB and changes the conformation of outer membrane receptor to dislodge the transported substrate from the outer membrane receptor (Bradbeer, 1993). Although considerable evidence supports the idea that TonB energizes the outer membrane, the nature of TonB action still remains enigmatic.

All of the TonB-dependent receptors and B-group colicins whose deduced amino acid sequences have been determined possess a conserved peptide at their N-terminus, called "TonB box". The existence of the TonB box consensus and genetic evidence that mutations in TonB box of several receptors or colicins can be suppressed by mutations in the *tonB* gene has led to the hypothesis that the TonB box represents a site of physical interaction of the TonB protein with the various receptor or colicin molecules (Mende & Braun, 1990). However, genetic suppression is not conclusive evidence that two proteins physically contact each other. *In vivo* crosslinking studies have detected cross-linked complex contained both TonB and FepA. However, the weak extent of crosslinking between TonB and FepA and the absence of crosslinking to other TonB-dependent outer membrane protein (Skare *et al.*, 1991; Larsen *et al.*, 1997) questions the conclusion that TonB spans the periplasmic space to interact physically with outer membrane receptors.

Part III. The Study of Ferric Enterobactin Receptor, FepA

Historical Background of FepA Study

Enterobactin is a microbial high affinity iron carrier which is overproduced by *E. coli* and related enteric bacteria under low iron stress. In 1975, Uemura and Mizushima first reported iron as responsible for regulation of certain outer membrane proteins of *E. coli* (Uemura & Mizushima., 1975). Relative to iron rich cultures, *E. coli* K-12 strains grown in low iron media show

an increased amount of a 81,000-dalton band on SDS-PAGE. In 1976, McIntosh & Earhart, and researchers from a number of other laboratories confirmed this observation (Pugsley & Reeves, 1976; McIntosh & Earhart, 1977). The 81,000 dalton protein was designated as FepA, Cbr, or FeuB by these different laboratories. The ferric enterobactin receptor was also reported as the binding site for colicins B and D, which compete with the siderophore for the receptor site (Guterman, 1971). Because FepA is easily observed in outer membrane preparations from iron-depleted cultures, some biochemical work was accomplished with this component of the ferric enterobactin transport system.

In 1978, Hollified and Neilands (Hollified & Neilands, 1978) reported that outer membrane preparations prepared in Tris-HCl, EDTA buffer containing Triton X-100 retained ferric enterobactin binding activity. They described an assay to measure the binding of [⁵⁵Fe] ferric enterobactin to receptor solubilized in Triton. Four years later, the isolation and partial characterization of this 81 kD protein was reported (Fiss *et al.*, 1982). The dissociation constant for FepA at 4°C in 2% Triton-0.1 M Tris, pH 7, was determined as 10 nM. The pI of FepA was determined from two-dimensional polyacrylamide gel electrophoresis to be 5.5. It was also noted that during the purification procedure, a novel proteolytic activity was identified that preferentially acts upon FepA. FepA is inactivated by cleavage to a smaller form, called 81 K*, which behaved on SDS-PAGE analysis as though it had lost a 6000-dalton polypeptide (Hollifield *et al.*, 1978; Fiss *et al.*, 1982).

Understanding the topology of FepA as it traverses the outer membrane is central to the understanding of its functional and structural domains. This question was primarily addressed with MAbs to surface and buried epitopes of FepA. Cell surface-exposed epitopes of FepA were identified and discriminated by cytofluorimetry and by the ability of MAbs that recognize them to block the interaction of FepA with its ligands (Murphy *et al.*, 1990). Immunochemical and biochemical characterization of the surface structures of FepA and analysis of its hydrophobicity and amphiphilicity were used to generate a model of FepA's transmembrane strand, surface peptides, and ligand-binding domains (Murphy *et al.*, 1990). Amino acids within region 208 to 339 were believed to participate directly in ligand binding. Deletion of the cell-surface ligand-binding peptides of FepA generated mutant proteins that were incapable of high-affinity uptake, and instead formed TonB-independent non-specific, passive channels in the outer membrane (Rutz *et al.*, 1991, 1992). These data suggested that TonB-dependent receptor proteins are gated porins that bind metal chelates within a cell surface domain and open in response to interaction with TonB to release the ligand into an underlying membrane channel. Liu *et al.* (1993) reported that the existence of a large hydrophilic channel within FepA that is considerably larger than OmpF-type pores, and the cell surface ligand-binding domain of FepA selectively controls transport through this underlying channel. The conformation of FepA was studied by site-directed spin labeling (SDSL). Initial SDSL studies on FepA focused on the residues E280 and E310 located in the large cell surface loop, PL5,

containing the ligand-binding site. The substituted glutamic acid residues are not expected to directly participate in binding of the acidic siderophore ferric enterobactin. These residues were individually replaced with Cys. In contrast to the native cysteine residues at 486 and 493 which are disulfide-linked and cannot be labeled without denaturation and reduction, the Cys-reactive nitroxides, MAL6 and MTSL, directly label both E280C and E310C, without reduction or denaturation of the receptor (Liu *et al.*, 1994).

Continuous wave (CW) ESR spectra of MTSL-labeled E280C and E310C showed a high degree of motional restriction for both sites, despite the hydrophilic nature of the surface loop as a whole (Liu *et al.*, 1994). E280C was surface-exposed, as indicated by its exposure to the aqueous paramagnetic relaxation agent, chromium oxalate (CROX), and low accessibility to O₂ which is a lipid-soluble paramagnetic probe. E310C apparently occupies a site near the membrane/aqueous interface. SDSL has also been used as first direct experimental test of β -sheet model of FepA membrane-spanning region (Klug *et al.*, 1997). Nine consecutive residues comprising a proposed β -strand immediately adjacent to the ligand-binding domain were individually mutated to cysteine, labeled with MTSL, and examined for accessibility to paramagnetic relaxation agents, O₂ and NiEDDA, in a reconstituted liposome system. Both reagents show biphasic periodicity that is characteristic of β -sheet structure, and accessibilities to polar and non-polar reagents are precisely 180° out of phase.

SDSL studies also showed a shift in the ESR spectra of MTSL-labeled E280C and E310C FepA upon addition of ferric enterobactin. Ligand binding produced a small, concentration-dependent change in the conventional ESR spectra, with decreased motion at both sites. This result demonstrated that PL5, the ligand-binding surface loop of FepA, does indeed undergo a conformational change upon the binding of ferric enterobactin (Liu *et al.*, 1993). It suggests that the FepA surface loops may contract or condense during ferric enterobactin binding, moving attached spin labels to a more restricted environment that is less accessible to hydrophilic spin probes. Kinetic analysis of ligand binding, furthermore, showed a biphasic binding reaction, and the second stage likely represents a conformational change in PL5 that locks the receptor and ligands in a slow-dissociating, transport competent complex (Payne *et al.*, 1997).

Significance

Iron is an essential nutrient for many pathogenic species. The relationship between iron and infection of animals is close (Bullen & Griffiths, 1987). An adequate iron supply for many bacterial pathogens to grow in the mammalian host is critical. Since eukaryotic proteins such as transferrin and lactoferrin have high affinities for iron, and these proteins are normally only about one-third saturated with iron, pathogenic bacteria will be in iron deficient condition *in vivo* (Gureinot, 1994). To survive in the host, many microbes have evolved iron binding and transport systems that allow them to compete for iron with host and transport iron

into these microbial species. Therefore, the molecular understanding of siderophore binding and transport is important to efforts against bacterial pathogenesis.

Iron uptake systems may also be used clinically as pathways for drug delivery. Naturally occurring iron chelating agents, siderophores, are expected to be not noxious. By building antibiotics into the molecules of the iron-binding functional groups of siderophore, the high affinity, siderophore-mediated iron uptake system of the bacteria can deliver this novel siderophore-antibiotics into pathogenic bacteria including species with very low cell envelope permeability (Watanabe *et al.*, 1987). So, the molecular understanding of siderophore transport is directly relevant to this promising clinical application.

TonB-dependent transport systems of Gram-negative bacteria provide the uptake of siderophores, vitamin B₁₂, group B colicins, and infection by T1 and Φ 80 bacteriophages (Bassford *et al.*, 1976; Pugsley & Reeves, 1977). The roles of TonB in these systems remain unknown. FepA is a TonB-dependent receptors that mediates the entry of ferric enterobactin into bacteria. Because its region of siderophore binding has been localized, and its secondary structure has been modeled from immunochemical and genetic data, FepA is an attractive prototype for the study of OM energized transport systems. The research on the structure of this protein will be the basis for prediction of structural domains of other TonB-dependent gated porins.

Part IV. Site-Directed Spin Labeling of Membrane Proteins

General Structural Difference between Water-Soluble Proteins and Membrane Proteins

The different solvent environments of membrane proteins and water-soluble proteins create the significant structural distinctions between them.

Water-soluble proteins are organized such that apolar amino acid residues are buried in the protein interior, while polar amino acid residues tend to be exposed on the protein surface. While the tendency for buried and surface residues in water-soluble proteins to be either apolar and polar, it should be emphasized that these are just trends and not an absolute distinction between buried and surface residues. The polar protein surface minimizes the surface area exposed to water. The packing of buried residues in the interior of water-soluble proteins is relatively efficient.

In contrast to water-soluble proteins, the tertiary structures of integral membrane proteins are adopted in the predominantly nonaqueous and apolar environment of the lipid bilayer. Consequently, hydrophobic interactions, believed to contribute substantially to the stability of water-soluble proteins, should play a less significant role in the stabilization of integral membrane proteins. The role of hydrophobic interactions in stabilizing the three-dimensional structures of water-soluble proteins could be replaced in membrane proteins by polar interactions (hydrogen bonds and salt bridge) occurring within the protein interior (Rees *et al.*, 1989).

The membrane protein surface should be relatively apolar to interact favorably with the hydrocarbon chains of the bilayer phospholipids. Since the surface tension of hydrocarbon liquids is much smaller than water, it is also expected that membrane proteins have a less compact interior and more irregular surface relative to water-soluble proteins, since the energetic penalty for creating larger molecular cavities in apolar environments would be less severe than for water.

Experimental Approaches for the Study of Membrane Protein Structure

Because studies of receptors, channels, and transporters have become one of the major activities of the biological research community, hundreds of amino acid sequences for membrane proteins have been reported in recent years. However, the structural determination of membrane proteins constitutes one of the most challenging problems of structural biology. Due to the lack of general and reliable methods for forming three-dimensional crystals suitable for crystallographic analysis, there is a limited database of membrane proteins of known structures. Of the over 500 solved protein structures in Brookhaven protein databank, less than ten of them are membrane proteins. In order to understand the functions of membrane proteins, we require the same high level of structural analysis that is now almost routinely applied to globular proteins.

X-ray crystallography seemed to be the only method in determining high-resolution structures of membrane proteins. However, structure determination by

x-ray diffraction requires high-quality single crystals. Because membrane proteins exist naturally in the quasi-two dimensional lipid bilayer, they are more likely to form two-dimensional crystals than three-dimensional ones. So membrane proteins are much more resistant to crystallization than water-soluble globular proteins. It is difficult to grow large and sufficiently well-ordered three-dimensional crystals of membrane proteins. This great difficulty precludes the use of standard crystallography as a routine direct structural approach.

Since Henderson and Unwin reported the first low-resolution three-dimensional structure of bacteriorhodopsin, several membrane proteins have been determined to high resolution with three-dimensional crystals: two photosynthetic reaction centers (PSRC) from *Rhodospseudomonas viridis* (Deisenhofer *et al.*, 1985) and *Rhodobacter sphaeroides* (Allen *et al.*, 1987), two porins from *Rhodobacter capsulatus* (Weiss *et al.*, 1991; Schmid B, *et al.*, 1997), two porins from *Escherichia coli* (Cowan *et al.*, 1992), and bovine heart cytochrome c oxidase (Tsukihara *et al.*, 1995; 1996). By using electron diffraction method, an incomplete structural model for bacteriorhodopsin (BR) from *Halobacterium halobium* has been determined by Henderson *et al.* (1990). An atomic model of plant light-harvesting complex II (LHCII) also determined by electron diffraction has been reported by Kuhlbrandt *et al.* (1994).

However, other approaches can be used to explore the structures of membrane proteins. On the other hand, taking advantage of that the thermodynamic constraints on the folding of membrane proteins are particularly

strong, at least for the membrane-embedded portions of the sequence, predicting the three-dimensional structures of unknown membrane proteins appears easier than predicting that of a totally unknown soluble proteins.

For the structure prediction of membrane proteins, researchers can always start from the hydropathy plot analysis of the amino acid sequence of a membrane protein. The amino acid sequence of a protein provides little information about how the sequence is folded in its normal three-dimensional structure. However, hydropathy plot analysis yields the first direct connection between sequence and structure. Because of the low solubility of polar side chains in nonpolar environments such as lipid bilayer, hydropathy plots assume that transmembrane sequences are comprised predominantly of hydrophobic residues. The backbones of the transmembrane segments should be hydrogen bonded so that their H-bonds can be satisfied internally (Rees *et al.*, 1989). This explains the observation that porins form β -barrels so that the transmembrane β -strands are fully hydrogen bonded. By plotting the average hydrophobicity along the sequence of a membrane protein, a preliminary two-dimensional model of this protein can be drawn.

After the sequencing has been done and the hydropathy analysis performed, the most important next step is to determine the correct topology of the membrane protein. The topological model of an integral membrane protein specifies which parts of the protein lie on which side of the membrane and which parts are embedded within the membrane. The topology of the membrane protein

can be tested by antibodies, enzymatic digestion or labeling, and chemical labeling. In recent years, several gene fusion methods for studying the membrane protein topology have been developed. With these methods, a DNA fragment coding for a reporter molecules, for example the secreted protein alkaline phosphatase, is fused to the gene for an integral membrane protein. The hybrid protein then produced from such a construct will have an N-terminal part from the membrane protein and a C-terminal reporter moiety. The reporter moiety performs as it is part of the membrane protein and is localized in the same way as part of the membrane protein to which it is joined. The reporter moiety will show different activities depending on where in the membrane protein the reporter was fused. The topology of the membrane protein can then be inferred from study of the activities of the report moiety in a set of fusion proteins. Information about the orientation of the membrane protein can then be provided by such an approach that cannot be provided by hydrophathy analysis. The most widely used of these gene fusion methods is the alkaline phosphatase fusion method.

The great difficulties involved in producing three-dimensional crystals of membrane proteins precludes the use of standard crystallography as routine direct structural approach. However, other methods can be used to gain direct structural information.

Circular dichroism (CD) and infrared (IR) spectroscopy are the most widely available methods to obtain useful information on the secondary structures

of membrane proteins. They are extremely important tools that can provide accurate and invaluable information.

Electron crystallography of two-dimensional crystals is a viable alternative of three-dimensional crystals. As we know, because of their natural propensity to form two-dimensional arrays in the two-dimensional lipid bilayer, membrane proteins are more likely to form two-dimensional crystals than three-dimensional ones. High-resolution electron crystallography has been used to study many membrane proteins. The first direct three-dimensional structure of a membrane protein was obtained by high-resolution electron crystallography of bacteriorhodopsin (BR) that naturally forms two-dimensional crystals (Henderson *et al.*, 1994). Atomic model of plant light harvesting complex (LHCII) (kuhlbrandt *et al.*, 1994) has also been proposed based on three-dimensional maps of 3.5 Å resolution in the membrane plane determined by electron crystallography. The structure of the bacterial porin PhoE (Jap *et al.*, 1990; 1991) and calcium ATPase (Stokes and Green 1990) have also been determined to low and moderate resolution by electron crystallography.

Nuclear magnetic resonance (NMR) spectroscopy also has been used in membrane protein structure study. Multidimensional solution NMR methods have been used to study peptides and proteins in micelles and used to determine structure of small, isotopically labeled proteins using high-field spectrometers. Solid-state NMR methods have also been developed for studying membrane protein in bilayers which has been very successful in the studies of Pfl viral coat

protein. However, NMR approaches are not general applicable for high MW membrane protein due to the lack of high-resolution spectra.

For integral membrane proteins, the technique of site-directed spin labeling (SDSL) offers an attractive alternative for obtaining structural information. Taking good advantage of the fact that one can replace virtually any amino acid in a membrane protein by cysteine through site-directed mutagenesis, nitroxide spin labels can then be attached at these sites to obtain information by electron magnetic resonance. The SDSL approach is very novel, and its potential applications has not yet been fully explored. Nevertheless, many membrane proteins like bacteriorhodopsin (Altenbach *et al.*, 1989a, 1990; Greenhalgh *et al.*, 1991), colicin E1 (Todd *et al.*, 1989; Shin *et al.*, 1993), and mellitin (Altenbach & Hubbell, 1988; Altenbach *et al.*, 1989b) have been studied by SDSL and the results demonstrate SDSL is a powerful approach for the study of membrane protein structure.

Electron Spin Resonance (ESR) Spin Labeling

Electron spin resonance is a unique type of spectroscopy. It only detects the paramagnetic centers in the system under study, as for example, an unpaired electron whose spin is not paired with another electron of opposite spin. In most biological systems, there are few unpaired electrons. Chemical bonding normally creates paired spins in molecules, resulting in an energetically favorable configuration. Such systems do not manifest an ESR signal. However, by

introduction of extrinsic paramagnetic spin labels, ESR has been applied to many biological systems for structural and dynamic studies (Likhtenstein, 1976).

Spin labels are usually stable free radicals that can be covalently attached to macromolecules, like proteins. Nitroxide spin labels are widely used, environmentally sensitive probes. The spectral anisotropy of the nitroxide free-radical group gives structural sensitivity to the spin-label ESR spectrum. The “partial motional averaging” of this anisotropy gives information about the nature and the amplitude of molecular segmental motion, and the line broadening and line shapes give a measure of the mode of motion and degree of conformational restriction of the spin-labeled group (Berliner, 1976, 1979, 1983; Berliner & Reuben, 1989).

Like other spectrometers, ESR spectrometer consists of a radiation source, a sample absorption cell, and a detector. The radiation is provided by microwave klystron or gunn diode microwave generators, which require a high-voltage DC power supply. It can be electronically tuned over a small frequency range or manually over larger ranges.

The microwave radiation is transmitted via a rectangular wave-guide-copper tube, whose dimensions are of the order of the microwave wavelength. For X-band (about 9 GHz) spectrometers, the wavelength is about 3 cm. A microwave resonant cavity serves as the absorption cell to concentrate the microwave radiation on the sample. The length of microwave resonant cavity is tunable, and the length of the cavity is determined by the frequency of the

radiation used. The iris of the resonant cavity allows the radiation to enter and leave the cavity. The detection element of a ESR spectrometer is a simple diode, sensitive to microwave frequencies. The rectified current provided by this diode is determined by the intensity of the microwave radiation incident on it.

The method used by the ESR spectrometer to scan the absorption spectrum of the sample differs from the methods used by most other spectrometers. Because of the difficulty of manually tuning the frequency of the microwave radiation source, and also the requirement that the microwave cavity be maintained in tune with this frequency, for ESR spectrometers, the magnetic field is scanned instead of the microwave frequency.

The absolute magnetic field position of the line of an ESR spectrum is characterized by the *g*-value.

$$h\nu = g\beta H_0$$

where H_0 is the magnetic field at which the center of the line occurs. ν is the microwave frequency used. β is a fundamental atomic constant, the Bohr magneton. h is Planck's constant. In nitroxides, the unpaired electron is essentially localized in a *p*-orbital of the nitrogen atoms. The *g*-values of nitroxide spin labels is about 2.

Due to the interaction of the paramagnetic electron with the magnetic moments of neighboring nuclei, the lines in an ESR spectrum can be split. These

splittings arise from the magnetic field associated with the nuclear moment. The nuclear spin, I , determines the number of hyperfine lines from a particular nucleus. This number is given by $2I + 1$. For nitroxide spin labels, the nitrogen hyperfine splitting is dominant because the free electron is essentially localized on the nitrogen atom. Nitrogen, with $I = 1$, has nuclear spins with three equally probable allowed orientations corresponding to the spin projections: $I_z = -1, 0, +1$ relative to the magnetic field. In this case, each nucleus gives rise three hyperfine lines.

One of the unique features of ESR spectra is that in many cases the positions and splittings of the lines depends on the direction of the magnetic field relative to the molecular axes. It is the anisotropy of hyperfine splitting with respect to the magnetic field direction which confers the structural and motional sensitivity on the spin-label method.

When the nitroxide groups are in non-viscous solutions, they have a high degree of mobility. The nitroxide is moving rapidly and isotropically in this environment, and its ESR signal consists of three narrow lines of equal heights. Increasing immobilization of the spin label leads to a differential line broadening in the spectrum. In the weakly immobilized situation, the high-field line is somewhat broadened relative to the other two. This broadening, which is a relaxation time effect arising from the modulation of spectral anisotropies by the molecular motion, is most easily seen from the decreased line height of the high-field line. As the rate of spin-label motion decreases, there is a progressive

differential broadening of the spectrum, up to the so-called moderately immobilized spectrum. Beyond this the spectra broaden out considerably and the line shape begins to change with lines appearing to low field and high field in the spectrum. This is because the rotational reorientation is no longer sufficiently fast to average out the spectral anisotropies. The resulting spectra are referred to as “strongly immobilized”.

For a membrane-associated protein, the technique of spin labeling offers an alternative for obtaining structural information. In this method, a stable nitroxide-free radical is attached at a specific site in the system of interest, and the electron paramagnetic resonance spectrum is analyzed to yield information regarding the local environment around the label.

Spin labeling has been highly successful in providing dynamic and structural information on lipids in membranes (Mason *et al.*, 1977; Marsh, 1981; Hemminga, 1983; Feix *et al.*, 1984, 1987; Volwerk & Griffith, 1988; Wu & Hubbell, 1993; Altenbach *et al.*, 1994). It has had much less application to the study of protein structure, primarily due to technical difficulties in achieving site-selective labeling in these complex molecules. However, taking advantage of modern molecular genetics, it has been possible to introduce spin labels at arbitrarily chosen sites using site-directed mutagenesis. This approach, referred as site-directed spin labeling (SDSL), has been highly successful in the study of protein structure.

In principle, SDSL can provide a three-dimensional structure at the level of the backbone folding in domains of regular secondary organization. Since integral membrane proteins are expected to have a high content of regular secondary structure, a significant fraction of the structure can be determined. The sensitivity and response time of conventional ESR spectrometers also make it possible to monitor real-time changes in protein structure during function, and this is one of the potentially most useful capabilities of SDSL.

SDSL has generated extensive structural and dynamic information about membrane proteins (Butterfield *et al.*, 1976; Beth *et al.*, 1984; Altenbach *et al.*, 1989a, 1990, 1996; Anthony-Cahill *et al.*, 1992; Millhauser, 1992; Calciano *et al.*, 1993; Miich *et al.*, 1993; Budker *et al.*, 1995; Barranger-mathys & Cafiso, 1996). So far, most of the nitroxide spin labels are cysteine specific. In labeling experiments, the reactive sulfhydryl group of cysteine is modified with a sulfhydryl-specific nitroxide spin label. SDSL has been highly successful in providing dynamic and structural information of bacteriorhodopsin (Altenbach *et al.*, 1989a, 1990, 1996; Resek *et al.*, 1993), colicin E1 (Todd *et al.*, 1989; Shin *et al.*, 1993), etc. All membrane-bound proteins show two-component spectra which represent two populations of spin labels differing in spin motion relative to the protein backbone. This consistent appearance of two-component (weakly immobilized and highly immobilized) spectra at many different sites in a number of labeled proteins with nitroxides of different structures suggests that this is a

general situation. The change in the relative populations of the motional components serves as a sensitive indicator of conformational change.

One of the most important applications of ESR spectroscopy is to determine topography of the polypeptide chain with respect to the bilayer interface. There are two obvious topological locations in which a spin label can be positioned: the interior of the protein where it experiences tertiary interactions with side chains of other amino acids, and the exterior surface where it contacts the hydrocarbon chains of bilayer. These locations can be distinguished experimentally by measuring the collision rate between the nitroxide and the free diffusing paramagnetic probe molecule introduced into the system. The Heisenberg rate, W_{ex} , of the nitroxide with diffusing paramagnetic probe (or exchange reagent) R can be written as (Shin & Hubbell, 1992):

$$W_{ex} = 4\pi g d D [C_R] \exp(-ZF\Phi/RT)$$

where d is the collision diameter, D is the relative diffusion coefficient of the nitroxide and R, g is a “steric factor”; $[C_R]$ and Z are the bulk concentration and valence of R, respectively, and Φ is the local electrostatic potential at the side of the nitroxide. The steric factor takes into account environmental features that reduce the collision rate of the nitroxide more with a diffusion species than with a free solution and contains direct structural information on the local site on the protein surface.

To determine whether a side chain is water exposed, a paramagnetic probe is chosen that it is water soluble, but less soluble in the membrane and protein interior. Chromium (III) oxalate (CROX) is an useful reagent for this purpose. On the other hand, if the nitroxide side chain is not water exposed, it may be located on an external surface of the protein, but in the bilayer interior phase. In this case, molecular oxygen is an outstanding relaxing agent. It has a higher solubility in a fluid bilayer interior than in the aqueous phase, a large diffusion coefficient, and a small size.

Accessibilities are implied by Heisenberg exchange rate. Relative collision frequencies of the paramagnetic probes O₂ or CROX with the nitroxide spin label are estimated through changes in the nitroxide electron spin-lattice relaxation, T₁, due to direct collision with the probe. Changes in T₁ are directly determined using continuous wave (CW) power saturation ESR methods. The experimental quantity measured in the saturation experiments is P_{1/2}, the power required to saturate the signal to one-half the amplitude it would have if it did not saturate at all. The difference between P_{1/2} in the presence and absence of O₂ or CROX is called ΔP_{1/2} and is proportional to the collision frequency of the nitroxide with the corresponding reagent (Subczynski & Hyde, 1981; Altenbach *et al.*, 1989a):

$$\Delta P_{1/2} = P_{1/2}^* - P_{1/2}^{\circ} \propto 1/T_1 T_2 - 1/T_1^{\circ} T_2^{\circ} \propto W_{ex}/T_2^{\circ}$$

where the superscript ⁰ refers to quantities in the absence of the exchange reagent, and T_2 is the effective spin-spin relaxation time of the nitroxide.

The topological location of a residue is most clearly displayed using the contrast in W_{ex} between the water- and lipid-soluble reagents. Nitroxides facing the lipid bilayer will have high W_{ex} with O_2 and low W_{ex} with CROX and vice versa for water exposed groups.

In addition to determining topography of the polypeptide chain with respect to the bilayer interface, SDSL has been used to identify regular secondary structural elements, their tertiary interactions, to investigate the dynamics of the above characteristics (Castle & Hubbell, 1976; Dalton *et al.*, 1987; Farahbakhsh *et al.*, 1993, 1995a, 1995b; He *et al.*, 1995; Zhan *et al.*, 1995; Farrens *et al.*, 1996; Mchaourab *et al.*, 1993, 1994, 1996, 1997). Perhaps the greatest strength of the SDSL method is its the resolution for detection of conformation changes, which has been used to time resolve the structural reorganization that occurs when colicin E1 binds to membrane.

The object of this dissertation is to study the structure and function of *E. coli* outer membrane protein, FepA. FepA is the receptor of ferric enterobactin, a bacterial siderophore. It has been proposed that ligand uptake through FepA, a TonB-dependent receptor, involves two distinct biochemical stages: binding and internalization. In this study, we designed our experiment based on the previous knowledge and understanding about FepA obtained by previous and current colleagues working in Dr. Klebba's laboratory and other related laboratories. By

taking great advantage of the powerful SDSL method, we localized the TonB-box of FepA, a very important domain for all TonB-dependent proteins. And most importantly, we developed a novel approach to identify conformational changes that occur in FepA, *in vivo*, as this receptor performs its transport function.

Chapter II

Methods

Media, Bacterial Strains, Plasmids, and Bacterophage

Bacterial were grown in YT, LB broth, or T medium (Klebba *et al.*, 1982; Messing, 1983). CJ236 and JM101 were used for M13 site-directed mutagenesis. *E. coli* strains KDF541, KDF570, and UT5600 were used as the host for all plasmids. pITSD12C, pITST13C, pITSI14C, pITSV15C, pITSV16C, pITST17C, pITSA18C, pITSA19C, pITSE20C, pITSE280C, pITSY289C, pITSW297C, pITSD298C, and pITSE310C are plasmids carrying mutated *fepA* alleles, while pITS449 carries wild type *fepA* allele. Mutant FepAs were expressed in the cells with substitutions of Cys for Asp, Thr, Ile, Val, Val, Thr, Ala, Ala, Glu, Glu, Tyr, Trp, Asp, and Glu at residues 12, 13, 14, 15, 16, 17, 18, 19, 20, 280, 289, 297, 298, and 310 respectively.

Table 1. Bacterial strains, plasmids, and phages

Strain, plasmid, or phage	Genotype or Phenotype	Reference
Strains		
JM101	<i>supE thi Δ(lac-proAB)</i>	Messing, 1979
CJ236	<i>dut1 ungl1 thi-1 relA1/pCJ105(cam^{F'})</i>	Kunkel <i>et al.</i> , 1987
KDF541	<i>pro⁻ leu⁻ trp⁻ thi⁻ tonA⁻ lac⁻ cir⁻ recA⁻ tonB⁺</i>	Rutz <i>et al.</i> , 1991
KDF571	<i>pro⁻ leu⁻ trp⁻ thi⁻ tonA⁻ lac⁻ cir⁻ recA⁻ tonB⁻</i>	Rutz <i>et al.</i> , 1991
UT5600	<i>pro⁻ leu⁻ trp⁻ thi⁻ entA⁻ lac⁻ tonA⁺</i>	McIntosh <i>et al.</i> , 1979
Plasmid		
pITS449	pUC18 <i>fepA⁺</i>	Armstrong
Phage		
M13		Messing <i>et al.</i> , 1977

Reagents

Bovine serum albumin and ovalbumin were purchased from United States Biochemical and Sigma respectively. Freund's complete and incomplete adjuvants were obtained from Sigma, and aluminum hydroxide gel (alum) was obtained from Superfos Biosector a/s (Vedbaek, Denmark). MAL6 (4-maleimido-tempo) and IASL [4-(2-iodoacetamido)-tempo] were obtained from Sigma. MTSL [S-(*-*-oxyl-2,2,5,5-tetramethylpyrroline-3-methyl) methanethiosulfonate] was obtained from Toronto Research Chemicals Inc. (Ontario, Canada). Anti-Rabbit IgG- and Anti-mouse IgG- Alkaline phosphatase conjugates were purchased from Sigma. Nitro blue tetrazolium [(2, 2'-Di-*p*-nitrophenyl-5,5'-diphenyl-3,3'-[3,3'-dimethoxy-4,4'-diphenylene] ditetrazolium]

and BCIP (5-bromo-4-chloro-3-indolyl phosphate) were obtained from Sigma. 1,2-Dioleoyl-*sn*-glycero-3-phosphatidylcholine (DOPC) and Egg *L*- α -phosphatidyl-*DL*-glycerol (EPG) were obtained from Avanti Polar Lipids. Ferric enterobactin was purified from cultures of *E. coli* strain AN102 as previously described (Murphy *et al.*, 1990). Colicin B was Purified from strain DM1187/pCLB1 (Payne *et al.*, 1997). Single-stranded oligonucleotide primers for mutagenesis (Table 2) were synthesized by Gibco BRL, and restriction enzymes were purchased from Gibco-BRL. T4 DNA polymerase and ligase were from Bio-Rad laboratories. Reagents and enzymes for DNA sequencing were obtained from United States Biochemical and Amersham.

Table 2. TonB-box mutant oligonucleotides used for mutagenesis

Mutation	Sequence of mutation oligonucleotide
D12C	CCT GTT TCA CAT GAC <u>TGT</u> ACT ATT GTC GTT ACC ³
T13C	GTT TCA CAT GAC GAT <u>TGT</u> ATT GTC GTT ACC GCC
I14C	TCA CAT GAC GAT ACT <u>TGT</u> GTC GTT ACC GCC GCC
V15C	CAT GAC GAT ACT ATT <u>TGT</u> GTT ACC GCC GCC GAG
V16C	GAC GAT ACT ATT GTC <u>TGT</u> ACC GCC GCC GAG CAG
T17C	GAT ACT ATT GTC GTT <u>TGC</u> GCC GCC GAG CAG AAC
A18C	ACT ATT GTC GTT ACC <u>TGC</u> GCC GAG CAG AAC TTA
A19C	ATT GTC GTT ACC GCC <u>TGCGAG</u> CAG AAC TTA CAG
E20C	GTC GTT ACC GCC GCC <u>TGC</u> CAG AAC TTA CAG GCG

Experimental Procedures

Generation and Characterization of Rabbit anti-Nitroxide Sera

Immunochemical reagents were generated to monitor the covalent attachment of nitroxides to outer membrane proteins.

Coupling of MAL6, IASL, or MTSL to bovine serum albumin (BSA) and ovalbumin (OVA)

Ten milligrams of BSA or OVA was dissolved in 1 ml of sodium borate buffer, pH 9.5, containing 0.3 M NaCl, 1 mM EDTA, and 7 M urea. The buffer was thoroughly degassed by vacuum, and 5 mg of MAL6, or MTSL, or IASL was added and mixed in the dark at room temperature. After 48 hr the reaction mixture was applied to a Sephadex G-50 column equilibrated with 0.05 M Tris-HCl, pH 7.5, 0.1 M NaCl, and 0.1 mM EDTA. Peak fractions of the void material were pooled and dialyzed against this same buffer. The concentration of protein in the purified conjugate sample was determined by the method of Lowry *et al.* (1951). The concentration of nitroxide spin labels attached to BSA was determined by double integration of their 1st derivative X-band spectra. Approximately 13 residues of nitroxide spin-label were found per albumin molecule.

Immunization and antiserum preparation

One milligram of BSA-MAL6 conjugate dissolved in 0.1 M NaCl, 0.05 M Tris-HCl, pH 7.5, and 0.1 mM EDTA was mixed with 1.6 ml of complete Freund's adjuvant to form a stable emulsion. New Zealand white rabbits were injected intramuscularly with approximately 0.1 mg of BSA-MAL6 weekly for a

month. After 2 weeks, the rabbit was injected with an emulsion of 0.1 mg of conjugate and 0.5 ml of Freund's incomplete adjuvant. Four weeks from the time of the initial injection, blood was collected. The blood was allowed to clot, and the sera were removed and clarified by centrifugation at 2000 x g. The clarified serum was stored frozen at -70°C.

Characterization of rabbit anti-nitroxide sera

Enzyme-linked immunosorbent assay (ELISA)

Usually, animals were injected with nitroxide-BSA conjugates, and their sera were assayed against nitroxide-OVA conjugates.

A 96-well microtiter plate was coated with antigens suspended at 1 mg/ml in 0.01 M NH₄Ac, 0.01 M (NH₄)₂CO₃, pH 8.3, and incubated overnight at 37°C. In the morning, Wells were filled with 200 µl TBS-OVA (1%) and let the plate stand at room temperature for 30 min to block its unreacted sites. The plate was emptied and refilled with 50 µl of appropriately diluted test serum, and allowed to incubate for 1 hr at room temperature. The assay plate was washed 3 time with TBS-Tween 20 (0.05% TBST) buffer, and 100 µl of goat anti-rabbit IgG-alkaline phosphatase, diluted in 1:1000 in TBS-BSA (1%), was added. After incubating for 1 hr at room temperature, the plate was washed 3 times with TBST and 50 µl of *p*-nitrophenyl phosphate (1 mg/ml) in diethanol amine substrate buffer was added. A bright yellow reaction product formed in those wells containing antibodies specific for the antigen been tested. 50 µl of 1 N NaOH was added to

stop the reaction. The plates were read at 410 nm on a microtiter plate reader to quantitate the results.

SDS-PAGE Electrophoresis

For denaturing SDS-polyacrylamide gel electrophoresis (PAGE) (Laemmli, 1970; Lanes, 1975), samples were suspended in SDS-containing sample buffer plus 3% β -mercaptoethanol, heated at 100°C for 5 min, and electrophoresed at room temperature.

Western Immunoblot

Proteins separated by SDS-PAGE were electrophoretically transferred from the polyacrylamide gel to a nitrocellulose (NC) membrane with transfer buffer (20 mM Tris, 150 mM glycine, pH 8.3) and a voltage of 60 V for 16 hr at 4°C. The nitrocellulose membranes were blocked by incubation for 1 hr at room temperature with TBS containing 1% gelatin (TBSG). The blocked NC was incubated with the primary antibody in TBSG for 2 hrs. Washed with 5 changes TBST over a 30 min period, then rinsed briefly in TBS. The NC was then incubated with the second antibody, a 1:1000 dilution of goat anti-rabbit IgG in TBSG, for 1 hr, washed with TBST as described above, incubated in 50 ml of substrate solution [16.7 mg nitro blue tetrazolium (NBT) and 8.5 mg of bromochloroindolyphosphate (BCIP) dissolved in 0.1 M Tris, 0.1 M NaCl, 5 mM $MgCl_2$, pH 9.5] until blue bands appeared. Color development was terminated by rinsing the membranes with distilled water. The stained membranes were

incubated with 50% glycerol for approximately 10 min, dried and stored under clear plastic film.

For [¹²⁵I]-labeled protein A western blots, 200 µl of [¹²⁵I] protein A in 50 ml of 1% gelatin in TBS was used instead of secondary Ab. Blots were washed 3 times with TBS-Tween 20, once with distilled water, and dried with a paper towel. The dry blot was then exposed to x-ray film overnight, or subjected to image analysis on a Packard Imager system.

M13 Site-Directed Mutagenesis

Preparation of uracylated M13 single strand DNA

Uracylation of M13 single strand DNA

The procedure of site-directed mutagenesis is based upon the method described by Kunkel (Kunkel, 1987).

An M13 plaque was picked with a sterile Pasteur pipette, and transferred into 1 ml 2 x YT liquid media in a microfuge tube. After incubating the tube at 65°C for 10 min to kill the bacteria, it was centrifuged at 14,000 rpm for 3 min. Fifty microliter of the supernatant was transferred to a 500 ml flask containing 50 ml of 2 x YT media with 0.25 µg/ml uridine, inoculated with 5 ml of a mid-log phase culture of CJ236. After growing at 37°C for 5-6 hr with vigorous shaking, 1 ml of the culture was pelleted by centrifugation at 14,000 rpm for 3 min. Fifty microliter of the supernatant was used to re-inoculate CJ236 under the same conditions, to increase the degree of uracylation.

Extent of uracylation

M13 lysates were diluted with LB broth in two sets of serial 10-fold dilutions. To one set of tubes, 75 μ l of JM101 culture was added. For the other set, 75 μ l of CJ236 culture was added to each tube. 2 ml of melted tryptone top agar was added to each tube and the mixtures were plated on tryptone plates and incubated 8 hr at 37°C. Phage titer was determined by counting M13 plaques on the plates. For successful uracylation, titer in CJ236 would be 10⁴ fold higher than in JM101.

Purification of uracylated M13 DNA

Single-stranded uracylated M13 DNA was isolated by phenol-chloroform extraction. 1 ml M13 phage were precipitated with 200 μ l 20% PEG, 2.5 M NaCl for 30 min. After centrifugation at 14,000 rpm for 15 min, the phage pellet was dissolved in 100 μ l of 10 mM Tris-HCl, pH 7.6. M13 DNA was then purified by treating with 100 μ l of saturated phenol, and then with 50 μ l phenol/50 μ l chloroform. DNA was then precipitated with 400 μ l 100% ethanol and the resulting crude DNA was washed with 200 μ l 70% ethanol. After centrifugation, DNA was resuspended in 30 μ l of distilled water.

Site directed mutagenesis

Phosphorylation of mutant oligonucleotide

Synthetic oligonucleotide primers were diluted to 10 pmol/ μ l in water, and phosphorylated by incubation with 1.5 μ l ATP (10 mM), 0.5 μ l T4 polynucleotide

kinase in kinase buffer (Giblo BRL) for 45 min at 37°C. The mixture was then incubated at 65°C for 10 min to inactivate enzyme.

Annealing, elongation and ligation reactions

BioRAD M13 mutagenesis kits were utilized. A mixture of 3 ul (200 ng) of uracylated M13 DNA, 1 ul (6 pmol) of phosphorylated oligonucleotide, 1 ul of 10 X hybridization buffer (BioRAD), and 5 ul of H₂O was incubated at 70°C for 2 min, and then allowed to slowly cool in a dish of 70°C water on bench for 30 min, until the temperature dropped below 35°C. To this 10 ul of hybridization mixture, 1 ul of 10 X synthesis buffer, 1 ul of T4 DNA ligase (3 units), and 1 ul of T7 DNA polymerase (1 unit) was added. The tube was incubated for 5 min on ice, for 5 min at 25°C, and finally for 45 min at 37°C. Ninety microliter of stop solution (10 mM Tris-EDTA, pH 8.0) was added to stop the reaction, and 1 ul of the reaction mixture was electroporated into competent JM101 cells, which were plated on tryptone plate to produce isolated plaques. For each mutant, 12 isolated plaques were picked at random with sterile Pasteur pipette and inoculated into 5 ml of LB broth containing 75 ul of JM101 culture, and incubated 6 hr at 37°C with shaking. Single-stranded M13 DNA was purified by phenol-chloroform extraction and sequenced to identify isolates that successfully incorporated the desired mutation.

Transfer of mutant *fepA* genes to an expression vector

Preparation of RF M13 DNA

After identification of mutant M13 *fepA* clones, described above, single-stranded DNA was isolated and electroporated into JM101. A single plaque was picked and inoculated in 5 ml of LB broth containing 75 μ l of JM101 culture. After shaking at 37°C for 4.5-5 hr, cells were pelleted by centrifugation, and replication form (RF) M13 DNA was purified using QIAprep Spin Plasmid Kit (Qiagen).

Digestion and ligation of FepA fragment from RF M13 into pUC18

Mutant M13 RF DNA and pITS449 plasmid DNA (Armstrong *et al.*, 1990) were digested with 1 unit of PstI and SacI at 37°C for 5 hr. The digestion reaction was terminated by the addition of 10 X stop buffer (10 mM EDTA, 0.25% bromophenol blue, 40% w/v sucrose in distilled water), and samples were loaded on 1% agarose gel and electrophoresed for 2 hr. DNA fragments of interest, containing the *fepA* from RF M13, and the vector fragment of pUC18 were excised under UV illumination. DNA fragments were recovered using a Gene Clean Kit (BIO 101, Inc) from the gel. One microliter of FepA fragment was incubated with 0.5 μ l vector pITS449 in the presence of T4 ligase overnight at 16°C. One microliter of the reaction mix was electroporated into competent host cells and plated on LB-Amp (10 μ g/ml) plates. After overnight growth, colonies were picked and grown in LB broth for plasmid DNA purification. The mutations were confirmed by sequencing these plasmids.

Phenotypic Tests

Siderophore Nutrition Assay

Bacteria were grown overnight in LB broth, and 10^8 cells were diluted into 3 ml NB top agar containing 3 μ l ampicillin (10 mg/ml), 30 μ l streptomycin (10 mg/ml), and 30 μ l 9 mM deferriferrichrome A to induce iron starvation. Filter discs (5 mm diameter) containing 5 μ l of 50 μ M freshly prepared ferric enterobactin were placed on top of the agar and, after overnight incubations at 37°C, scored for ability to utilize the siderophore as determined by a halo of cell growth around the disc.

ColB killing Assay

Purified colicin B was serially diluted in LB broth in microtiter plates, from 10^{-1} to 3.2×10^{-9} , and transferred with a sterile CloneMaster™ (Immunosine) to an LB plate containing ampicillin (10 μ g/ml) that was seeded with a tester strain. Colicin titers were measured after overnight incubation, as the inverse of the highest dilution that cleared the bacteria lawn.

Quantitative immunoblots to determine FepA expression level

Western blot was carried out according to the procedure described before. Fifty million bacteria were lysated and subjected to western immunoblot to quantitative FepA expression.

FepA purification

For purification of FepA and FepA mutants, *E. coli* strain UT5600 was used as the host for all plasmids carrying mutated *fepA* alleles. Bacteria were grown in 5 ml LB culture at 37°C for overnight, subcultured in 300 ml of LB and incubated with vigorous shaking at 37°C for 6 hr. This culture was used to inoculate 15 l of T media in 20 l carboy. Bacteria were grown with vigorous aeration at 37°C overnight, and harvested by centrifugation at 5,000 x g for 30 min. Cells in the pellets were resuspended and washed twice with 10 mM Tris, 10 mM benzamidine, pH 8.0, and resuspended in 40 ml of 100 mM Tris, 10 mM benzamidine. The bacteria were placed in a French pressure cell and slowly bled through an orifice at 14,000 psi to induce lysis. Under these conditions the cells literally explode, fragmenting their membranes and releasing the cytoplasmic contents. Unlysed cells were removed by centrifugation and discarded. The cell envelopes were then pelleted by ultracentrifugation at 100,000 x g for 40 min, washed twice with 50 ml of 10 mM Tris, 10 mM MgCl₂, 10 mM benzamidine, pH 8.0, and pelleted cell envelope fraction was next resuspended in, and extracted with 50 ml 2% Triton X-100, 100 mM Tris, 10 mM benzamidine, pH 8.0. This procedure solubilizes the inner membrane, but not outer membrane proteins (Schnaitman, 1971). The OM pellet was washed with 50 ml 10 mM Tris, 10 mM benzamidine, pH 8.0 and pelleted by centrifugation for 40 min. The OM was resuspended in, and extracted with 50 ml 2% Triton X-100, 10 mM Tris, 5 mM EDTA, 10 mM benzamidine, pH 8.0. This procedure destabilizes the OM, solubilizing its protein. The insoluble murein fraction was pelleted by

centrifugation; the supernatant contained most of the OM proteins. The extraction of this outer membrane fraction was repeated, and the supernatants were combined.

The collected outer membrane proteins were dialyzed against 4 l of 50 mM Tris, 2% Triton X-100, 5 mM EDTA, pH 7.2 (TTE) and loaded onto a 20 ml column of ColB-Sepharose (Payne *et al.*, 1997). After loading, the affinity column was washed with 10 column volumes of TTE, and FepA protein was eluted with a 20 column volumes of 0 to 2.5 M NaCl gradient in TTE. The fractions were analyzed by SDS-PAGE. The affinity column could be regenerated by washing with 10 column volumes of 1 M TCA neutralized in TTE, then with 20 column volumes of a reverse 6.0 to 0 M urea gradient in TTE.

Spin labeling of FepA and ESR

Since the two natural cysteines of FepA, at residues 486 and 493, exist as a disulfide in native FepA, and cannot be readily labeled without reduction and denaturation of the receptor, Cys residues have been introduced at sites within the FepA ligand binding domain by site-specific mutagenesis. These engineered Cys residues, at positions 280 and 310 in mature FepA, can be covalently modified with the nitroxides spin labels MAL6 or MTSL, without denaturation of the receptor (Liu *et al.*, 1994). Preliminary experiments have established that the substitution of Cys at these positions, and then covalent modification with nitroxides, do not impair either the tertiary structure of the receptor or its ability to

bind ferric enterobactin (Liu *et al.*, 1994). In this research, we extended this methodology to E280C and E310 mutants and other engineered Cys residues of FepA in detergents, liposomes, and live bacteria.

Spin labeling of FepA proteins in TTE

Spin labeling of FepA cysteine mutant proteins was accomplished by incubating 0.1 mM protein in 50 mM Tris-HCl, pH 7.2, 5 mM EDTA, 2% Triton X-100 (TTE) buffer with 2 mM MTSL at 4°C for 8 hours. Excess free spin label was removed by extensive dialysis (48 hours, six buffer changes).

Spin labeling of FepA in liposomes

liposome reconstitution

Spin labeled FepA was reconstituted into liposomes by method previously established for liposome-swelling experiments (Nikaido *et al.*, 1991; Liu *et al.*, 1993, 1994). A thin film of 1, 2-Dioleoyl-*sn*-glycero-3-phosphatidylcholine (DOPC) (2.25 μ mol) and Egg *L*- α -phosphatidyl-*DL*-glycerol (EPG) (0.25 μ mol) was dried onto a glass tube under a soft stream of N₂, and incubated 10 hr in vacuum at 25°C. Approximately 1 mg of protein in 50 mM Tris-HCl, pH 7.2, 5 mM EDTA (TE) buffer was added to the lipid film and vortexed to homogeneity. This suspension was dried under vacuum at room temperature. The lipid/protein film was finally hydrated with 100 μ l TE buffer at 37°C for 30 min and shaken vigorously by hand.

Spin labeling FepA in liposomes

E280C and E310C FepA protein had been spin labeled and reconstituted into liposomes in preliminary experiments (Liu *et al.*, 1994). Before we spin label these proteins on cell surface, spin labeling experiments have been carried out to covalently modify E280C proteins which has been reconstituted in liposome.

FepA reconstituted into liposomes in TE buffer was incubated with 2 mM MAL6 or MTSL at pH 7.5 at 4°C or room temperature for different periods. Unbound spin labels were removed by extensive dialysis (48 hr, six buffer changes) against TE buffer. Samples were collected and loaded on SDS-PAGE gel. Proteins were transferred to nitrocellulose paper. Immunoelectroblots were carried out using anti-MAL6 to study if E280C reconstituted in liposomes could be spin labeled. Appropriate reaction time was determined by this experiment. ESR measurements were made on a Bruker EMX spectrometer.

Spin labeling FepA in live cells

Labeling experiments

KDF541 containing pITS449, pFepAE280C, or pFepAE310C was grown in LB medium and subcultured into T medium plus appropriate nutritional supplements at 1%. After 16 hr, bacteria were harvested and suspended in labeling buffer (50 mM Mops and 60 mM NaCl, pH 7.5). Spin labels were added (to a final concentration of 20 μ M MTSL and 10 μ M MAL6) and incubated 2 hr

at room temperature with shaking, and the cells were washed twice with reaction buffer containing 0.05% Tween 20 and once with reaction buffer alone.

MAL6 (4-maleimido-tempo), IASL [4-(2-iodoacetamido)-tempo], and MTSL [s-(2,2,5,5-tetramethylpyrroline-3-yl)methyl] methanethiosulfonate] were used to spin label cells. The reaction condition is the same for all these three probes.

Specificity of in vivo spin labeling

ESR analysis

ESR was used to examine the specifically modification of FepA *in vivo*. For ESR analysis, 10^{10} cells were suspended in 100 μ l of 0.01 M NaHPO₄ (pH 6.9) containing 0.4% glucose. X-band spectra of MTSL-labeled KDF541/pFepAE280C, KDF541/pITS449 (*fepA*⁺), or KDF541 (*fepA*) were recorded on a Bruker EMX spectrometer, operating at 9.8 GHz with a total scan range of 150 G and 100-KHz modulation frequency, at 4°C in a quartz flat cell.

[¹²⁵I]-labeled protein A Western blot

5×10^7 cells of KDF541, KDF541/pITS449, and KDF541/pFepAE280C, previously labeled with MAL6, were suspended in SDS-PAGE sample buffer and lysate were used for western blot, which reacted with the anti-MAL6 polyclonal serum, according to the procedure described before.

ESR analysis of outer membrane and inner membrane of labeled KDF541/pFepAE280C

E280C cells labeled with MAL6 were washed with 200 ml 10 mM Tris, pH 7.4, then pelleted by centrifugation. Pellets were resuspended in 27 ml of the same buffer in a 30 ml Corex tube. 1 mg of each DNase and RNase were added. French press was used to break the cells. Cell lysate was spun at 3000 x g for 5 min to remove debris. The supernatant was transferred to an ultra-centrifuge tube and spun at 150,000 x g for 1 hr. The supernatant was discarded and the pellet was resuspended in 7.5 ml 10 mM Tris, pH 7.4 with syringe and needles. The membrane suspension was layered onto sucrose gradients (2.02 M, 1.44 M, and 0.77 M) and spun in a SW27 rotor for 16 hr at 26,000 rpm. Inner membrane fraction was collected from the top of 1.44 M sucrose gradient. Outer membrane fraction was collected from 2.02 M gradient and washed with 10 mM Tris, pH 7.4. The purified outer and inner membrane residues were obtained by spinning at 150,000 x g for 2 hr which could then be frozen at -70°C. X-band spectra of outer and inner membrane were recorded on a Bruker EMX spectrometer.

Functions of spin-labeled cells

Viability of the spin-labeled cells

After the labeling reaction, the viability of the bacteria was confirmed. Labeled bacteria were serially diluted in LB broth in test tubes and plated on LB agar. After incubating at 37°C overnight, the titer of living bacteria was measured.

Siderophore binding and transport

⁵⁹Fe-enterobactin binding experiments were performed. Six 10-ml aliquots of 10⁹ labeled cells were transferred into culture tubes and incubated on ice for 1 hr. Appropriate volumes of freshly prepared, purified, ice-cold ⁵⁹Fe-siderophore were mixed in the six tubes. After 1 and 6 min, 5-ml aliquots were withdrawn and filtered through glass fiber filters, and the filters were counted. The absence of a differential in the siderophore associated with the cells at 1 and 6 min confirmed the inability of the bacteria to transport under these conditions.

Colicin binding and killing Assay

Purified colicin B was labeled with ¹²⁵I. Its adsorption to labeled cells was measured. Labeled bacteria were resuspended in cold 40 mM Mops (pH 6.9) containing 0.9% NaCl, at 4 x 10⁹ cells per ml. Aliquots of 50 µl were incubated with 10 µl of colicin B (containing 2.6% ¹²⁵I-colicin B) for 1 hr on ice. The mixture was diluted with 500 µl of Mops buffer and spun at 14,000 rpm for 2 min at 4°C. The radioactivity of the pellets was compared with that of the colicin solutions to calculate the amount bound. Incubation times were varied from 5 min to 3 hr, and the level of trace ¹²⁵I-colicin B varied from 1.3% to 7.5% without any alteration in results.

ESR study of FepA conformational changes in living bacteria

ESR study the effects of FeEnt and colicin B on the mobility of MTSL attached to FepAE280C in live bacteria

KDF541/pFepAE280C was grown, spin-labeled, and prepared as described before. Signal-averaged X-band spectra (six field sweeps collected over

a 8-min period) of spin labeled bacteria were recorded, with or without saturating FeEnt (300 μ M) or colicin B (10 μ M). Each of the spectra was double integrated from 3405 to 3555 G to determine the total number of MTSL spins and from 3443 to 3477 G to determine the spins derived from the strongly immobilized and weakly immobilized peaks.

TonB- and energy-dependence of conformational changes in FepA E280C

fepA, tonB⁺ or *fepA, tonB* bacteria (KDF541 or KDF571) expressing pFepAE280C were spin-labeled with MTSL and analyzed in the presence or absence of glucose. Bacteria were incubated at 4°C with or without added ligands and warmed to 37°C after 5 min. The intensity of the weakly immobilized peak was monitored versus time by setting the spectrometer center magnetic field at peak maximum (3472.3 G) and the sweep width to zero.

TonB- and energy-dependence of conformational change in FepA E280C at different temperature

Bacteria were spin-labeled with MTSL as described before. They were incubated at 4°C and warmed to 30°C and 42°C. The intensity of the weakly immobilized peak was monitored versus time by setting the spectrometer center magnetic field at peak maximum (3472.3 G) and the sweep width to zero.

Signal-averaged X-band ESR and time-course ESR experiments were also carried out in the presence of CROX with different concentrations. The effect of CROX is studied by the changes in the X-band and time-course spectra.

General ESR methods

X-band spectra

Spin-labeled samples were placed in quartz capillaries, and ESR spectra were recorded by signal averaging scans at a microwave power of 20 mW and a modulation amplitude of 2 G. Measurements of individual samples were found to be reproducible within 3% error upon reinserting and rescanning the sample.

For live cell ESR analysis, 10^{10} cells were suspended in 100 μ l of 0.01 M NaHPO₄ (pH 6.9) containing 0.4% glucose. X-band spectra of MTSL-labeled cells were recorded on a Bruker EMX spectrometer, operating at 9.8 GHz with a total scan range of 150 G and 100-KHz modulation frequency, at 4°C in a quartz flat cell.

ESR was also used to investigate the accessibility of the single Cys residues of FepA to spin labeling probes *in vivo*. X-band spectra of MTSL-labeled KDF 541 cells carrying mutated FepA alleles were recorded on a Bruker EMX spectrometer, operating at 9.8 GHz with a total scan range of 150 G and 100-KHz modulation frequency in a quartz flat cell. KDF541/pITS449 (fepA⁺) and KDF541/pFepAE280C were used as control. In control experiments, we also applied SDSL to cells harboring single cysteine mutations reside in a defined transmembrane strand of FepA.

Time-course experiment

Continuous monitoring of spin label mobility over time was carried out by time-course experiment. The intensity of the weakly immobilized peak was monitored versus time by setting the spectrometer center magnetic field at the peak maximum and the sweep width to zero.

Power saturation experiments: spin label-spin probe studies

ESR power saturation experiments were performed on a Bruker EMX X-band spectrometer equipped with a loop-gap resonator (model#XP-0201, Medical Advances, Milwaukee, WI). To obtain saturation curves in the absence and presence of CROX, all traces of oxygen were removed from the sample by using gas-permeable polymethylpentone (TPX or PMP) plastic sample capillary tubes, and continuously surrounded by flowing nitrogen gas during the measurements. For experiments in the presence of molecular oxygen, nitrogen gas was replaced by 20% oxygen (air). Spectra were recorded at 100 KHz modulation frequency and 2.0 G modulation amplitude, varying microwave power in the range 0.1-40 mW. To obtain a saturation curve, the peak-to-peak amplitude of the first-derivative $M_l = 0$ resonance line was measured and plotted against the square root of microwave power. The $P_{1/2}$ values were determined from the curve as the intersection point with a straight line that has half the initial slope of the saturation curve. Thus the $P_{1/2}$ value is the square root of the microwave power needed to reach 1/2 of the maximum intensity in the absence of any saturation. $\Delta P_{1/2}$ for O_2

and CROX represent $P_{1/2}$ determined in the presence of the relaxing agent (spin probe) minus $P_{1/2}$ determined in the absence of any relaxing agent (bathed in N_2).

Chapter III

Results

Part I. ESR Analysis of Conformational Changes of FepA *in vivo*

Introduction

Outer membrane receptors of *E. coli* and other Gram-negative bacteria scavenge Fe(III)-bearing siderophores and vitamin B₁₂ from the environment (Guterman, 1971; Wayne & Neilands, 1975; Bradbeer & Woodrow, 1976). FepA is one of a special class of OMPs called “TonB-dependent” that mediate the entry of siderophores into bacteria (Neilands, 1981; Klebba *et al.*, 1982). Siderophore transport systems play an important role in the infectivity of bacteria (Neilands, 1982, 1995; Guerinot, 1994). For many pathogenic species, an adequate iron supply is critical for the survival of the bacterial pathogens in mammalian hosts. FepA is a ligand-specific, high-affinity transport protein that binds an iron chelate and transports it through the bacterial outer membrane.

The purpose of this research is to understand the transport mechanism of ferric enterobactin (FeEnt) through its *E. coli* outer membrane receptor, FepA. Ligand uptake through such TonB-dependent receptors involves two distinct biochemical stages: binding and internalization (Rutz *et al.*, 1992). This dissertation focused on the latter aspect, the release of ligand through the outer membrane bilayer into the periplasm. In this project, electron spin resonance (ESR) spectroscopy was used to identify conformational changes that occur in FepA, *in vivo*, as the receptor performs its transport function. Stable nitroxide spin labels, like MTSL, were coupled to genetically engineered Cys residues in FepA. By determining the mobility of the spin label and its accessibility of spin probe relaxing agents, the microenvironment surrounding the spin label was evaluated *in vivo* and *in vitro*. Ferric enterobactin and colicin B were added to bacteria that had nitroxide spin labels attached to FepA, and the changes of microenvironment around these labels were monitored by ESR as the cells transported these ligands. The dependence of spin label motion on metabolic energy, TonB, and temperature was also determined.

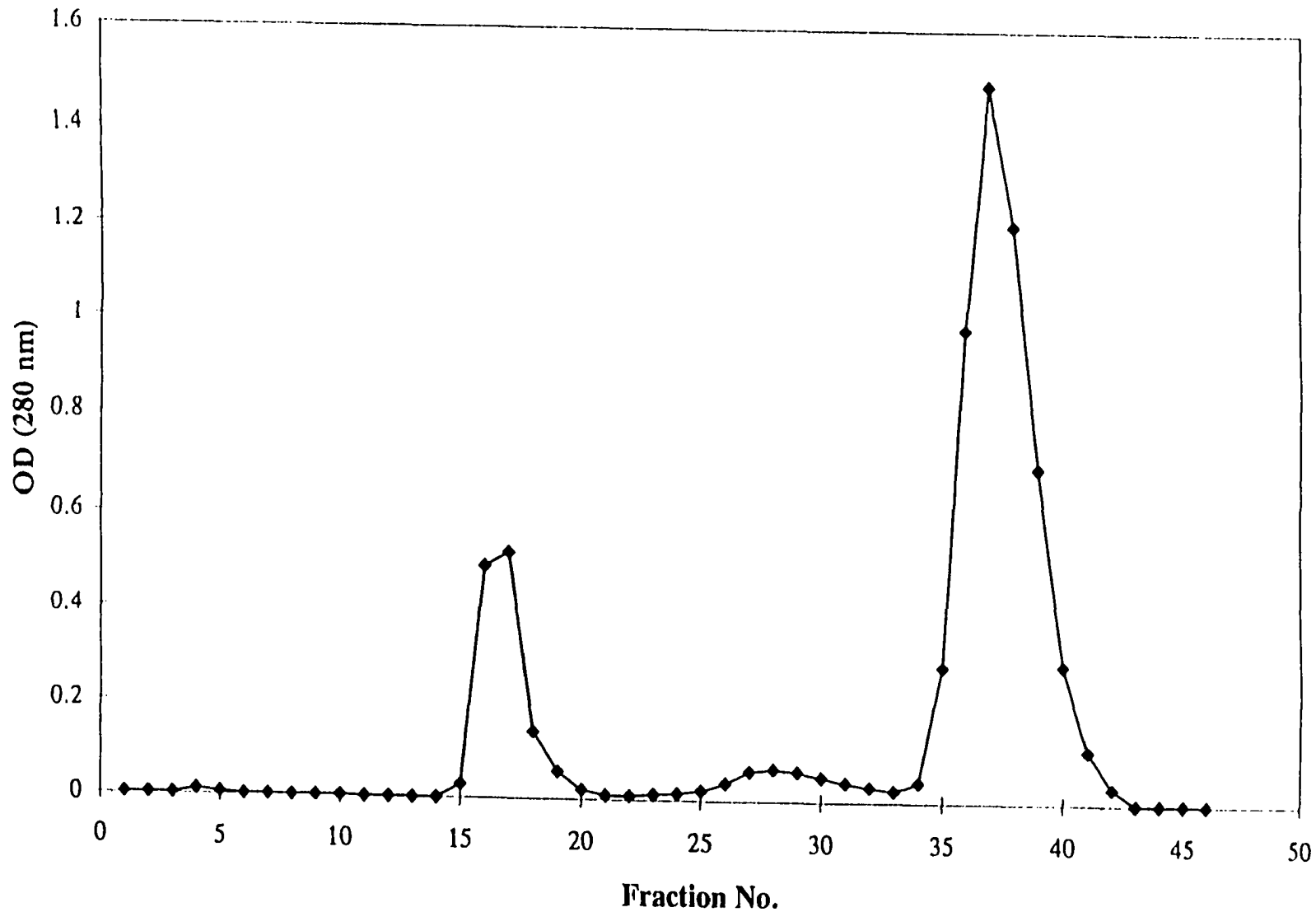
Generation and characterization of Rabbit anti-Nitroxide Sera

Ligand complexed to a protein carrier is an established approach to elicit antiserum to specific ligands (Balakrishnan *et al.*, 1982; Eichler *et al.*, 1985; Martinez-Yamout *et al.*, 1994). Bovine serum albumin (BSA) is one such protein used as a carrier. In order to effectively couple the nitroxide spin label 4-

maleimido-tempo (MAL6) to bovine serum albumin, we took advantage of the relatively high number of titratable sulfhydryl groups present in the albumin molecules. It was previously reported that the titration of albumin thiol groups depended not only on the presence of a denaturant such as urea but also on the pH (Eicher *et al.*, 1985). For this reason, the sulfhydryl-reactive spin-label was reacted with the albumin carrier in 7 M urea under alkaline conditions to maximize the substitution. The reaction mixture was applied to a Sephadex G-50 column which separated the BSA-MAL6 conjugate from unlabeled BSA (Fig. 1). Covalent modification of the accessible groups of bovine serum albumin by MAL6 resulted in a significant change in the ESR spectrum of the bound nitroxide (Fig. 2), reflecting a decrease in the rotational mobility of the conjugated spin-label. The concentration of nitroxide spin labels attached to BSA was determined by double integration of its 1st derivative X-band spectra. Approximately 13 residues of nitroxide spin-label were found per albumin molecule.

Anti-MAL6 serum was assayed for antigen specificity by ELISA in microtiter plates coated with BSA, BSA-MAL6, OVA, and OVA-MAL6. The titer of this serum against MAL6 was 15,000 (Fig. 3). The specificity of the anti-MAL6 sera was also determined by Western blot (Fig. 4). The antibodies to the nitroxide were used to detect labeled proteins after fractionation by sodium dodecyl sulfate-polyacrylamide gel electrophoresis (SDS-PAGE). BSA, BSA-MAL6, OVA, and OVA-MAL6 were heat-denatured in the presence of sodium

Figure 1. Separation of BSA-MAL6. One milliliter of the reaction mixture was loaded on a Sephadex G-50 column (2.5 cm in diameter, 30 cm in length) equilibrated with 0.05 M Tris-HCl, pH7.5, 0.1 M NaCl, and 0.1 mM EDTA. The size of each fraction is 3 ml. The absorption of the fraction at 280 nm is plotted against the fraction number.



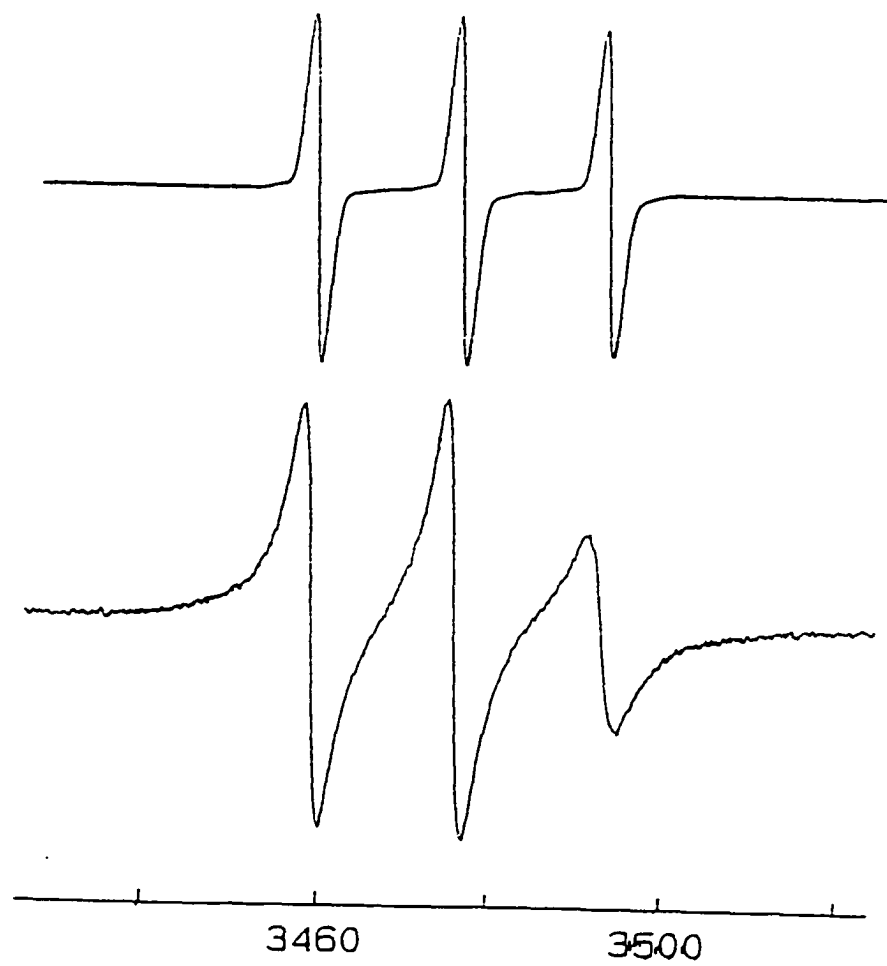
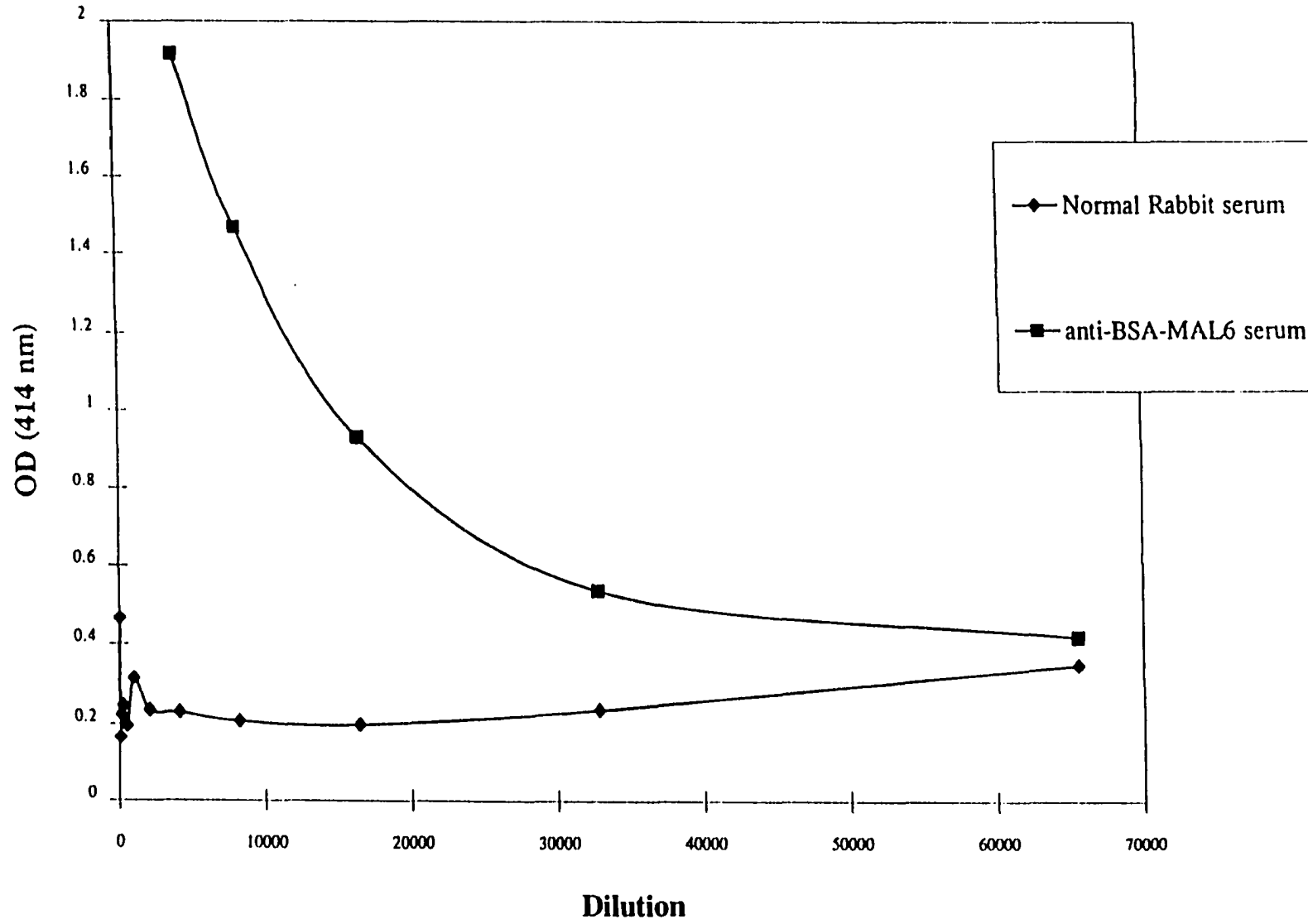


Figure 2. ESR spectra of MAL6 (top) and BSA-MAL6 (bottom).

Figure 3. ELISA (anti-BSA-MAL6 Serum, 4°C)



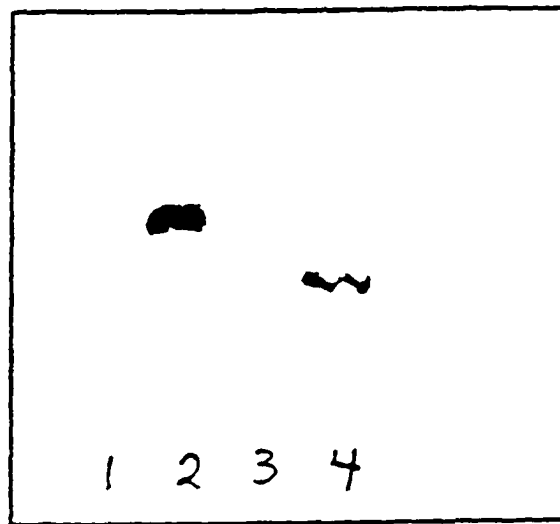


Figure 4. Immunoblot to detect the specificity of anti-MAL6 serum. From left to right: BSA, BSA-MAL6, OVA, OVA-MAL6.

dodecyl sulfate and β -mercaptoethanol prior to loading them onto the polyacrylamide gel. Following electrophoresis and transfer to nitrocellulose membranes, the labeled proteins were detected by anti-MAL6 sera. Little cross-reactivity was observed against unsubstituted bovine serum albumin, demonstrating that the response was primarily directed against the nitroxide spin-label hapten. The same experiment was carried out for proteins labeled with 4-(2-Iodoacetamido)-tempo(IASL). The ESR spectra of IASL, BSA-IASL, and OVA-IASL are shown in Fig. 5. Compared to free IASL, IASL attached to BSA or OVA had lower mobility than free IASL. However, compared to BSA-MAL6, IASL attached to BSA had higher mobility because it has a longer arm between the Cys and the nitroxide to allow faster motion than MAL6. BSA, BSA-IASL, OVA, and OVA-IASL were denatured and loaded onto SDS-PAGE. After electrophoresis and transfer to nitrocellulose, anti-MAL6 serum was used to detect these proteins (Fig. 6). In western blots, BSA, BSA-IASL, and OVA-IASL were recognized by anti-MAL6 serum, while OVA was not. These results demonstrate that each constituent of the nitroxide spin-label conjugate, BSA-MAL6, contributes to the overall recognition by antibodies, but that the six-membered nitroxide spin-label ring structure, TEMPO, appears to be the most important antigenic determinant.

Specific labeling of FepA in live bacteria

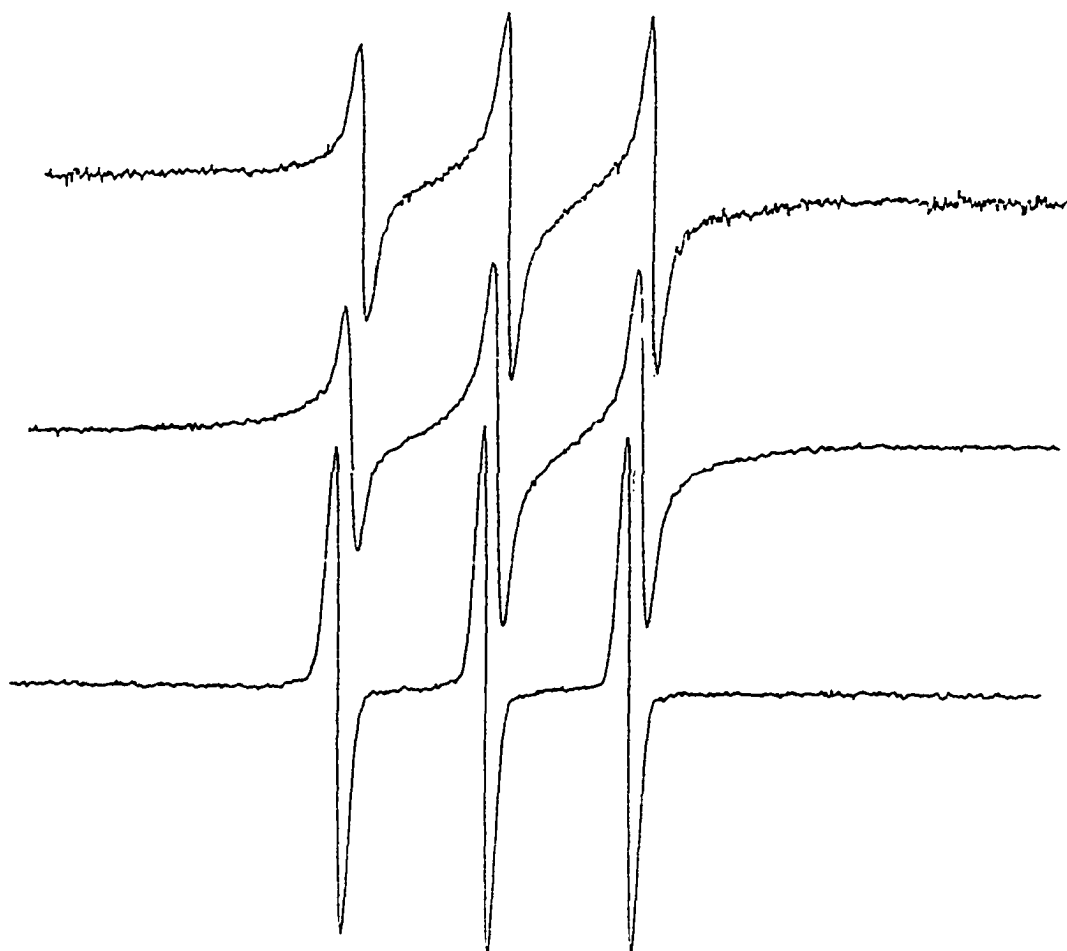


Figure 5. ESR spectra of IASL, BSA-IASL, and OVA-IASL (from top to bottom).

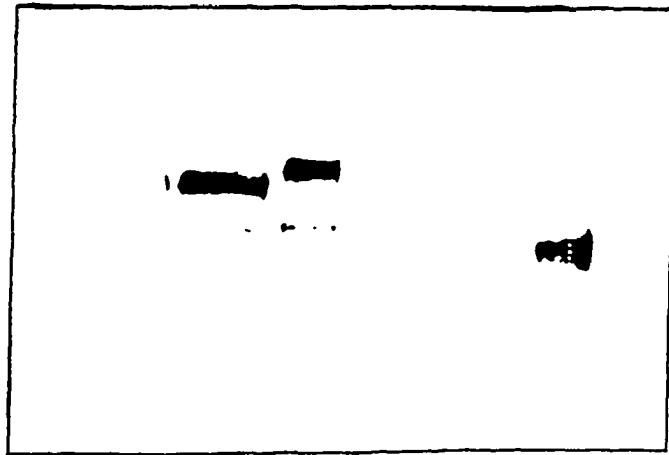
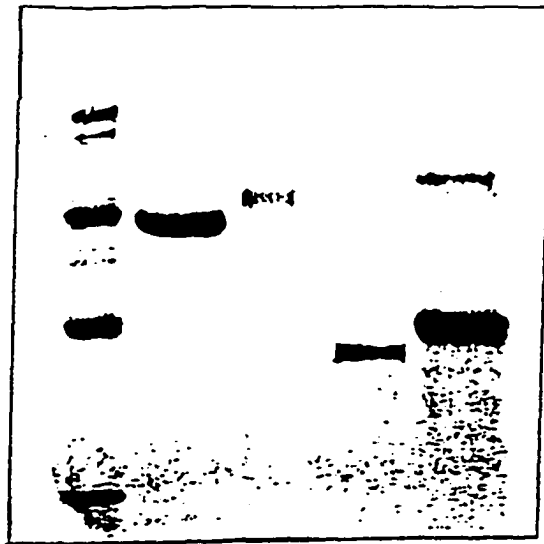


Figure 6. SDS-PAGE and Immunoblot analysis of IASL-labeled proteins: For SDS-PAGE, from left to right: MW markers, BSA, BSA-IASL, OVA, OVA-IASL; For Western blot using anti-MAL6 serum, from left to right: BSA, BSA-IASL, OVA, OVA-IASL.

Previous study suggested that the two native cysteines (Cys486 and Cys493) within wild-type FepA were disulfide-linked (Liu *et al.*, 1994). Spin labeling of these two native cysteines occurred only after both reduction with a thiol-reducing agent (e.g.; DTT) and unfolding in 6 M urea. Two FepA substitution mutants, FepAE280C and FepAE310C, were readily spin labeled *in vitro* without either reduction or denaturation (Liu *et al.*, 1994). These data and a body of data from other experiments (Murphy *et al.*, 1990; Rutz *et al.*, 1992) suggest that the proposed loop in which these residues occur (250-339) exists on the *E. coli* cell surface. This loop is involved in the binding and transport of FeEnt. One aim of the work in this dissertation was to evaluate this question *in vivo*, using live bacterial cells expressing the mutants of interest. As a preliminary experiment, we replicated the experiments of Liu *et al.* (1994) in liposomes. FepA E280C was first purified, reconstituted into DOPC liposomes, and then labeled with MAL6. The labeling reaction was analyzed by western blot with anti-MAL6 serum (Fig. 7) and conventional X-band ESR spectroscopy (Fig. 8).

Western blot results showed that residue E280C in liposome vesicles was accessible to spin labeling. As the reaction time increased, the FepA-MAL6 band in the blot became darker and wider, which suggests more and more FepA proteins were labeled by the nitroxide until the reaction was ended after 2 hrs.

ESR of the nitroxides demonstrated that they were protein-bound with limited mobility. As shown in Fig. 8, compared to spectra of free nitroxide spin label, nitroxide in FepA-MAL6 complex was weakly immobilized, and nitroxide

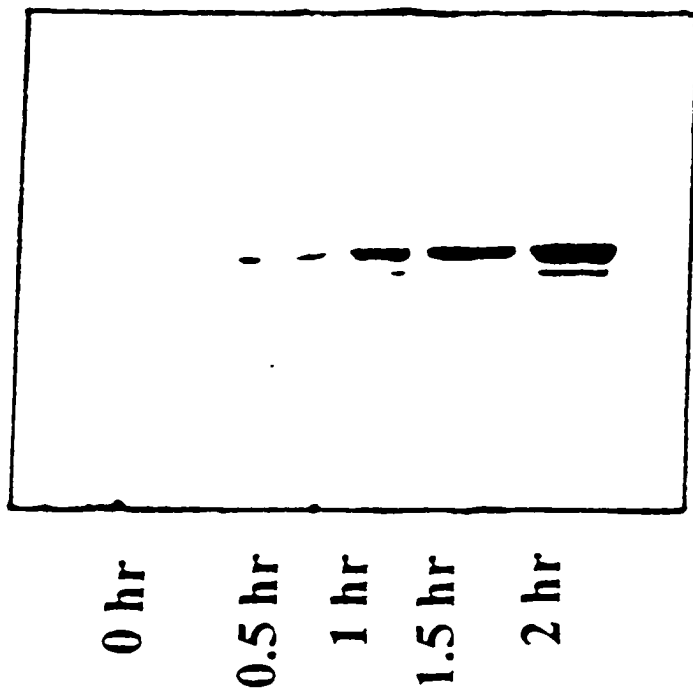


Figure 7. Western blot of spin labeled FepAE280C proteins which were reconstituted into liposome.

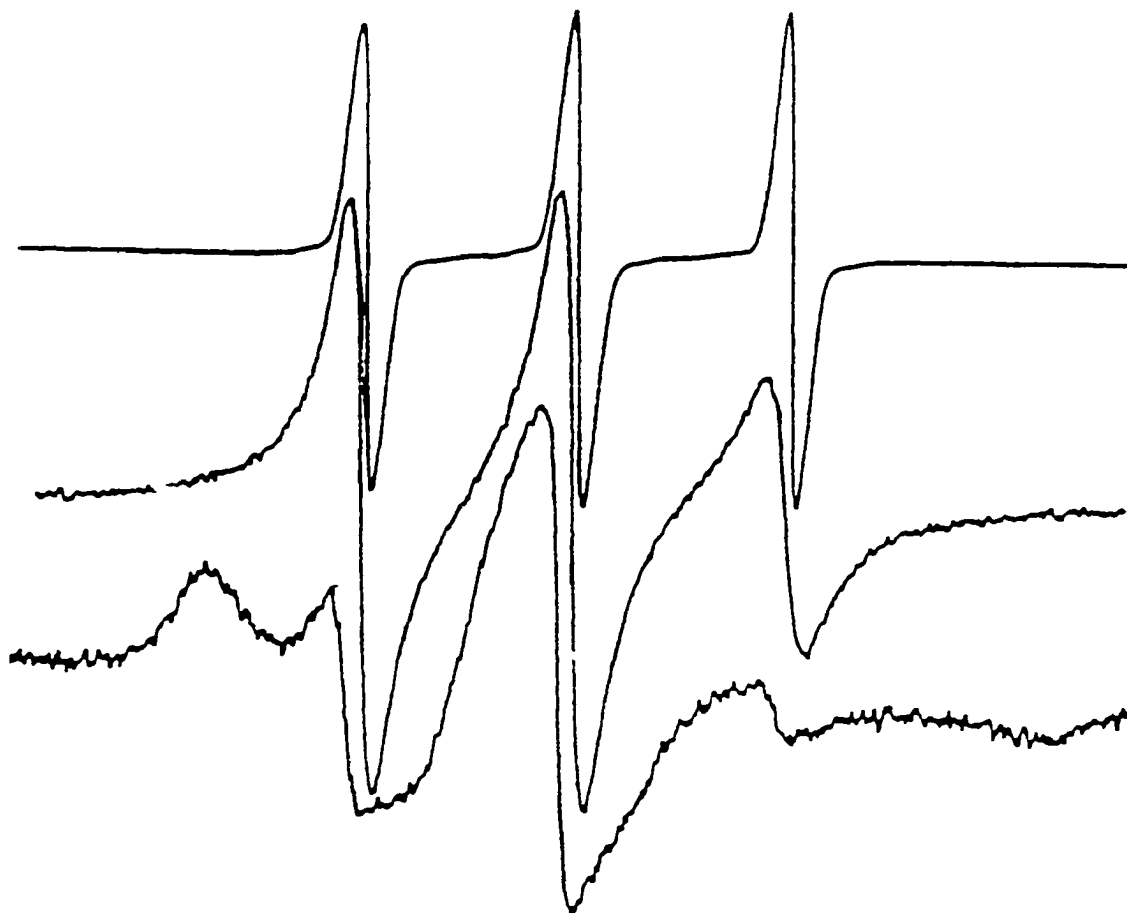
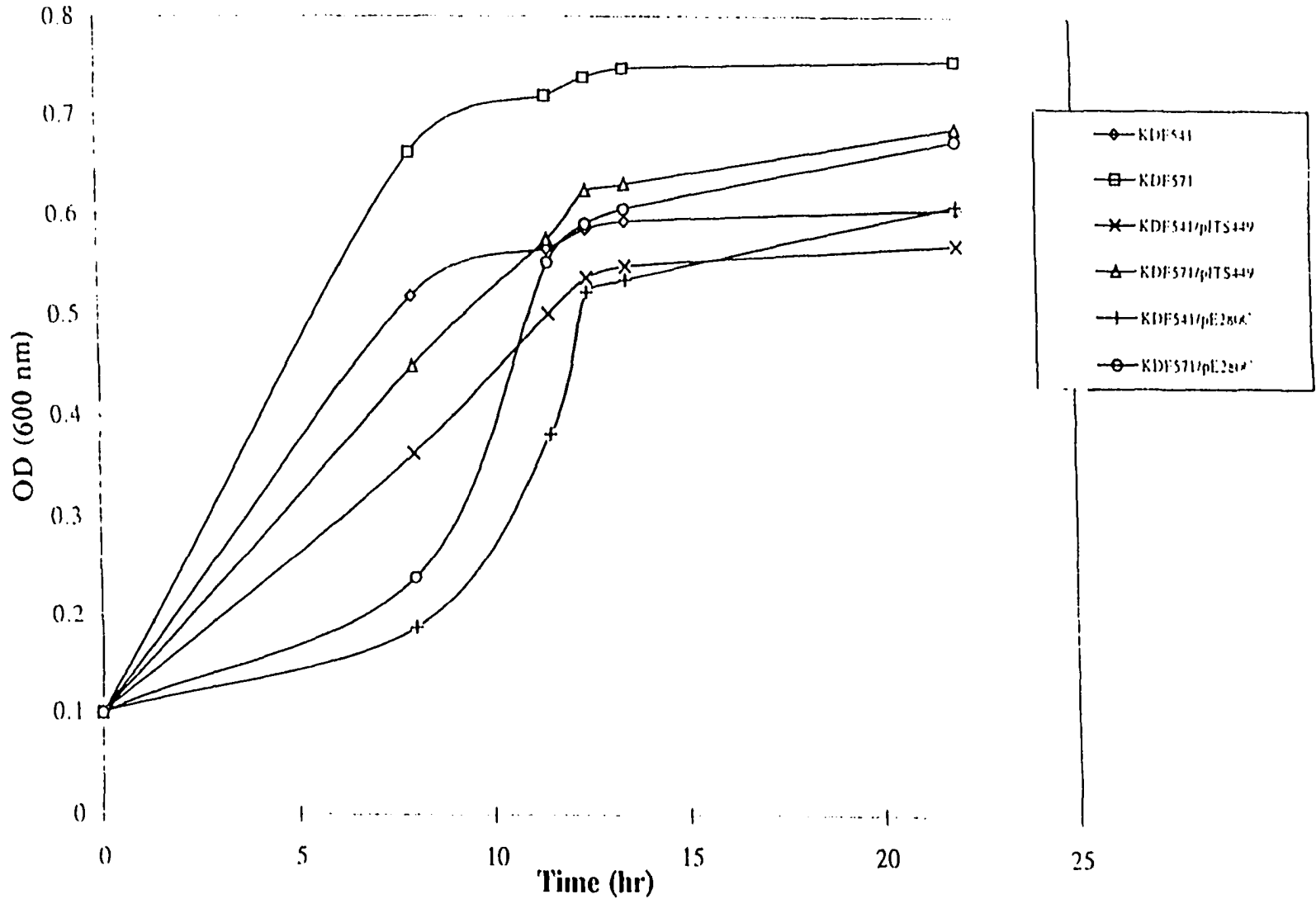


Figure 8. ESR spectra of MAL6, FepA-MAL6 in TTE, and FepA-MAL6 in liposome (from top to bottom).

in membrane-bound FepA-MAL6 was strongly immobilized. The motion of the protein as a whole is too slow to produce much significant effect on the spin-label spectrum in the range of the spin label time scale. Consequently the degree of immobilization of label depends on the flexibility of the covalent linkage, which is very sensitive to the environment at the point of attachment (Hubbell & Altenbach, 1994a, b). The weakly immobilized spectrum suggested the 280 position of FepA was likely in a surface loop with a distance away from the protein body to obtain more mobility and flexibility. This result is very consistent with previous results about E280C FepA (Liu *et al.*, 1994). On the other hand, the spectrum of the spin-labeled membrane-bound E280C FepA corresponded to a very strongly immobilized spin label with the sharp lines of some mobile spin label superimposed.

To extend the site-directed spin labeling approach to the study of membrane biochemistry in live bacteria, we utilized MTSL to label FepAE280C *in vivo*, with wild type FepA (pITS449) as a control. Bacteria were grown in LB medium and then subcultured into T medium plus appropriate nutritional supplements at 1%. The growth curves were obtained by measuring the optical density at 600 nm at various times (Fig. 9). After 16 hr, bacteria were harvested and spin labeled. The labeling conditions were optimized. The labeling reaction was carried out at room temperature at pH 7.5 with the ratio of nitroxide spin label probes to FepA copy number 100:1 in 15 ml reaction buffer. When the labeling reaction was carried out at 4°C, there was very weak labeling with no significant

Figure 9. Bacterial Growth Curves. Bacterial KDF541, KDF541/pITS449, KDF541/pFepAE280C, KDF570, KDF570/pITS449, and KDF570/pFepAE310C, first grown in LB, were subcultured into T media. The absorption of the culture at 600 nm is plotted against the time of growth.



difference between bacteria harboring pfepAE280C and the fepA host strain KDF541 expressing the wild-type fepA allele. The pH 7.5 of labeling buffer was used to match the pH of T media of bacterial culture. This pH worked well for *in vitro* spin labeling experiments. *In vitro* experiment also showed that 2 hrs of the labeling reaction ensured strong labeling of E280C FepA.

The conclusion that FepA could be specifically modified and analyzed *in vivo* was supported by two results: Bacteria harboring pfepAE280C were labeled 30- to 50-fold more than the fepA host strain KDF541 or KDF541 expressing the *fepA*⁺ allele that lacks the E280C mutation (Fig. 10). Furthermore, in Western blots of cell lysates with anti MAL6 sera, the engineered Cys residue at FepA residue 280 was the major spin-labeled site in the bacteria (Fig. 11).

Our result also showed that the outer membrane of nitroxide labeling FepAE280C cells has strong ESR signal. No ESR signal was detected for the inner membrane (Fig. 12).

After the labeling reactions, the viability of the bacteria was measured by plating on LB agar. These results showed about 70% of bacteria were still alive and active after labeling and washing. The siderophore binding and transport experiment and colicin binding and killing experiment suggested these labeled cells were still normally functioning (Fig. 13).

Structural changes in FepA during ligand transport in live bacteria

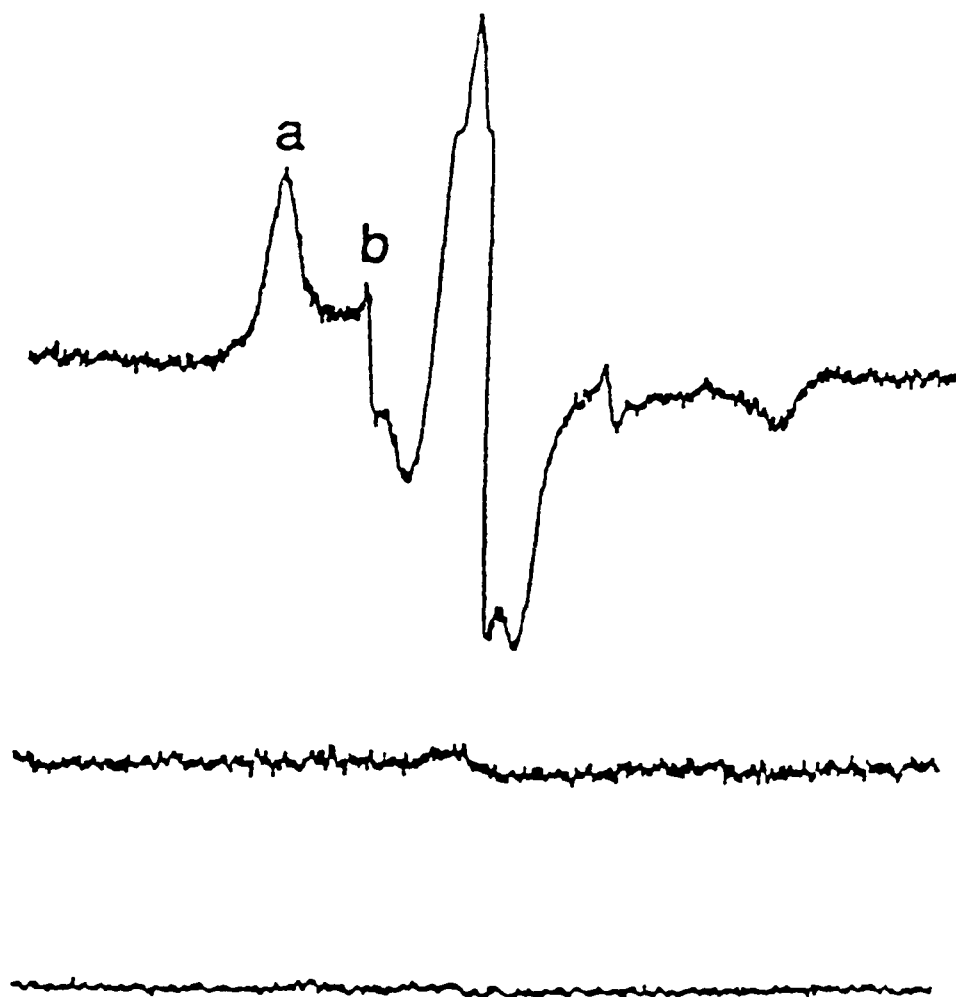


Figure 10. ESR analyses of MTSL-labeled bacteria expressing FepAE280C. From top to bottom: MTSL-labeled KDF541/pFepAE280C, KDF541/pITS449 (*fepA*⁺), and KDF541 (*fepA*).

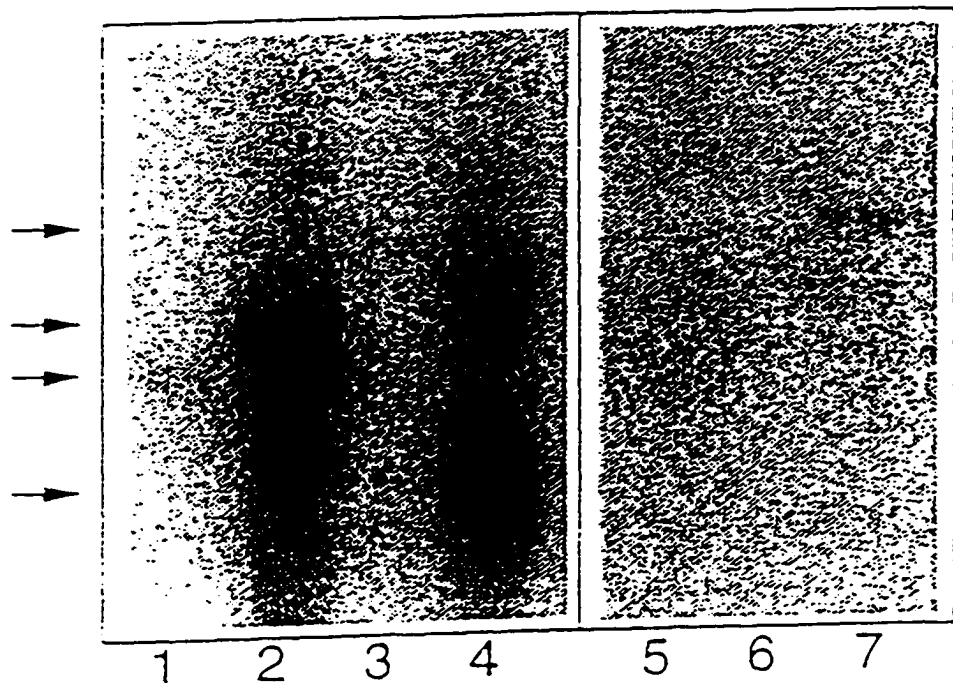


Figure 11. [^{125}I]-labeled protein A Western blots with anti-MAL6 sera. Lane 1 through 7: BSA, BSA-MAL6, OVA, OVA-MAL6, lysates of KDF541, KDF541/pITS449, and KDF541/pFepAE280C.

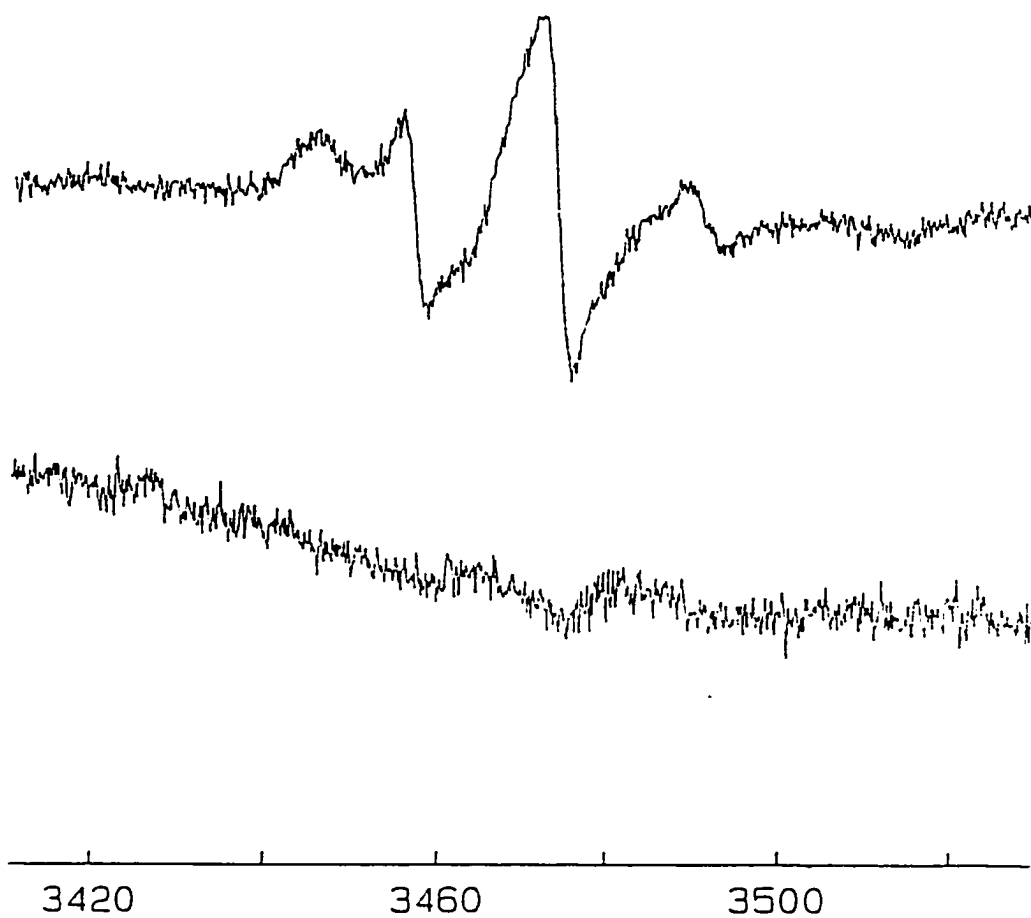
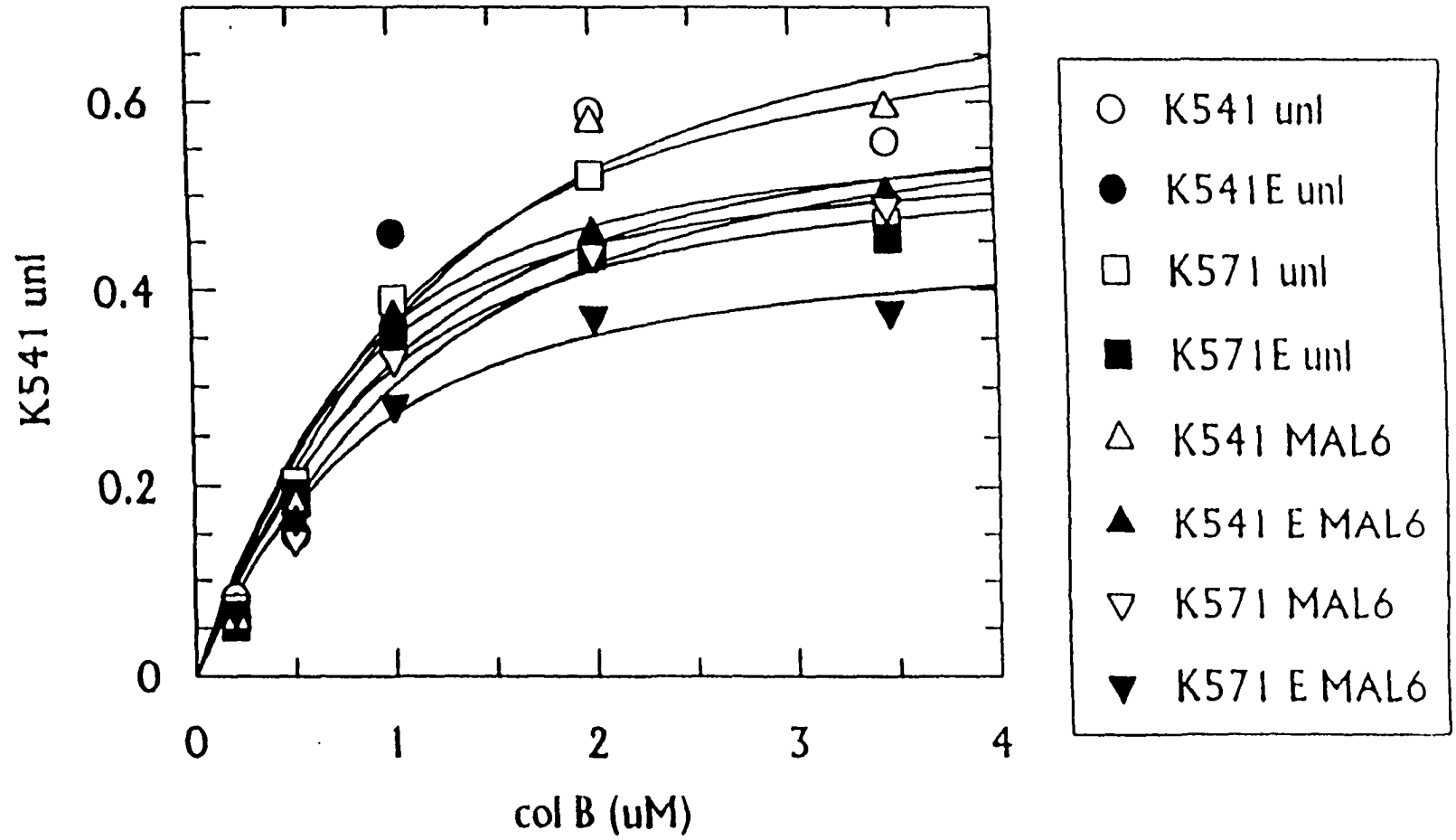


Figure 12. ESR spectra of OM (top) and IM (bottom) of MTSL-labeled KDF541/pFepAE280C cells.

Figure 13. Concentration dependence of colicin B binding by MAL6-spin labeled cells.



Spin-labeled bacteria were incubated with saturating levels of FeEnt (300 μM) under binding conditions (MOPS media, 4°C), spectra were recorded, and the cells were shifted to 37°C by heating the flat cell sample tube in the resonator cavity. A time course of sequential X band spectra was also recorded over a 20 min period. The effects of ferric enterobactin on ESR spectra of MTSL-labeled cells are shown in Fig. 14. At 4°C, FepA recognized and bound ferric enterobactin. FepAE280C-MTSL showed a two-component spectrum *in vivo*, with the majority of its spins strongly immobilized and a small percentage weakly immobilized, very similar to *in vitro* MTSL-labeled FepA spectrum (Liu *et al.*, 1993; Klug *et al.*, 1995, 1997). At 37°C, the strongly immobilized component changed in the presence of the siderophores: 16% of the spins shifted to the weakly immobilized state, indicating a change in protein conformation that relocated the nitroxides into a more mobile environment. The bacteria were then recooled to 4°C for 30 min and their ESR spectrum was recorded. The regeneration of the properties and proportion of strongly immobilized spins ruled out the possibility that the mobilization of spins in the presence of FeEnt was caused by chemical release of MTSL from FepA by ferric enterobactin.

The experiment was repeated with another FepA ligand, colicin B, and in this case, different TonB-dependent energy-dependent changes in spin label motion were observed (Fig. 15). Addition of saturating levels of colicin B (10 μM) to nitroxide-labeled FepA *in vivo* progressively converted the weakly immobilized spins and enhanced the strongly immobilized peak. The separation

Figure 14. Effect of ferric enterobactin on the mobility of MTSL attached to FepAE280C in live bacteria, observed in signal-averaged X-band spectra. Signal-averaged X-band spectra (six field sweeps collected over an 8-min period) of spin-labeled bacteria were recorded at 4°C (A) and again after warming the flat cell to 37°C (B). A fresh aliquot of cells from the same labeling reaction was suspended in saturating ferric enterobactin (300 μM) at 4°C (C), the sample was warmed to 37°C, and spectra were recorded after 5 (D) and 15 (E) min (midpoints of the signal-average measurements). The bacteria were then cooled again to 4°C for 30 min, and spectra were recorded (F). Each of the spectra was double-integrated (G) from 3405 to 3555 G to determine the total number of MTSL spins (○) and from 3443 to 3477 G to determine the spins derived from the strongly immobilized (a) and weakly immobilized (b) peaks (●). (Copied from Jiang *et al.*, 1997)

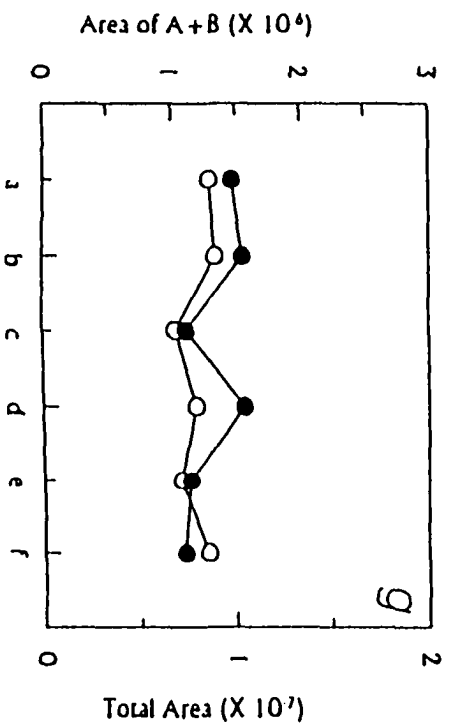
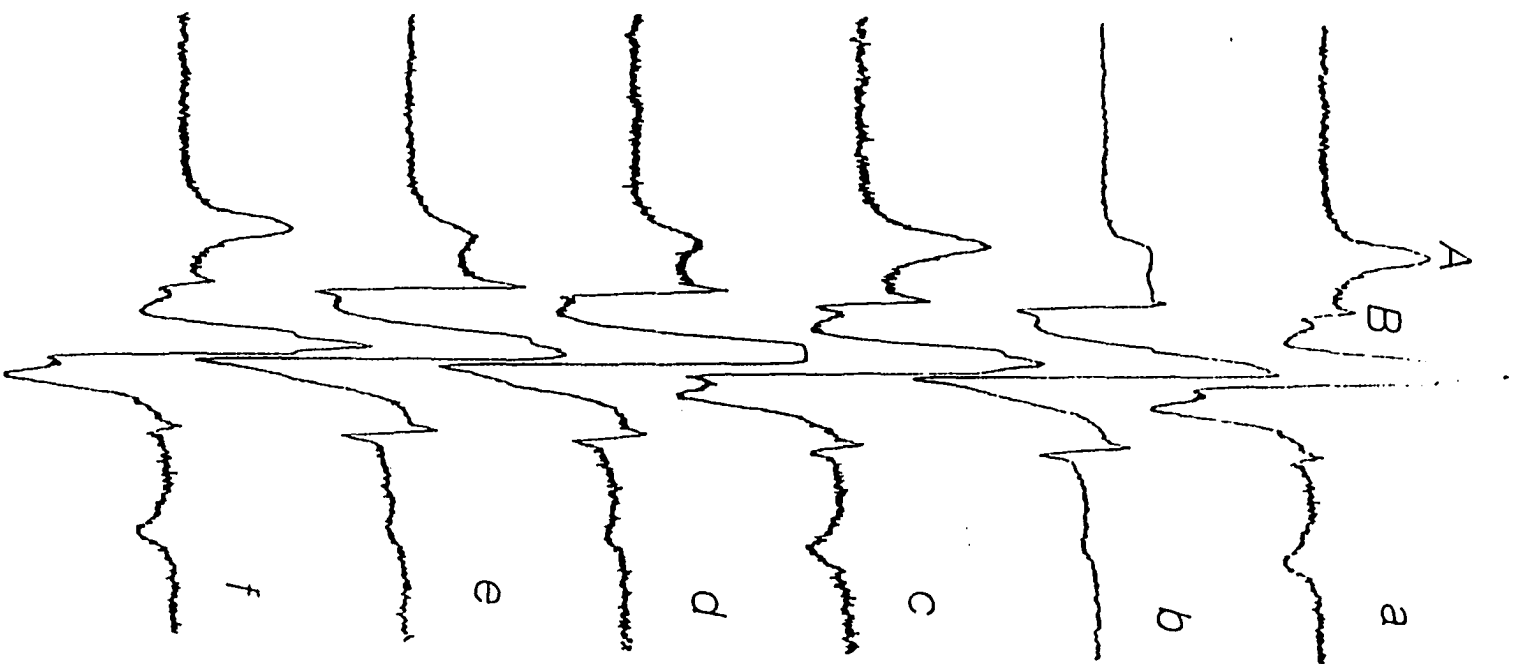
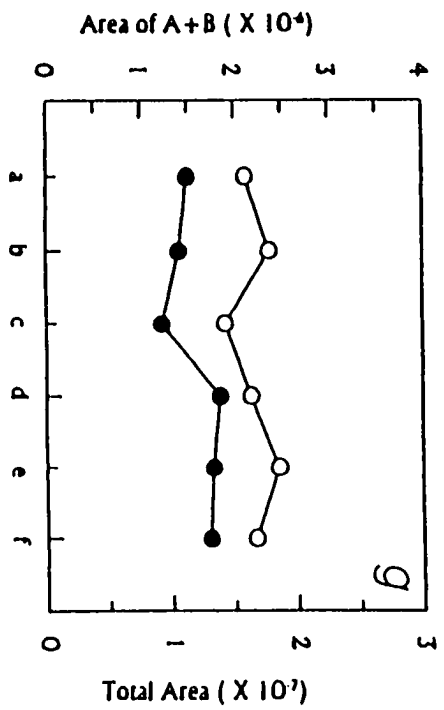
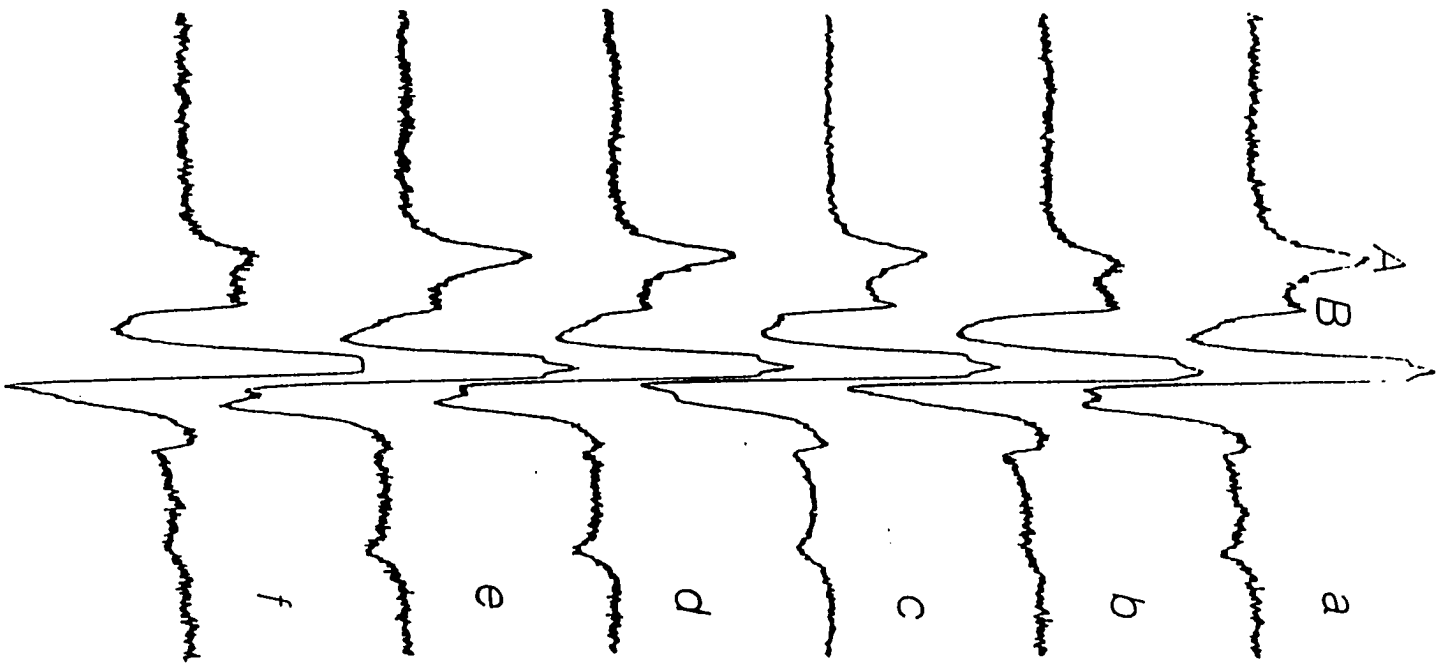


Figure 15. Effect of colicin B on the mobility of MTSL attached to FepAE280C in live bacteria, observed in signal-averaged X-band spectra. Signal-averaged X-band spectra (six field sweeps collected over an 8-min period) of spin-labeled bacteria in the presence of saturating levels of colicin B (10 μ M) were recorded at 4°C (A) and after warming in the flat cell to 37°C after 5 (B), 15 (C), and 75 (D) min (midpoints of the signal-average measurements). The bacteria were then cooled again to 4°C for 30 min, and spectra were recorded (E). The same strain was grown in minimal media and starved for glucose for 2 hours to deplete its energy stores, spin-labeled, and exposed to colicin B (10 μ M) at 37°C for 30 min (F). (Each of the spectra was double-integrated (G) from 3405 to 3555 G to determine the total number of MTSL spins (O) and from 3443 to 3477 G to determine the spins derived from the strongly immobilized (a) and weakly immobilized (b) peaks (●). (Copied from Jiang *et al.*, 1997)



between low- and high-field extrema also increased. These changes were distinguishable from colicin binding, because they were not observed by continual incubation of the cells at 4°C for 1 hr. This result supports the prediction that the colicin threads through the surface loops of FepA and into its underlying domain, in the process restricting nitroxide motion by direct contact with the toxin polypeptide (Wiener *et al.*, 1997). The same strain was grown in minimal media and starved for glucose for 2 hr to deplete its energy stored, spin-labeled, and exposed to colicin B at 37°C for 3 min, no mobility changes were observed. This result indicates that the changes of spin label motion is energy-dependent. Addition of colicin B to MTSL-E280C reconstituted in liposomes did not induce those changes observed in Fig. 15 either (Fig. 16).

Fig. 17 shows the statistical analysis of ferric enterobactin- and colicin B-induced variation in FepAE280C-MTSL motion. Multiple signal-averaged spectra were collected from several independent preparations of bacteria, and the mean and standard derivative of the ratio b/a , the most sensitive measure of changes in spin-label mobility, was calculated at the indicated points after addition of ferric enterobactin (A) ($n = 4$) and colicin B (C) ($n = 6$). These figures showed the tendency of the siderophore to mobilize spin labels and the colicin to immobilize them.

Time course of spin label motion

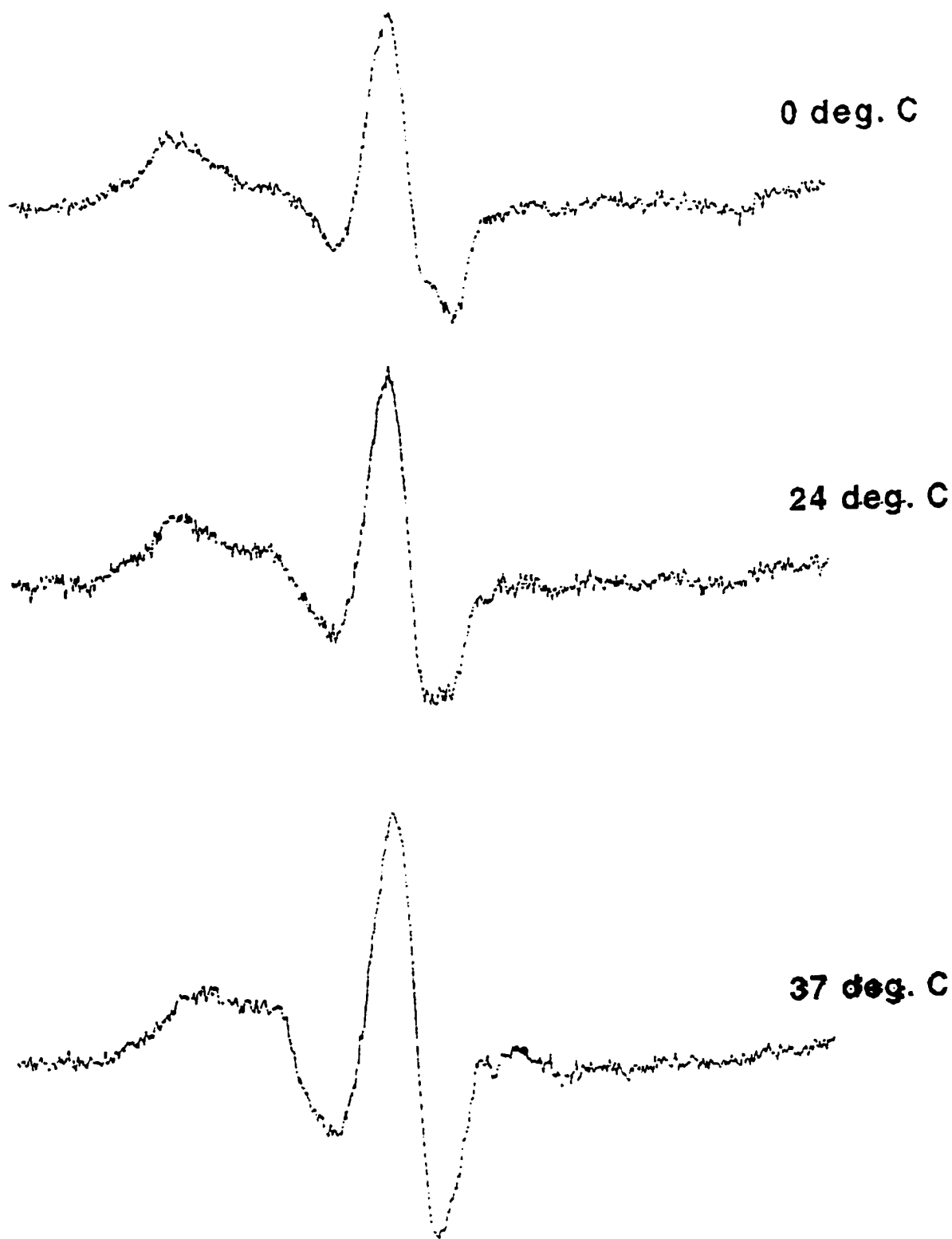
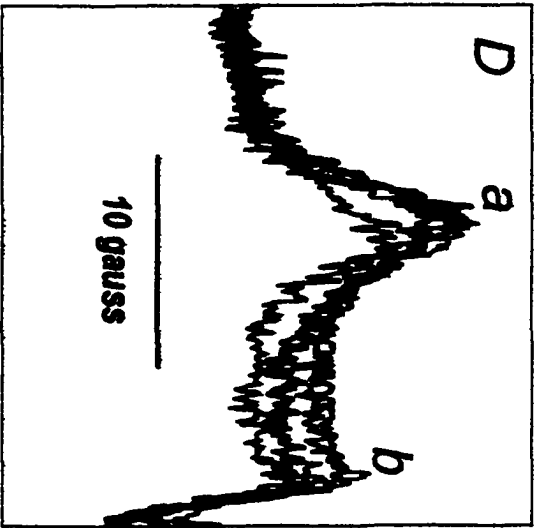
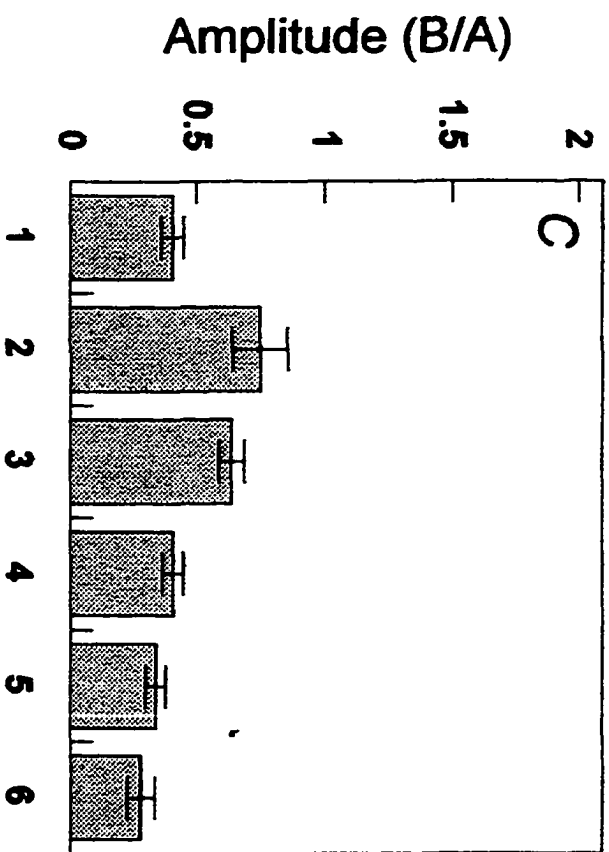
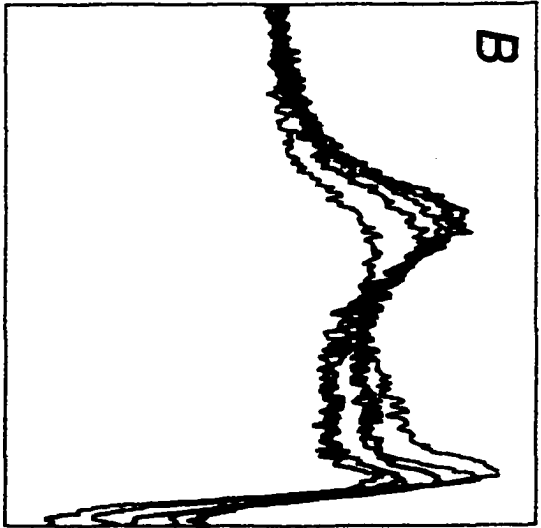
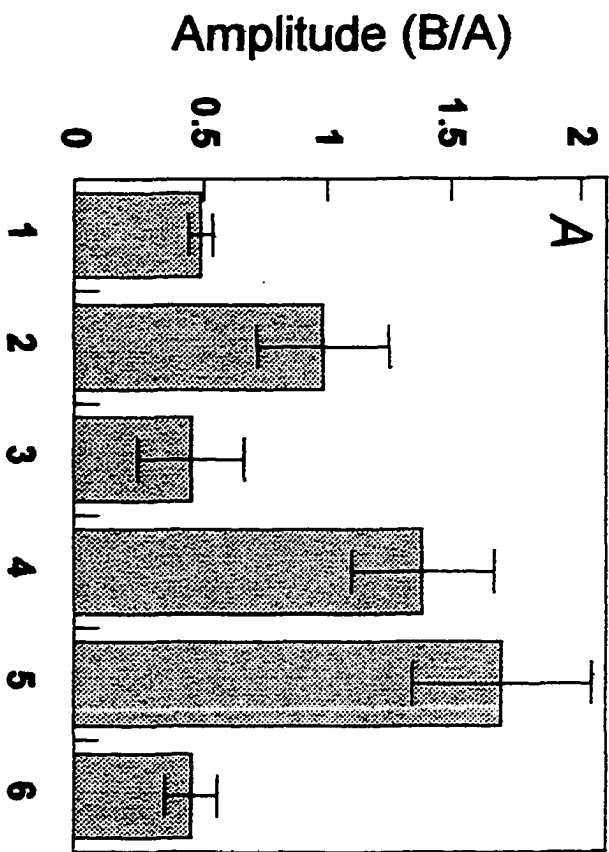


Figure 16. ESR spectra of MTSL-E280C in liposomes with colicin B at different temperature.

Figure 17. Statistical analysis of ferric enterobactin- and colicin B-induced variations in FepAE280C-MTSL motion. (A) Bars 1 through 6 correspond to samples A through F, respectively, of Fig. 28. (C) Bars 1, 2, 3, 5, and 6 correspond to panels A through E, respectively, of Fig. 29; bar 4 shows the effects of collicin after 30 min at 37°C. Superimposed spectra from single experiments are also shown, in the region of the strongly and weakly immobilized peaks. (B) Spectra were collected in the absence of ferric enterobactin at 37°C (purple), in the presence of ferric enterobactin at 4°C (blue), after increasing the temperature to 37°C for 5 (green) and 15 (red) min, and after recooling the sample to 4°C (black). (D) Spectra were collected in the presence of colicin B at 4°C (purple), after increasing the temperature to 37°C for 5 (blue), 15 (green), and 75 (red) min, and after recooling the sample to 4°C (black). (Jiang *et al.*, 1997)



KDF541/FepAE280C was spin labeled with MTSL and analyzed in the presence of glucose. The intensity of the weakly immobilized peak was monitored versus time by setting the spectrometer center magnetic field at the peak maximum (3472.3 GHz) and the sweep width to zero (Fig. 18). In the presence of ferric enterobactin (300 μ M), the continuous monitoring of MTSL mobility showed a burst of motion that peaked and receded over a 5-min period. The mobility of MTSL attached to FepAE280C in live bacteria peaked in 140 s and decayed in 140 s. This result suggests conformational changes in FepA during the internalization of bound FeEnt through the closed surface loops. The surface loops of FepA may spread apart folded polypeptides and open the channel to dislodge the bound ligand into underlying channels.

Time-course experiment was also carried out for MTSL-labeled KDF541/E280C bacteria in the presence of 10 μ M colicin B. At 37°C, the intensity of weakly immobilized peak was progressively eliminated which reflected the steric constraints placed on the spin-labeled site as the colicin polypeptide passes through the FepA pore.

Conformational change of FepA was also studied in conditions of glucose deprivation (Fig. 18), and by using a *tonB* strain (Fig. 18). Both glucose starvation and the *tonB* mutation prevented changes in the mobility of MTSL attached to the FepAE280C in live cells: Neither ferric enterobactin nor colicin B stimulated the conformational changes of FepA.

Figure 18. (top) TonB and energy dependence of conformational changes in FepAE280C. *fepA*, *tonB*⁺ bacteria (KDF541) expressing pFepAE280C were spin-labeled with MTSL and analyzed in the presence of glucose. The intensity of the weakly immobilized peak was monitored versus time by setting the spectrometer center magnetic field at the peak maximum (3472.3 G) and the sweep width to zero. Bacteria were incubated at 4°C without added ligands (blue tracing) and warmed to 37°C after 5 min (marked by an arrow). The experiment was repeated in the presence of ferric enterobactin (300 μM; yellow) or colicin B (10 μM; red).

(middle) Time-course ESR for *fepA*, *tonB*⁺ bacteria (KDF541) expressing FepAE280C subjected to the conditions described above under glucose starvation condition.

(bottom) Analysis of *fepA*, *tonB* bacteria (KDF570) expressing FepAE280C, subjected to the conditions above. (Jiang *et al.*, 1997)

Time-course ESR experiments of MTSL-labeled KDF541/E280C cells in the presence of FeEnt were also carried out at different temperatures (Fig. 19). The conformational changes in FepAE280C were a function of temperature: At different temperatures, FepA behaved differently. Incubation at 4°C, even in the presence of FeEnt, prevented the relocation of spin labels attached to E280C. At 30°C, the response to ferric enterobactin was slower than 37°C: It took longer to stimulate the increase and decrease of MTSL mobility. At 42°C, however, ferric enterobactin stimulated a dramatic increase in MTSL mobility which did not recede during a 20-min period. As mentioned above, the changing mobility of the spin label likely reflects the opening and closing of the gated FepA channel during siderophore uptake, so this observation suggests that the opening and closing of FepA channel at 30°C is slower than at 37°C. However, at 42°C, FeEnt stimulates the opening of gated FepA channels which stay at open state and do not close.

Effect of CROX on the mobility of MTSL attached to FepAE280C in live bacteria

To confirm whether the E280C is exposed in the aqueous milieu, chromium (III) oxalate (CROX) was chosen as a water soluble diffusing radical. CROX is insoluble in the membrane bilayer and the protein interior (Altenbach *et al.*, 1990). Collisions between nitroxides and CROX resulted in Heisenberg exchange, an effect which was directly measured from the nitroxide magnetic

Temperature and CROX Effect on the Mobility of MTSL attached to FepAE280C on Cell Surface in Presence of FeEnt

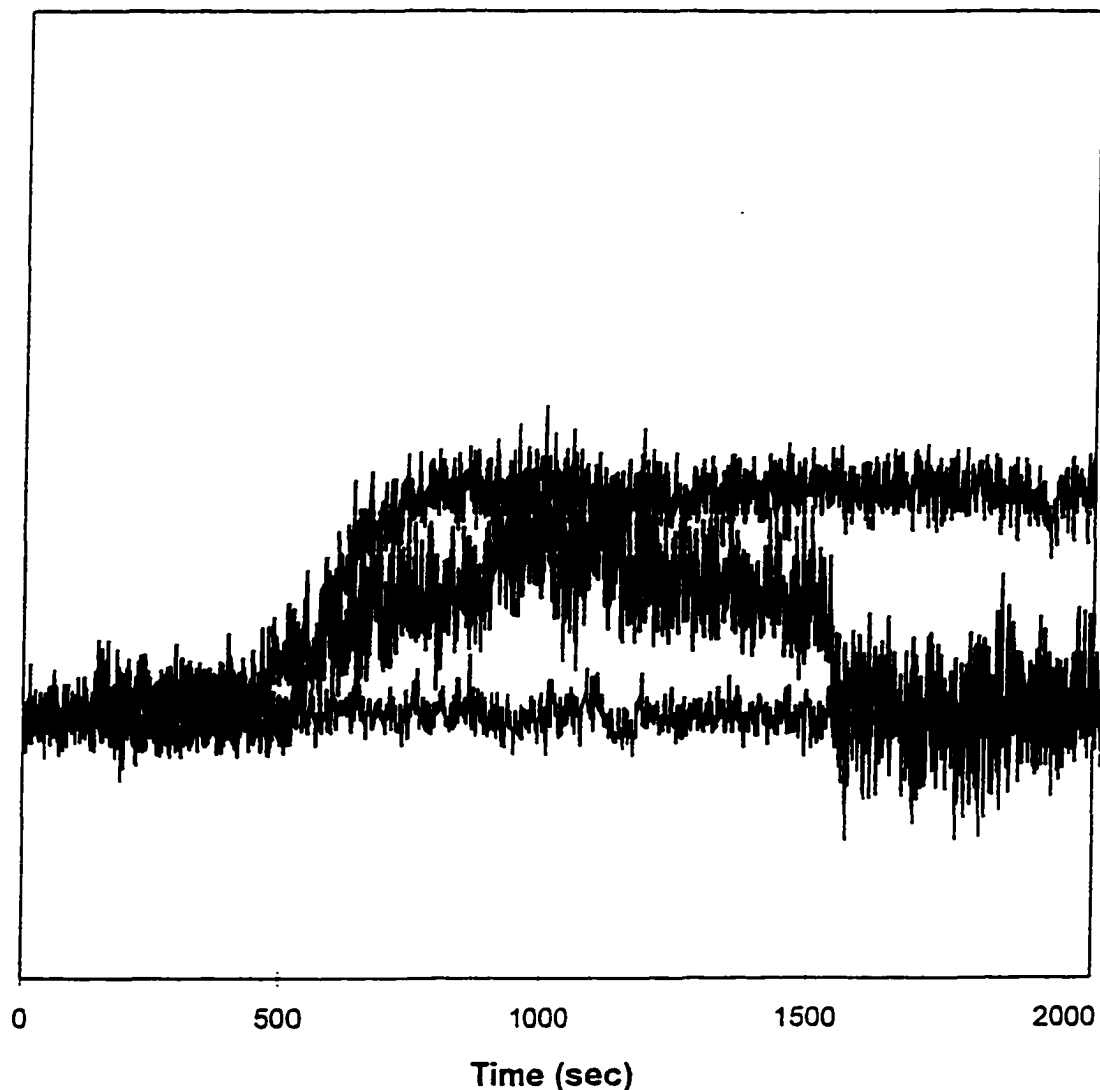


Figure 19. Conformational changes in FepAE280C at different temperature. From top to bottom: 42°C (in 300 μ M FeEnt), 30°C (in 300 μ M FeEnt), and 37°C in the presence of CROX (25 mM) and FeEnt (300 μ M FeEnt).

resonance. As the concentration of CROX increased, the ESR spectra of MTSL attached to FepAE280C in live bacteria gradually changed, until the weakly immobilized components were totally diminished at high CROX concentration (Fig. 20). This result indicated that the weakly immobilized nitroxides were water exposed and had high W_{ex} with CROX.

Continuous monitoring of the mobility of MTSL attached to FepAE280C in live bacteria in the presence of 300 μ M FeEnt and 25 mM CROX is shown in Fig. 19. The motion of spin labels stimulated by FeEnt was not observed. Aqueous phase exposed MTSL probes collided with CROX, and the relocation of spin labels stimulated by FeEnt was not detectable under this condition.

Comparison of spin-label probes used for in vivo spin labeling

Spin labels, MAL6, MTSL, and IASL, have been employed and compared for the purpose of this *in vivo* study, and the ESR spectra of KDF541 pFepAE280C cells labeled with these three spin probes are shown in Fig. 21. In all cases, two significant populations were observed: a strongly immobilized component and a weakly immobilized component. These two populations could arise from different degrees of interaction of the nitroxide with the immediate environment. Spectra for MAL6- and MTSL-labeled cells are very similar, while spectrum for IASL-labeled cells has significantly higher weakly immobilized peak (Fig. 21). This is because IASL has a spacer arm between the attachment point and the nitroxide to allow rapid motion relative to the protein.

The Effect of CROX on Spin Motion of MTSL Attached at FepAE280C on Cell Surface

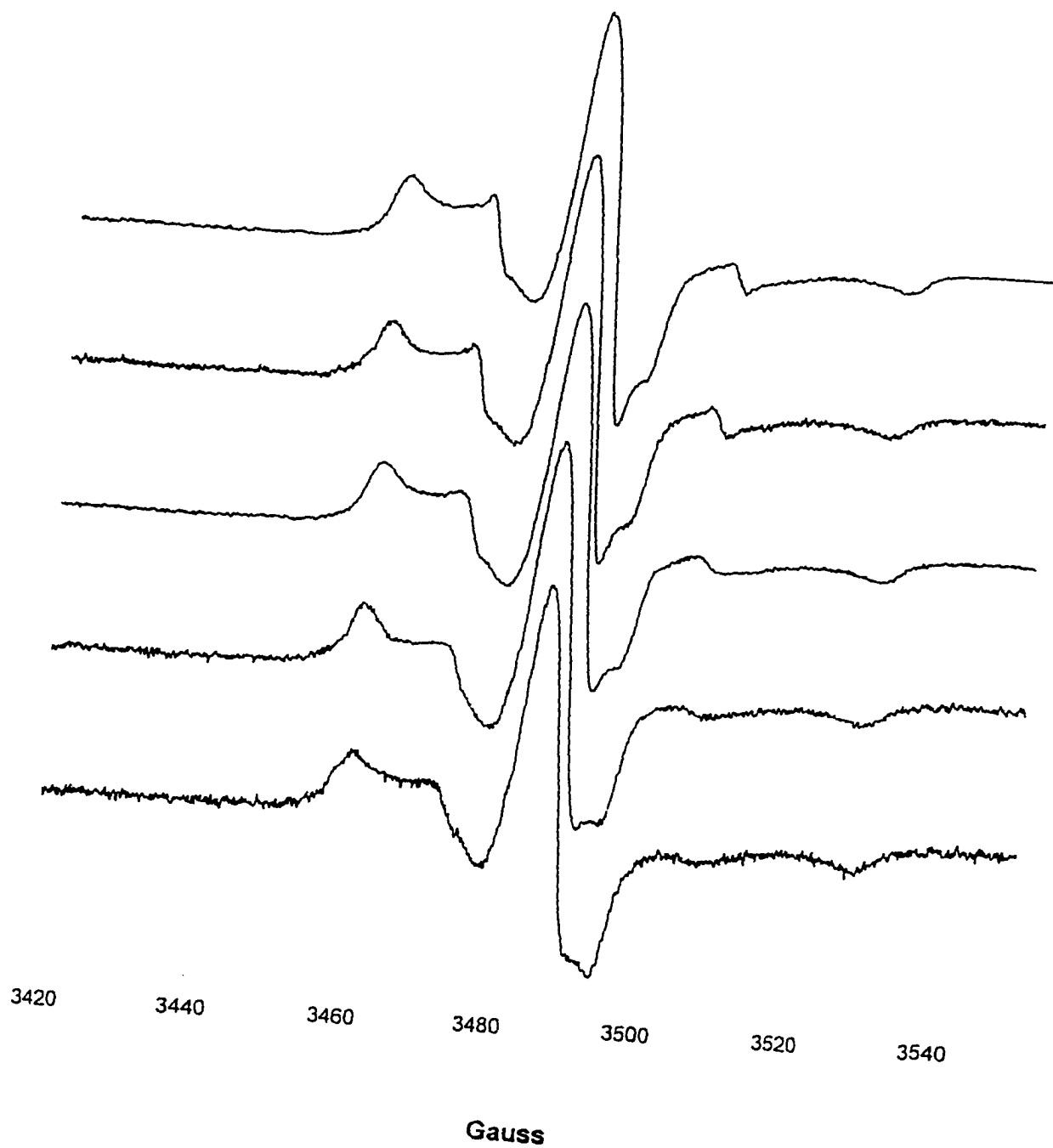


Figure 20. Effect of CROX to the mobility of MTSL attached to FepAE280C in live bacteria. From top to bottom: 0, 5, 10, 25, and 50 mM of CROX.

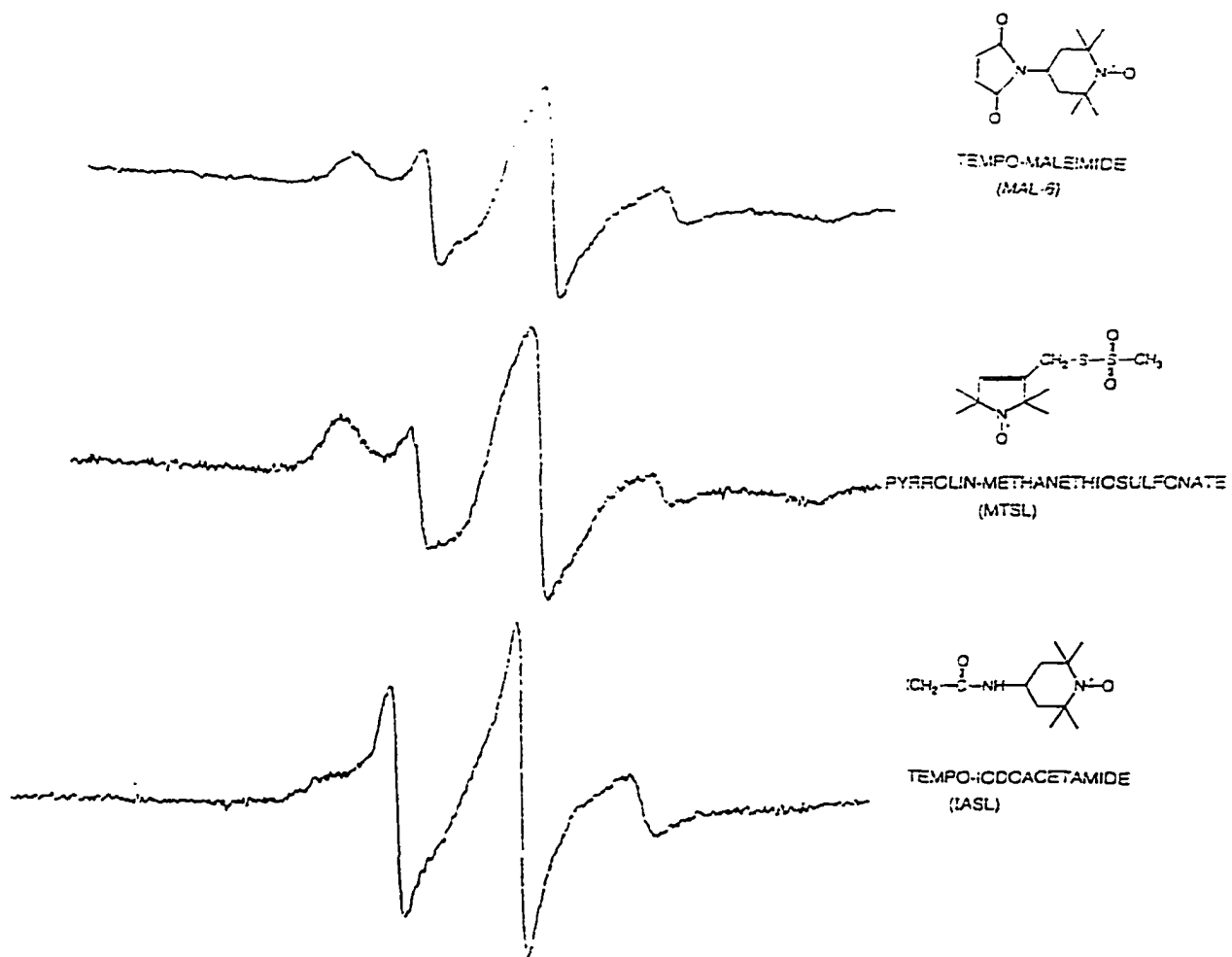


Figure 21. Comparison of spin-label probes used for *in vivo* spin labeling. From top to bottom: MAL6, MTSL, and IASL.

Accessibility of engineered FepA Cys residues to spin-label probe

To extend the site-directed spin labeling approach to the study of membrane biochemistry in live bacteria, we utilized *fepAE280C*, *fepAE310C*, and three other new substitution mutants, *fepAY289C*, *fepAW297C*, and *fepAD298C*, using *E. coli* strain KDF541 (*fepA*) as the host for these alleles.

When the nitroxide spin labels were added to live bacteria, they reacted chemically with available sites on the cell surface. The accessibility of the five different sites of interest to spin labeling was examined by comparing their ESR spectra, shown in Fig. 22. Nitroxide spin labels modified these five different sites within FepA to varying extents, but all five showed a high degree of motional restriction. The labeling on D298C mutants was not very strong, and the intensity of labeling Y289C and W297C was intermediate between E280C and D298C. Western blots of cell lysates from these bacteria, with anti-FepA sera indicated that the level of FepA expression was approximately the same in all 6 *fepA*⁺ strains (Fig. 22). Their accessibility to covalent modification was in the following order: E280C > E310C > Y289C > W297C > D298C. The high degree of immobilization of these spin labels *in vivo* for E280C and E310C virtually exactly reproduce the ESR spectra of the same mutants, purified and measured *in vitro* (Liu *et al.*, 1994). Furthermore, like the E280C and E310C sites, reported previously (Liu *et al.*, 1994), the degree of immobilization of site D298C correlated well with its accessibility to realization by the spin probes CROX and O₂: D298C was strongly immobilized, difficult to label with aqueous nitroxide

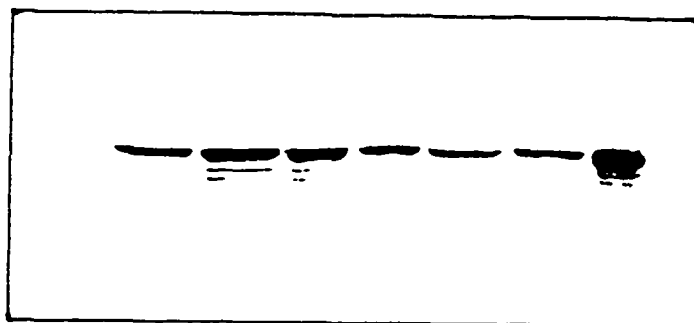
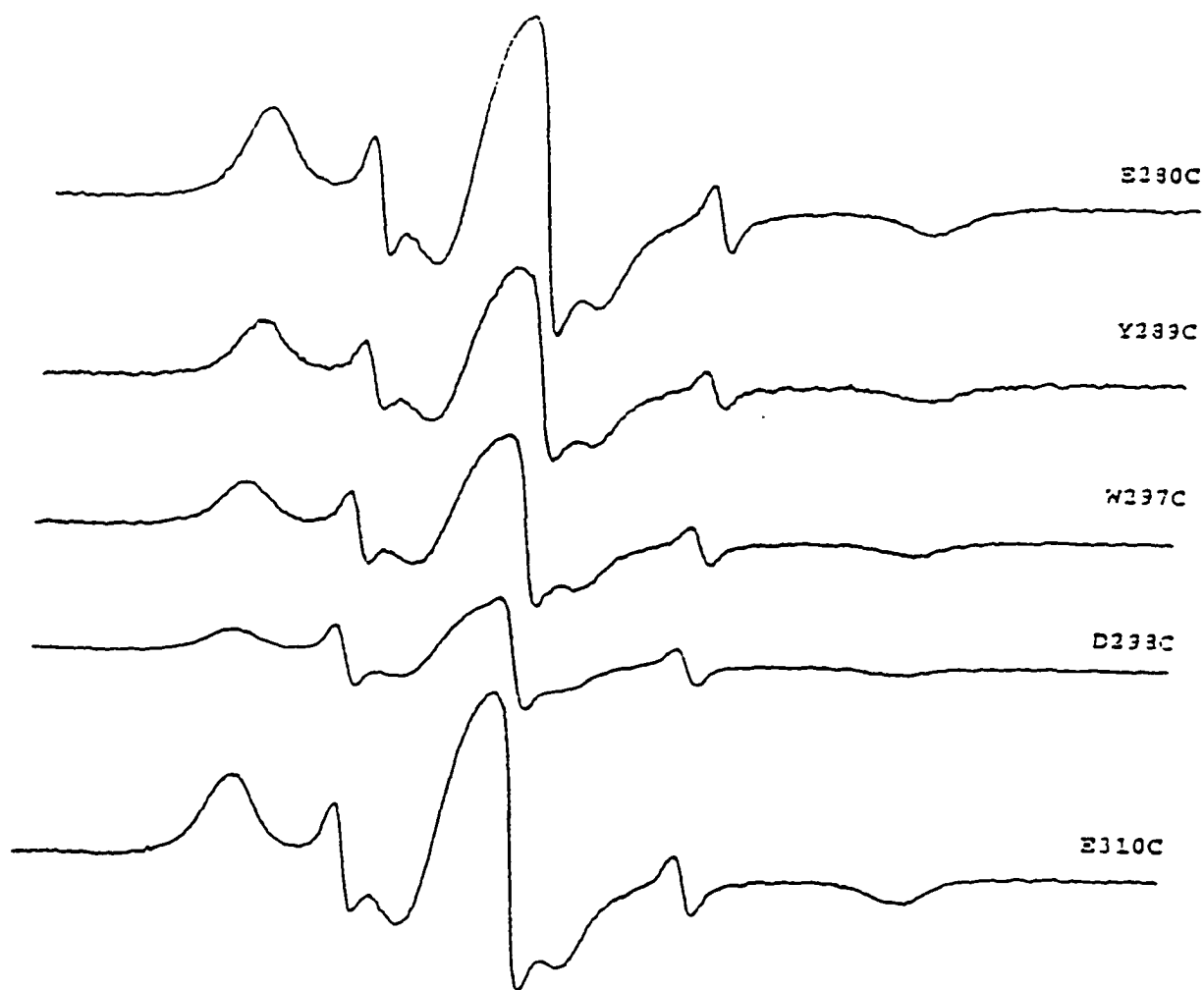


Figure 22. Top: Accessibility of engineered FepA Cys residues to spin-label probe. Bottom: An equal number of cells, 5×10^7 , were loaded onto SDS-PAGE and transferred to nitrocellulose paper. A cocktail of anti-FepA MAbs were used to probe proteins. From left to right: KDF541, KDF541/pITS449, KDF541/E280C, KDF541/Y289C, KDF541/W297C, KDF541/D298C, KDF541/E310C, and FepAE280C-MAL6 complex.

reagents, and more accessible to molecular oxygen than CROX (Dr. Feix's data). These results indicate that this site is more deeply buried within protein structure (or the membrane bilayer) than the E280 and E310 residues, both *in vitro* and *in vivo*.

Part II. Location of the TonB-box domain of FepA

Introduction

The ferric enterobactin receptor, FepA, is a TonB-dependent gated porin that transports the siderophore ferric enterobactin across the outer membrane of Gram-negative bacteria (Neilands, 1981; Klebba *et al.*, 1982). TonB is proposed to provide a functional link between the inner and outer membranes by energizing the OM with potential energy generated by proton gradients across the IM (Hannavy *et al.*, 1990; Bradbeer, 1993). However, so far the nature of TonB action still remains enigmatic. Proteinase studies and fusion protein studies suggest that TonB is anchored in the cytoplasmic membrane by an uncleaved hydrophobic amino-terminal signal sequence (Plastow & Holland, 1979; Roof *et al.*, 1991; Karlsson *et al.*, 1993; Jaskula *et al.*, 1994). The conserved central (Glu-Pro)_n and (Lys-Pro)_m repeat motifs are predicted to assume a rigid and extended conformation in the periplasm (Evans *et al.*, 1986; Brewer *et al.*, 1990; Klebba *et al.*, 1993). The localization of the C-terminal amphiphilic region is unknown.

TonB may promote OM transport by physically contacting TonB-dependent proteins (Postle, 1990; Tuckman & Osburne, 1992; Larsen *et al.*, 1997; Letain & Postle, 1997). Supporting this hypothesis, TonB-dependent receptors possess a conserved peptide at their N-terminal, the “TonB box” (for review see Klebba *et al.*, 1993). Evidence exists that this region directly interacts TonB: mutations in the TonB-box, TIVVTAA, that inactivate transport may be compensated by mutations in TonB. The proposed physical interaction between FepA in the OM and TonB in the periplasm suggests that the TonB box of FepA resides on the inner surface of the OM bilayer, but the proposed model of FepA, on the other hand, postulates these residues as the first transmembrane strand of its β -barrel. To resolve this issue, we determined the localization of the TonB box region of FepA using site-directed spin labeling and ESR spectroscopy. We generated Cys substitutions within and around the TonB-box of FepA at the nine sequential sites: DTIVVTAAE. These nine mutant FepA proteins that introduce Cys at positions 12-20 were purified, spin-labeled, reconstituted into liposomes, and analyzed by conventional ESR and spin label relaximetry to assess their localization in a membrane or an aqueous environment. If the TonB box polypeptide is a component strand of the FepA β -barrel, the sequential residues within it will alternate between interior and exterior of FepA channel.

Site-directed Mutagenesis using M13

To explore the location of TonB-box domain of FepA by site-directed spin labeling, cysteine was substituted for amino acids from 12-20, DTIVVTAAE, which reside within and around the TonB-box of FepA. Among these mutants, T13C was generated by Dr. Sally Newton.

Site-directed mutagenesis was carried out using Kunkel's method (Kunkel, 1985). Phage were grown on the *E. coli* host strain CJ 236, which is deficient in dUTPase (*dut*) and uracil glycosylase (*ung*). The *dut* mutation increases intracellular dUTP levels and the *ung* mutation permits the incorporation of deoxyuridine into the DNA in place of thymidine at some positions. Phage M13 grown in a *dut ung* host contains 20-30 uracil residues per genome and are propagated with reduced efficiency in an *ung*⁺ host, like JM101. Using uracylated M13 DNA, a heteroduplex composed of a uracil-containing parental strand and a mutant strand synthesized *in vitro* in the presence of dTTP gives rise to mostly mutant progeny when plated on a wild-type (*ung*⁺) host, because the wild type template DNA does not propagate efficiently. Sequential mutations can be made using this system by growing the first mutant on a *dut ung* host before subjecting it to another round of mutagenesis.

Using the uracil-containing DNA template prepared by standard procedures (Messing, 1983) after selection for the mutant strand *in vivo*, these site-directed mutagenesis procedures produce mutations at approximately 10%-40% efficiency. The M13 DNA was fully sequenced by the ALFExpress. For FepA, appropriate PstI/SacI bands from mutant M13-fepA and pITS449 were

purified by 1% agarose gel electrophoresis and recovered from the gel by using GeneClean kit. The purified DNA was used in ligation reactions as described in Chapter II. A control ligation was performed using the purified pUC vector DNA band, and electroporated into recipients. The single Cys substitution mutations were transferred to the FepA expression vector pITS449 at 50%-100% efficiency. Mutant clones in pITS449 (a pUC18 derivative) were also verified by determination of their DNA sequence.

Siderophore Nutrition Assays of FepA Mutants

To determine the effects of the single Cys substitution mutations in the TonB-box domain on FepA physiology, we examined the ability of the altered receptors to function in siderophore nutrition assays and colicin B sensitivity tests.

In siderophore nutrition assays, a total of 10^7 cells were plated in 45-mm-diameter dishes with 9 mM deferriferrichrome A. Deferrichrome A was used to scavenge any residual iron, so no adventitious iron was on the plate to enable the bacteria to grow. A sterile disk containing 5 μ l of 50 μ M ferric enterobactin was applied to the center of the dish, and the plate then incubated at 37°C overnight. The presence of a growth halo around the disk was observed for pITS449, E280C, E310C, D12C, T13C, I14C, V15C, V16C, T17C, A18C, A19C, and E20C. This observation suggests that all the FepA mutant strains were viable, and they obtained iron from enterobactin. The experiments indicated that the single

mutations in the TonB-box domain of FepA were well tolerated, and that mutant strains were still able to transport ferric enterobactin.

The ability of the FepA mutant receptors to transport ferric enterobactin was estimated by measuring the diameter of the growth halos around the ferric enterobactin. The diameters of the growth halos for all these strains are listed in Table. 3. Each plate was measured and compared. The diameter of the disk itself was 6.5 mm, so the diameters of the growth halos included this distance.

pITS449 which encodes wt FepA, and mutants E280C and E310C were used as controls for the nutrition studies. The growth halos of E280C and E310C had essentially the same diameter as pITS449. The substitutions with Cys did not alter regional protein conformation or the ability of FepA to bind ferric enterobactin.

The TonB box mutants all mimicked wild-type behavior in the transport of the siderophore and had very clear growth halos. This results may support the observation that only mutations to residues participating in ligand binding will affect the transport of ferric enterobactin. However, all the halos of TonB-box mutants were slightly smaller than that of wild type. Since the phenotype of TonB box mutants is dependent upon substitution with Cys that may alter regional protein conformation to some degree, the mutations may not precisely define residues involved in the interactions with siderophore but rather may reflect regional perturbations that affect the interaction between TonB-box domain of FepA and TonB.

Table 3. The effects of single Cys mutation on ferric enterobactin growth halo diameters and colicin B killing (Average of three different experiments)

Plasmids	Nutrition Assay (diameter of growth halo, in cm)	Colicin B Killing Assay (titer)
pITS449	1.90 ± 0.02	1 x 10 ⁶
E280C	1.90 ± 0.02	1 x 10 ⁶
E310C	1.90 ± 0.02	1 x 10 ⁶
D12C	1.65 ± 0.01	2 x 10 ⁵
T13C	1.84 ± 0.01	2 x 10 ⁵
I14C	1.80 ± 0.02	1 x 10 ⁵
V15C	1.85 ± 0.01	2 x 10 ⁵
V16C	1.80 ± 0.03	2 x 10 ⁵
T17C	1.82 ± 0.02	2 x 10 ⁵
A18C	1.73 ± 0.03	1 x 10 ⁵
A19C	1.82 ± 0.03	2 x 10 ⁵
E20C	1.67 ± 0.03	1 x 10 ⁵
D12C/E20C	no halo	0

Finally, a double Cys substitution mutant in TonB-box of FepA, D12C/E20C, was totally different. In the siderophore nutrition assay, no growth halo was observed for this double mutant. This result may suggest that the mutations alter FepA conformation, which may perturb the ligand binding domain of FepA; It is also possible that these mutations specifically disrupt local regional protein conformation, destroying the interaction between TonB-box of FepA and TonB.

Colicin B Killing Assay

The ferric enterobactin porin, FepA, transports the siderophore ferric enterobactin across the outer membrane, and also serves as the receptor for colicin

B and D (Pugsley & Reeves, 1976; Timmis, 1981; Mende & Braun, 1989). Colicins are water-soluble cytotoxins. They are antibiotic proteins produced by colicinogenic bacteria that kill other coliform bacteria. The colicinogenic bacteria are specifically immune to killing by the colicin that they make, but not to other colicins.

The colicin B protein contains a receptor binding domain, translocation domain, and a channel forming domain. The lethal action of colicin B does not result in bacterial lysis or leakage of cellular macromolecules. The biochemical effect of colicin B is to interfere with energy metabolism by making channels in the cytoplasmic membrane, which dissipates the proton motive force across the inner membrane (Davies & Reeves, 1975; Benedetti *et al.*, 1991; Wiener *et al.*, 1997).

Colicin B killing assays were used to test the affinity of mutant FepA receptors for colicin B. Purified colicin B was serially diluted in LB broth over 200,000-fold in microtiter plate, and then transferred with a sterile CloneMaster™ onto an LB plate containing the test bacteria, that contained the mutant *fepA* genes on pUC. After incubation at 37°C overnight, colicin titers were measured as the inverse of the lowest dilution that cleared the bacteria lawn.

The host bacterial strain KDF541 was fully resistant to colicin B, as expected for a *fepA*⁻ strain. Mutants E280C and E310C FepA were indistinguishable from wild type FepA on pITS449, again suggesting that single mutations at 280 and 310 did not affect the FepA ligand binding ability. On the

other hand, the TonB box mutants with single Cys substitutions behaved differently. The titers of these single mutations were about 10 fold lower than the controls, indicating that the single substitutions somehow impaired colicin killing. This result was very comparable to the siderophore nutrition assay results, confirming that these mutations caused either global or local perturbation in protein conformation, affecting either the ligand binding domain of FepA, or the connection between receptor and TonB protein respectively.

The most dramatic change in the sensitivity of colicin B killing was caused by double mutation D12C/E20C in FepA TonB-box domain. No sensitivity to colicin B was showed in this mutant strain. This result suggests that substitution combination may somehow seriously impaired the binding or transport ability of the receptor.

Western Blot

5×10^7 bacteria cells used for above assays were boiled with sample buffer and loaded onto SDS-PAGE. After transferring to nitrocellulose, a mixture of anti-FepA MAbs were used to recognize the FepA proteins.

Fig. 23 shows a western blot of TonB-box mutants analyzed in this study. All of these strains, wild-type or mutated, have almost identical FepA expression level. Even the double mutation, D12C/E20C, has high expression level. These data confirmed that the differences observed in siderophore nutrition assay and colicin B killing assays were directly caused by the Cys substitutions. The bacteria somehow tolerated the single substitution of Cys in FepA TonB-box

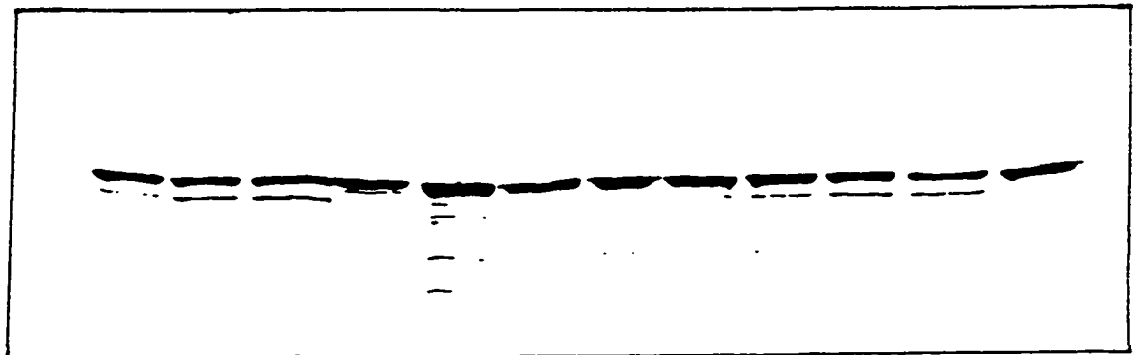


Figure 23. Western blot of FepA receptors. An equal number of cells, 5×10^7 , were loaded onto SDS-PAGE and transferred to nitrocellulose paper. A cocktail of anti-FepA MAbs were used to probe proteins. From left to right: pITS449, E280C, E310C, D12C, I14C, V15C, V16C, T17C, A18C, A19C, E20C, and D12C/E20C

domain, but the D12C/E20C double mutation totally impaired the binding and transport functions of FepA.

Affinity Purification of mutant FepA proteins

FepA mutants were purified by using affinity chromatography (Payne *et al.*, 1997) (Fig. 24). ColB-Sepharose was used to purify FepA from Triton X 100-solubilized OM fractions of UT5600/pITSFepA. Colicin B was coupled to cyanogen bromide-activated agarose. The polysaccharide resin, which has many free hydroxyl groups was briefly treated with aqueous cyanogen bromide to form an intermediate. This activated intermediate was then reacted with the colicin to form a covalently attached ligand for affinity chromatography. This method was more effective than other methods, which required multiple steps including ion-exchange and gel filtration chromatography. It is even more effective than immunoaffinity chromatography, because 81 K^{*}, the OmpT-generated degradation product of FepA, stuck tightly to anti-FepA-Sepharose, but not to ColB-Sepharose. Secondary, a mild salt gradient could release FepA from ColB-Sepharose, while only high concentrations of the chaotropic agent trichloroacetate eluted the receptor from the immunoabsorbent, and these harsh conditions also released antibodies from the resin that contaminated the FepA product.

Spin Labeling and ESR of Purified Receptors

Wild type FepA has two cysteine located at residues 486 and 493. No labeling of wt FepA with MTSL was observed without prior treatment with a

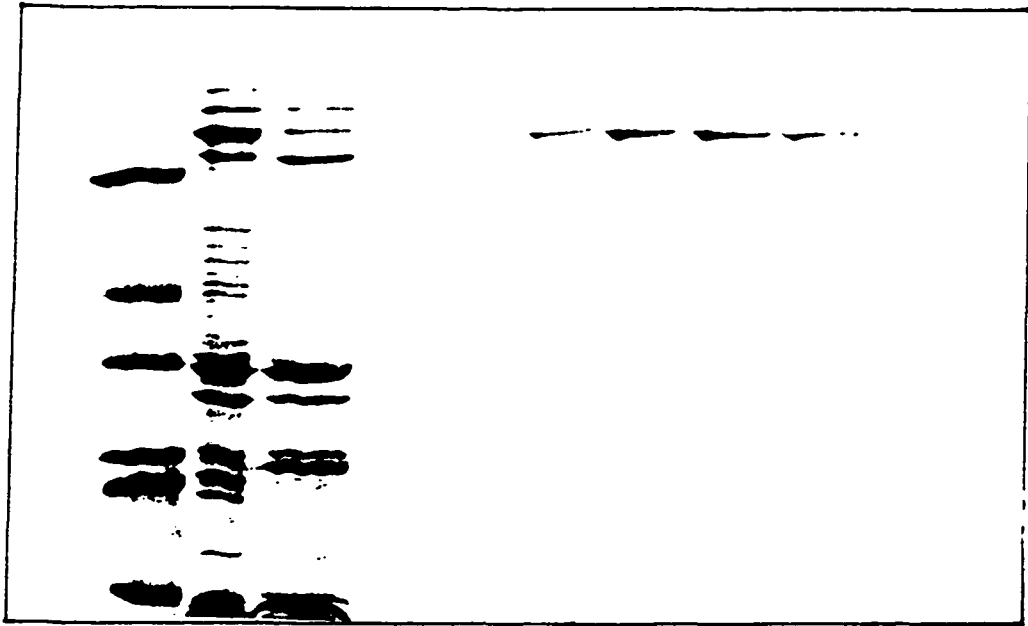


Figure 24. Purification of FepA using ColB-Sepharose affinity chromatography. SDS-PAGE is showing elution of adsorbed FepA-V16C from regenerated ColB-Sepharose column. The first lane contains M.W. markers [Bovine serum albumin (66 kD), Ovalbumin (45 kD), Glyceraldehyde-3-phosphate dehydrogenase (36 kD), Carbonic Anhydrase (29 kD) Trypinogen (24 kD), Trypsin inhibitor (20.1 kD), and α -Lactalbumin (14.2 kD)]; The second lane contains UT5600/pFepAV16C outer membrane preparation; The third land contains the wash effusion; The remaining lanes show the elution of the adsorbed FepA with a 0 to 2.5 M NaCl gradient.

disulfide reducing agent (DTT or β -mercaptoethanol) and partial unfolding in urea ($\geq 4\text{M}$) (Liu *et al.*, 1994). Similar results were obtained with MAL6, a less hydrophobic label. These results indicate that Cys-486 and Cys-493 are disulfide-linked and occupy a tightly folded region of the protein. Concentrations of urea less than 4 M led to incomplete labeling. In contrast, just like E280C and E310C, most of the Cys substitution mutants in FepA TonB-box domain were readily labeled without either reduction or denaturation, and consistently had labeling stoichiometries (spin label:FepA) of approximately 1:1. Labeling without DTT and urea thus allowed selective spin labeling of mutationally inserted Cys residues under circumstances in which the native cysteines were not modified. T13C was the only single Cys substitution in the TonB box that could not be labeled by MTSL in TTE without denaturation. This result indicates that this residue resides in an area of structure that is inaccessible to MTSL, perhaps from strong interactions with nearby amino acid side chains.

Table 4. Labeling stoichiometry and w/s ratio for MTSL-labeled TonB-box Cys mutants

Mutant	Spin label:FepA	b/a (in TTE)	b/a (in liposomes)
D12C	0.87	0.16	0.02
T13C	0.94	0.18	0.01
I14C	0.93	0.19	0.01
V15C	0.86	0.06	0.02
V16C	0.93	0.06	0.03
T17C	0.90	0.05	0.02
A18C	0.97	0.06	0.02
A19C	0.98	0.10	0.04
E20C	0.94	0.12	0.03
D12C/E20C	1.76	0.00	0.04

Each Cys single substitutions of FepA TonB-box mutants was reacted with MTSL to generate the nitroxide-FepA. ESR spectra of the labeled mutants are shown in Fig. 25-33. The line shapes of the spin-labeled mutants in TTE are complex and reflect at least two significant spin populations: one of high mobility (a) and the other more immobilized (b) with respect to the protein. These regions of the X band spectra are also called s and w, respectively, in some other publication. Since the protein contains only a single spin-labeled site, the populations must arise from different degrees of interaction of the nitroxide with the immediate environment in the protein. The a state is attributed to nitroxides interacting with nearby structure of the protein, while the b state arises from nitroxides projecting into solution, where the motion is limited primarily by rotational isomerization about the bonds which connect it to the backbone (Flitsch & Khorana, 1989; Altenbach *et al.*, 1989a, 1990; Farahbakhsh *et al.*, 1992, 1995; Perozo & Hubbell, 1993; Calciano *et al.*, 1993; Carreras *et al.*, 1994; Oh *et al.*, 1996).

To determine whether a particular spin-labeled site on a protein is buried or surface-exposed, spin labeled FepAs were reconstituted into liposomes (Nikaido & Rosenberg, 1983a, b). The ESR spectrum of each MTSL-labeled FepA mutant in liposomes are shown in Fig. 25-33. All the mutants appeared to contain two components in the low field region (Fig. 34). Unlike in TX100, the nitroxide side chains were fairly strongly immobilized for most of the MTSL-labeled mutants.

D12C in TTE, Liposomes, and Cells

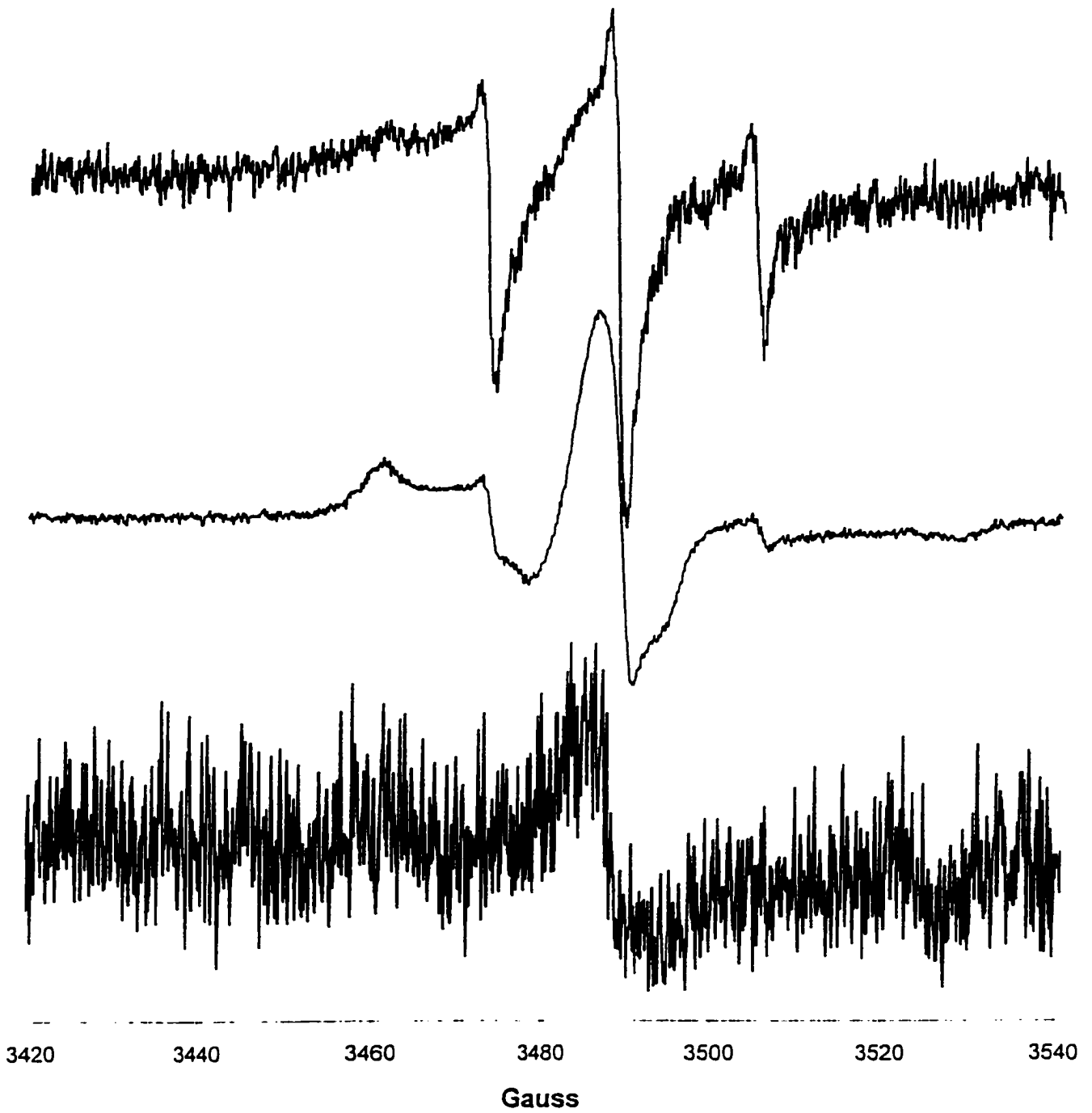


Figure 25. ESR spectra of D12C in TTE, liposomes, and live cells

T13C in TTE, Liposomes, and Cells

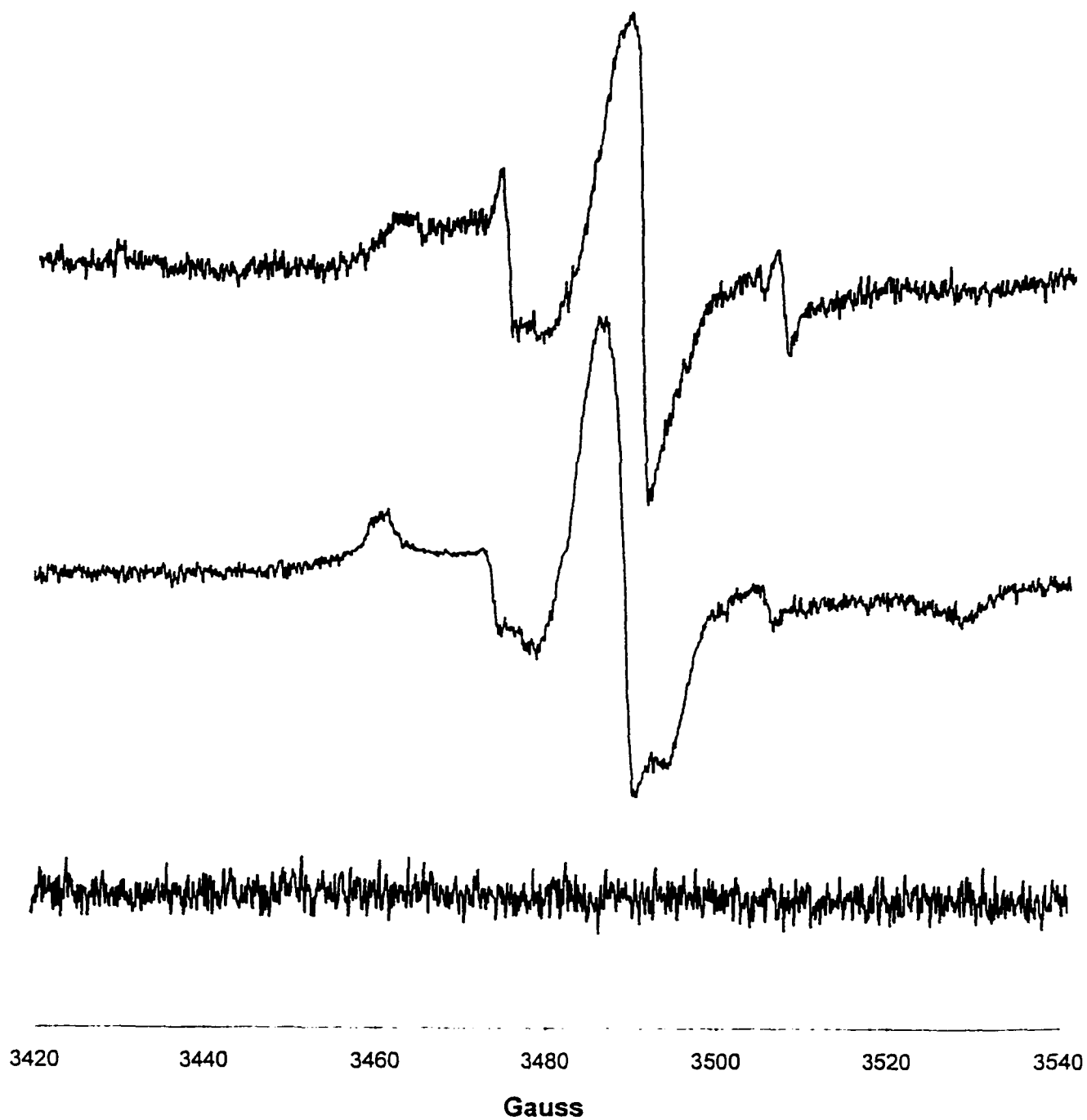


Figure 26. ESR spectra of T13C in TTE, liposomes, and live cells

I14C in TTE, Liposomes, and Cells

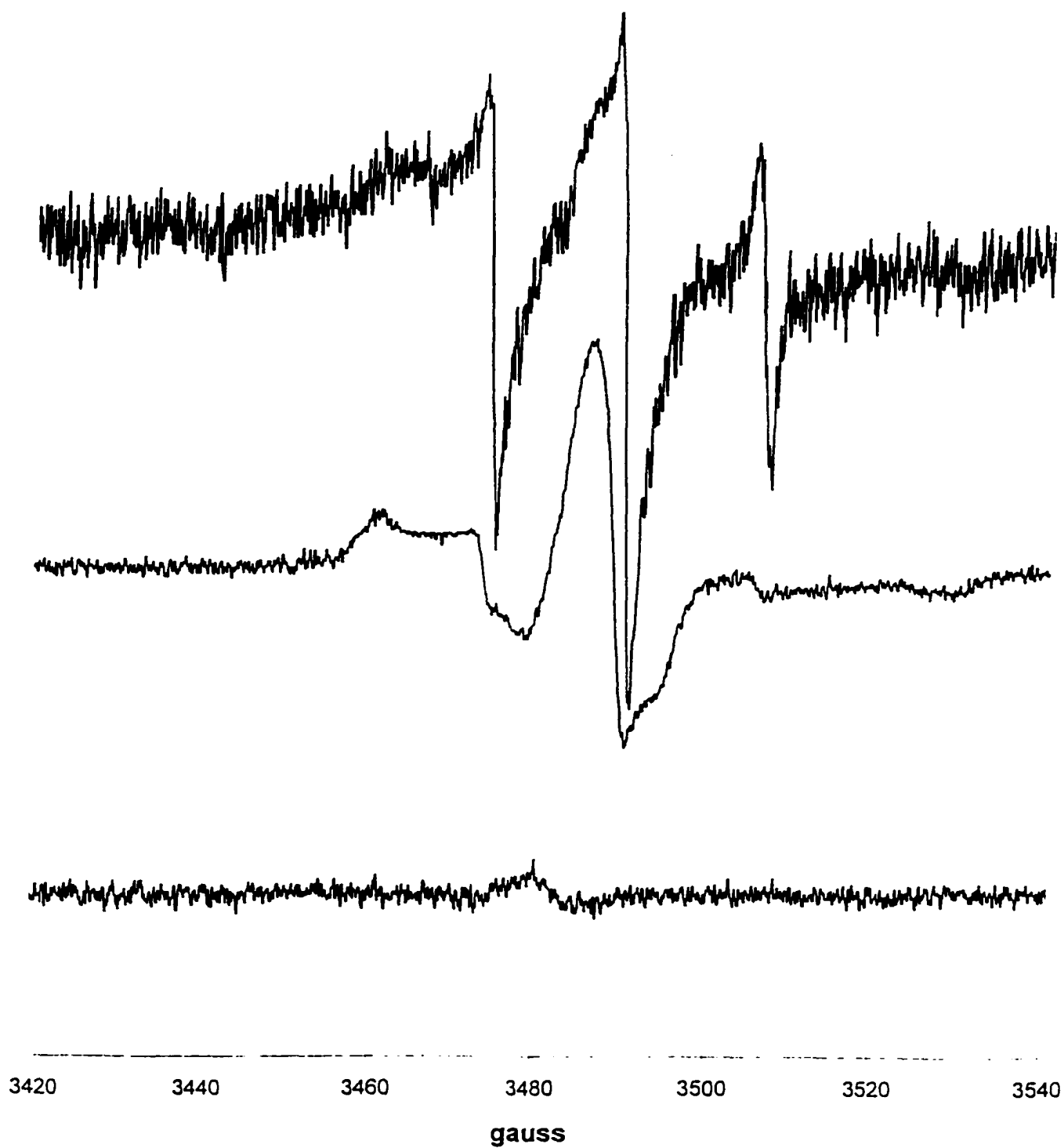


Figure 27. ESR spectra of I14C in TTE, liposomes, and live cells

V15C in TTE, Liposomes, and Cells

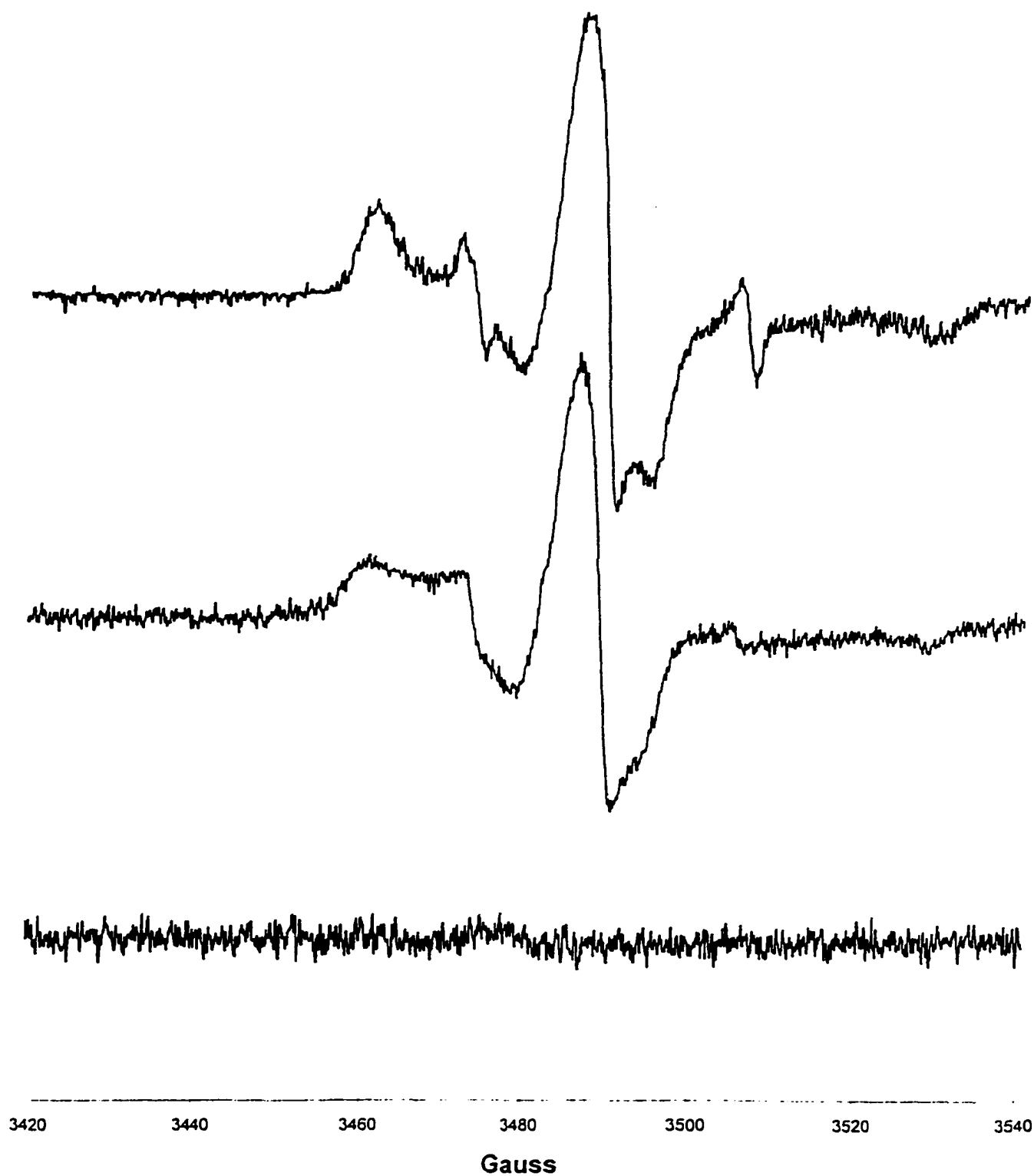


Figure 28. ESR spectra of V15C in TTE, liposomes, and live cells

V16C in TTE, Liposomes, and Cells

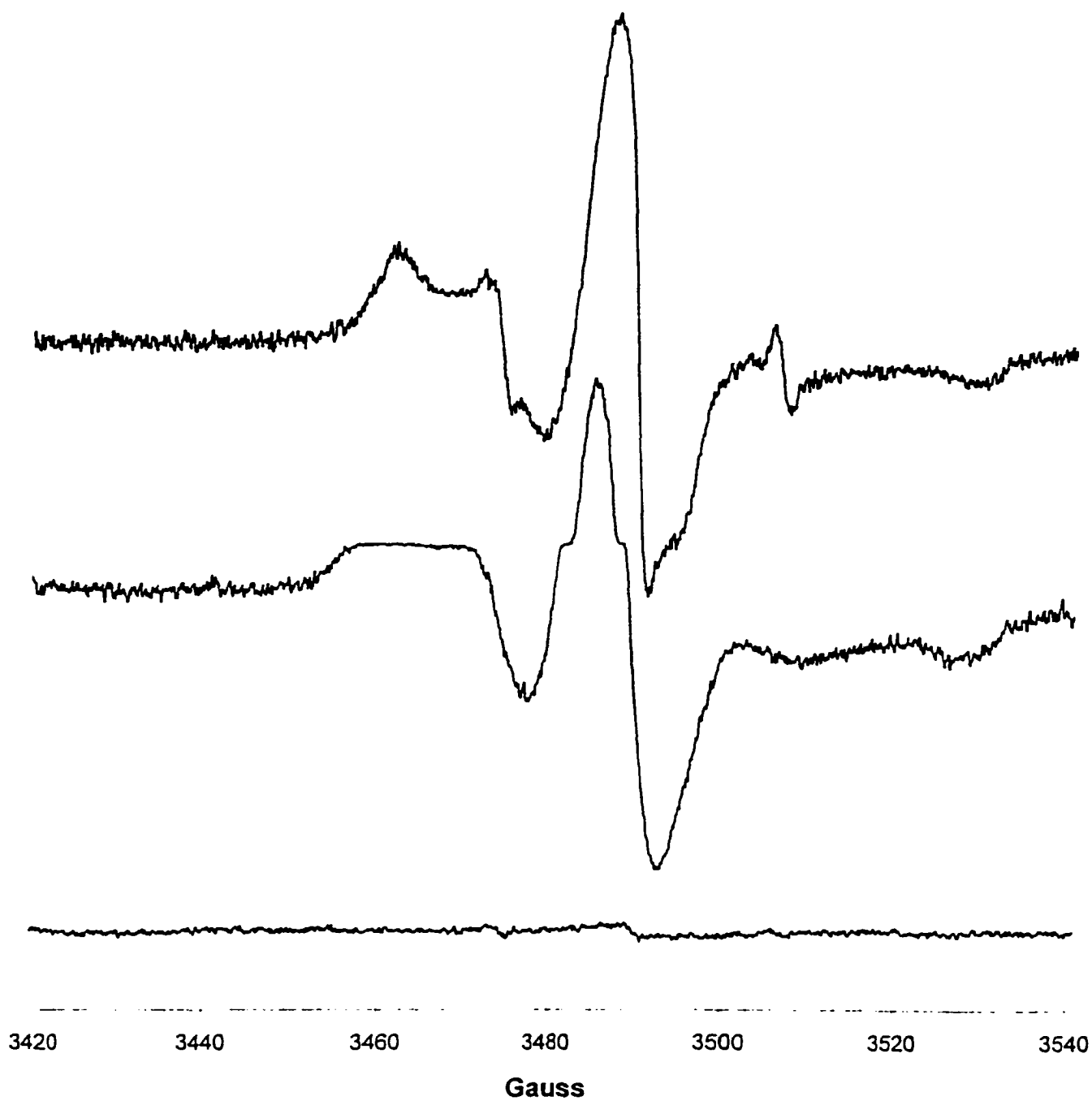


Figure 29. ESR spectra of V16C in TTE, liposomes, and live cells

T17C in TTE, Liposomes, and Cells

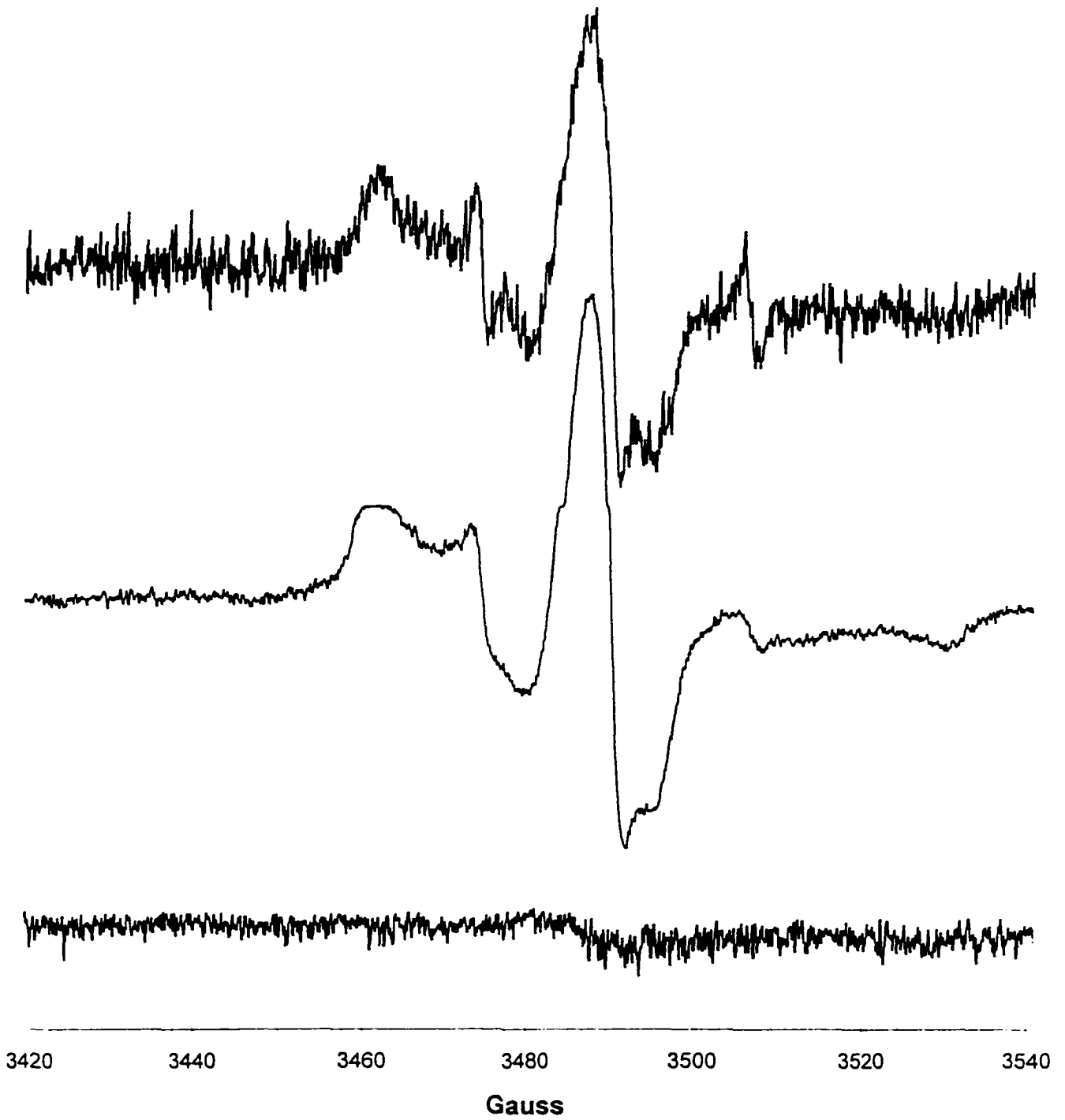


Figure 30. ESR spectra of T17C in TTE, liposomes, and live cells

A18C in TTE, Liposomes, and Cells

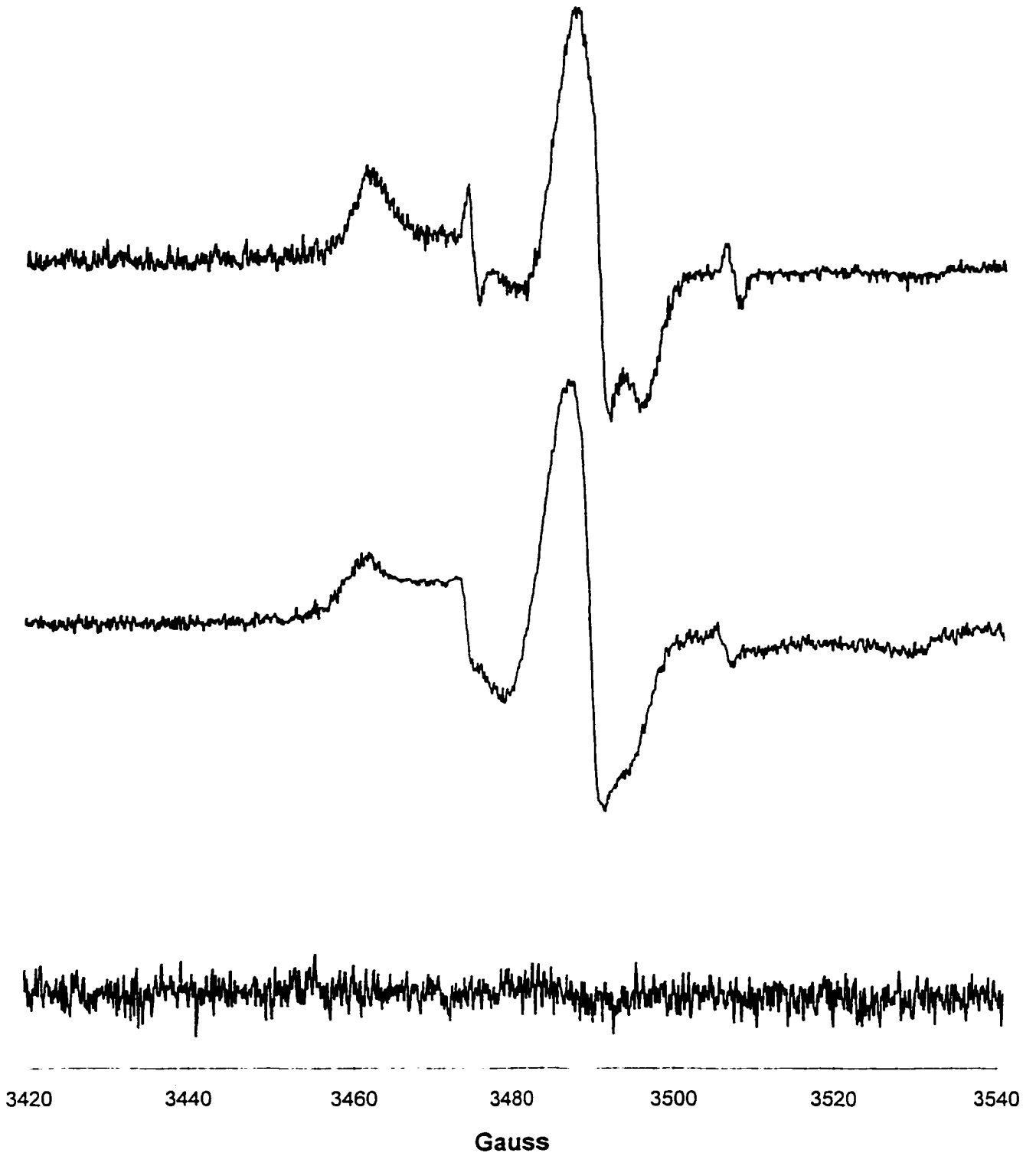


Figure 31. ESR spectra of A18C in TTE, liposomes, and live cells

A19C in TTE, Liposomes, and Cells

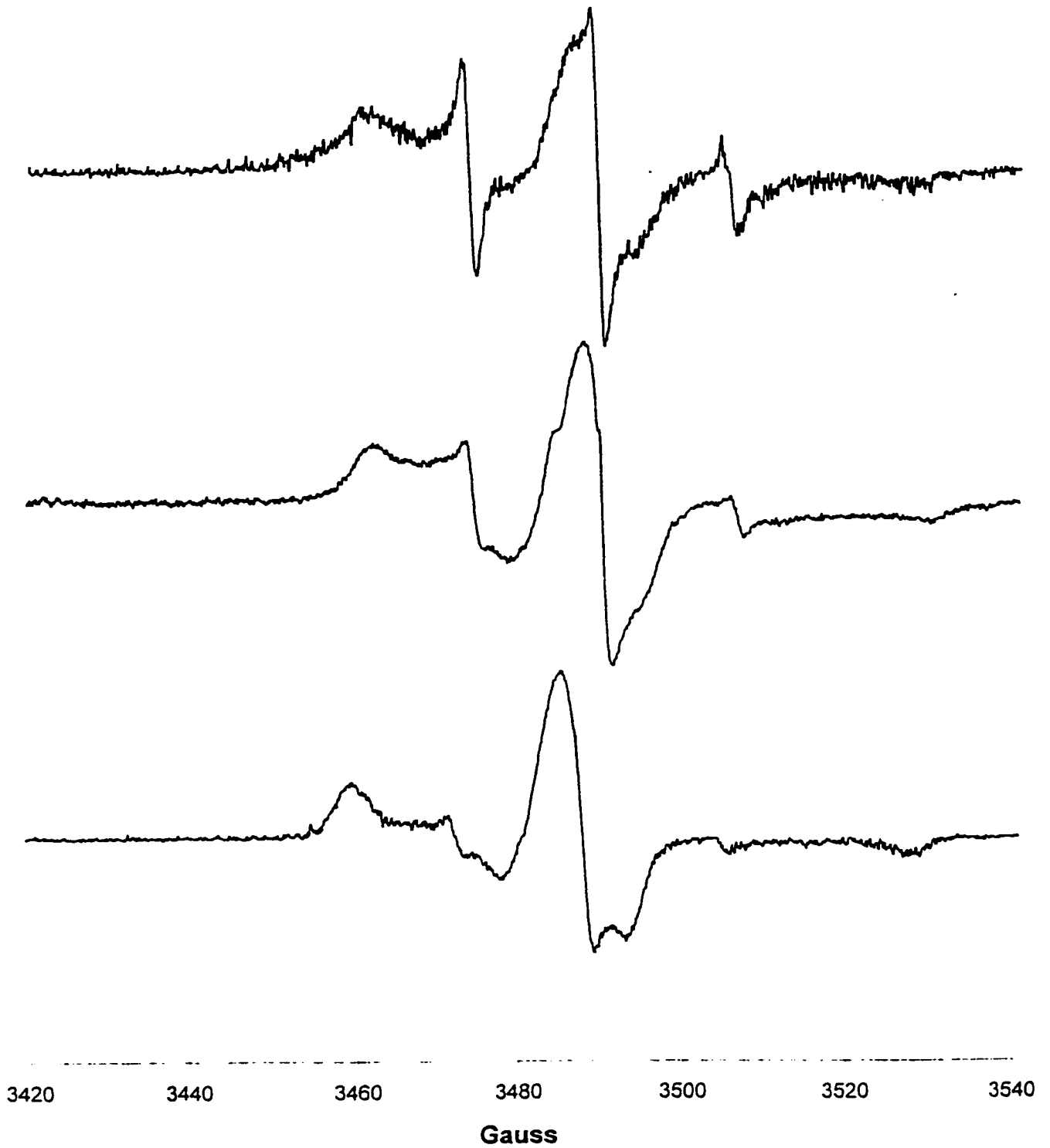


Figure 32. ESR spectra of A19C in TTE, liposomes, and live cells

E20C in TTE, Liposomes, and Cells

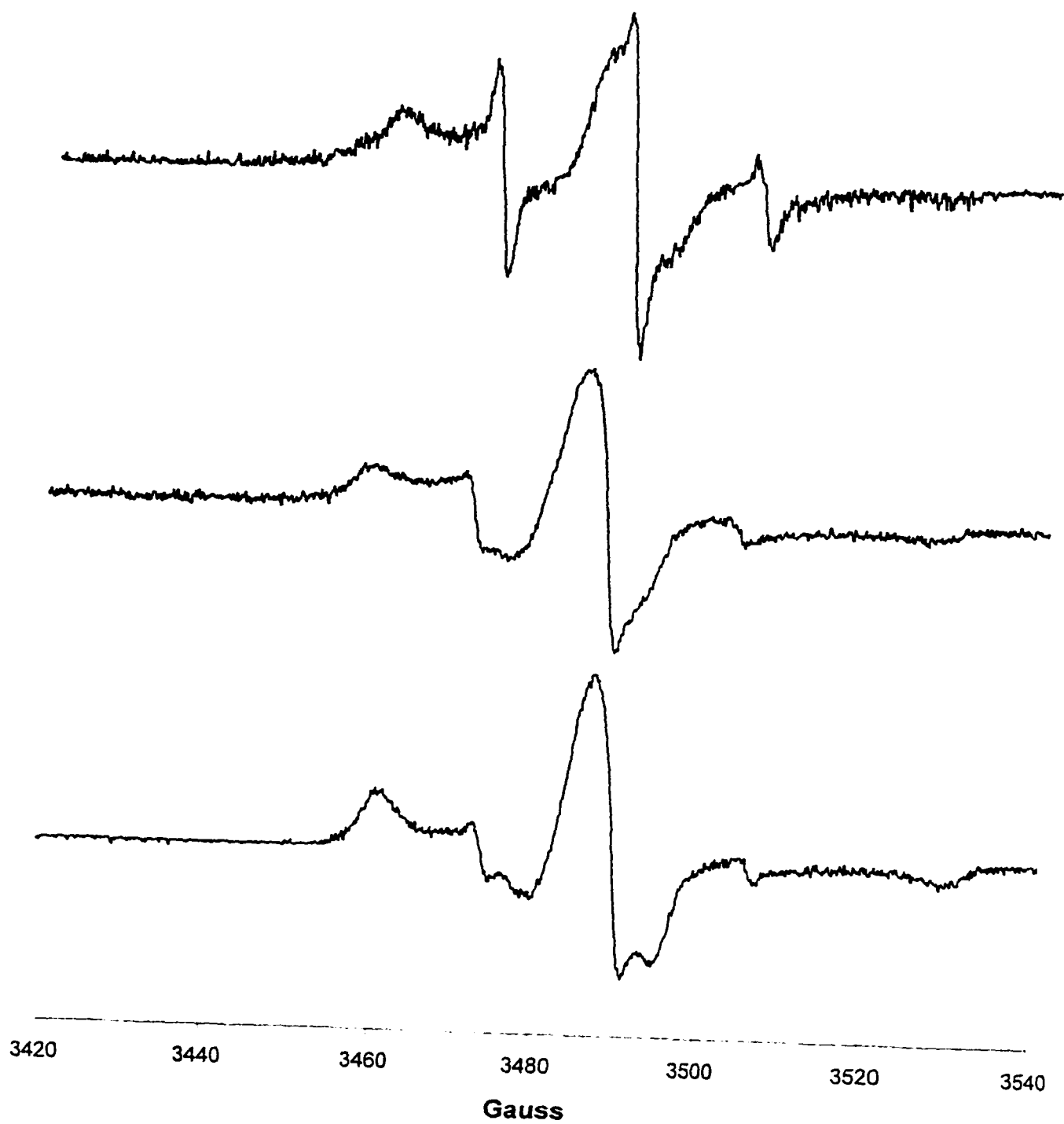


Figure 33. ESR spectra of E20C in TTE, liposomes, and live cells

ESR Spectra of MTSL-Labeled TonB-Box Mutants (in Liposomes)

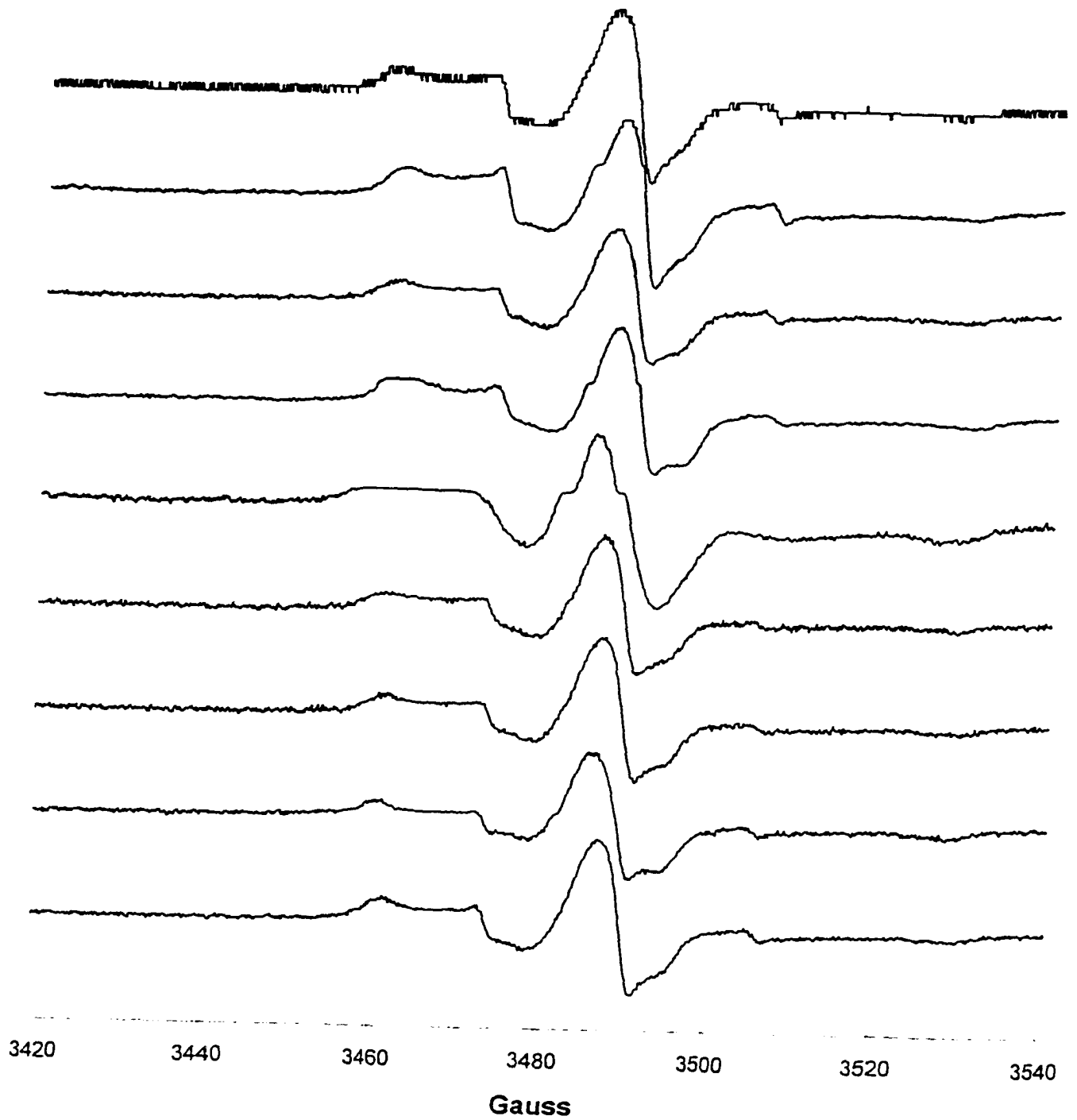


Figure 34. ESR spectra of spin-labeled TonB-box mutants in liposomes

Our *in vivo* SDSL experiments results also suggested that the majority of the residues in the TonB box domain were not localized on cell surface. KDF541 cells expressing derivatives of pITS449 (*fepA*⁺) carrying mutated *fepA* alleles were spin labeled (Fig. 25-33), while using KDF541/pITS449 and KDF541/pFepAE280C as controls. The ESR signal of these bacteria was very weak for the most part, suggesting the poor accessibility of the cysteine side chain to the nitroxide spin labeling probes. On the other hand, the ESR spectra of A19C and E20C exhibited remarkable intensity of spin labeling which suggested that these residues may locate on the external surface of the cells. To further confirm these results, *in vivo* SDSL experiments were carried out using cells harboring single cysteine mutants which are localized in lipid bilayer (Klug *et al.*, 1997). Spin labeling of all these cells was also very weak.

In addition to study protein structure and dynamics, site-directed spin labeling can also be used to measure distance in protein (Dalton *et al.*, 1987; Greenhalgh *et al.*, 1991; Jung *et al.*, 1995; Budker *et al.*, 1995; Rabenstein & Shin, 1995; Voss *et al.*, 1995). To test the feasibility of the nitroxide-nitroxide approach with respect to distance measurements in FepA, two cysteine residues were introduced into FepA TonB-box in place of D12 and E20. This mutant was purified, spin labeled, and studied by ESR.

D12C/E20C proteins were readily labeled and had labeling stoichiometries (spin label : FepA) of approximately 2:1. X-band ESR spectra of spin labeled D12C/E20C FepA are shown in Fig. 35. In TTE, significant dipolar interaction was observed for spin labels attached to D12C and E20C in TonB-box: linewidth

D12C/E20C in TTE, and Liposomes



Figure 35. ESR spectra of D12C/E20C in TTE and in liposomes

of $m_I = 0$ peak increased and hence its amplitude decreased, also the weakly immobilized peak disappeared due to the strong interspin interaction. Dipolar interactions between spin labels are reflected by the intensity ratio I/I_0 (I_0 and I stand for the amplitudes of the $m_I = 0$ resonance without and with interspin interaction respectively) (Pali *et al.*, 1992). The interspin distance between two spin labels was estimated from molecular modeling given by Voss *et al.* (1995). I/I_0 value of 0.72 for D12C/E20C corresponds to a distance about 16 Å between the unpaired electrons. No dipolar interaction was observed for the spin labeled D12C/E20C reconstituted into liposomes, indicating a separation greater than 35 Å.

Power Saturation Experiments

ESR power saturation experiments were performed on EMX X-band spectrometer equipped with a loop-gap resonator (LGR). The LGR consists a small cylinder made of ceramic that contains two cylindrical holes (loops) connected by a slot (gap). The feature of the resonator is that the electric flux of the microwave field is mainly concentrated within the slot, while the magnetic flux is concentrated within the holes portions of the structure. The magnetic flux density that the sample is exposed to in the LGR is greater than for an air filled cavity at the same operating frequency. “Lossy” samples such as aqueous solutions can then be readily studied. The use of loop-gap resonator technology

increases the sensitivity of ESR, facilitating the analysis samples with limited available material (Froncisz & Hyde, 1982).

To determine the topographical location of the spin-labeled site in the FepA, the accessibility of the nitroxide to collision with O₂ and chromium(III) oxalate (CROX) was investigated for each of the spin-labeled mutants (Altenbach *et al.*, 1989a, 1990). Spin exchange, resulting from the direct collision of a paramagnetic species with the nitroxide, was detected by ESR. By this method it is possible to determine whether a nitroxide at a particular site on a protein is within the membrane interior or in the aqueous phase, simply by measuring the exchange frequency in the presence of a lipid- or water-soluble paramagnetic exchange reagent.

Molecular oxygen O₂ is an outstanding choice for the probe because of its small size and finite solubility in all domains of the system. It is soluble in both the membrane interior and aqueous solutions, although it prefers hydrocarbon phases to water by about 10 to 1 in concentration. If a spin label on a protein does not collide and spin exchange with O₂, it is safe to conclude that it is buried in a compact domain (Subczynski & Hyde, 1981; Popp & Hyde, 1981; Altenbach *et al.*, 1989a, 1990).

Chromium oxalate (CROX) is an ideal choice for a water-soluble exchange reagent. CROX is highly insoluble in the membrane interior and restricted to the aqueous phase (Altenbach *et al.*, 1989a, 1990). Spin exchange can only occur if the spin label on a protein located in a water-exposed region of

the protein. No collisions with CROX would be observed for a spin label located in the protein or membrane interior. CROX is a negatively charged ion at physiological pH. It has a bulky molecular volume and is strongly affected by steric constraints in the local environment around the nitroxide.

Relative collision frequencies of a nitroxide spin label with a fast relaxing paramagnetic spin probe like O₂ or CROX are estimated through changes in the nitroxide electron spin-lattice relaxation time, T₁. Continuous wave (CW) power saturation ESR is used to determine changes in T₁. The experimental quantity measured in the saturation experiments is P_{1/2}, the power at which the ESR signal amplitude of the central line is 50 percent of that corresponding to no saturation. The difference between P_{1/2} in the presence and absence of a relaxing agent is called ΔP_{1/2} and is proportional to the collision frequency of the nitroxide with the corresponding reagent.

The loop-gap resonator technology greatly facilitated the determination of power saturation effects: First, very high values of the microwave magnetic field component can be attained at the sample by using a gunn diode microwave generator without amplification. This permits the study of relatively short relaxation times with simple instrumentation. Second, the microwave magnetic field is very homogeneous over the sample volume, greatly simplifying the analysis (Froncisz & Hyde, 1982).

In the experiments below, we applied CROX, O₂, and the CW power saturation approach to investigate the locations of spin labels attached to TonB

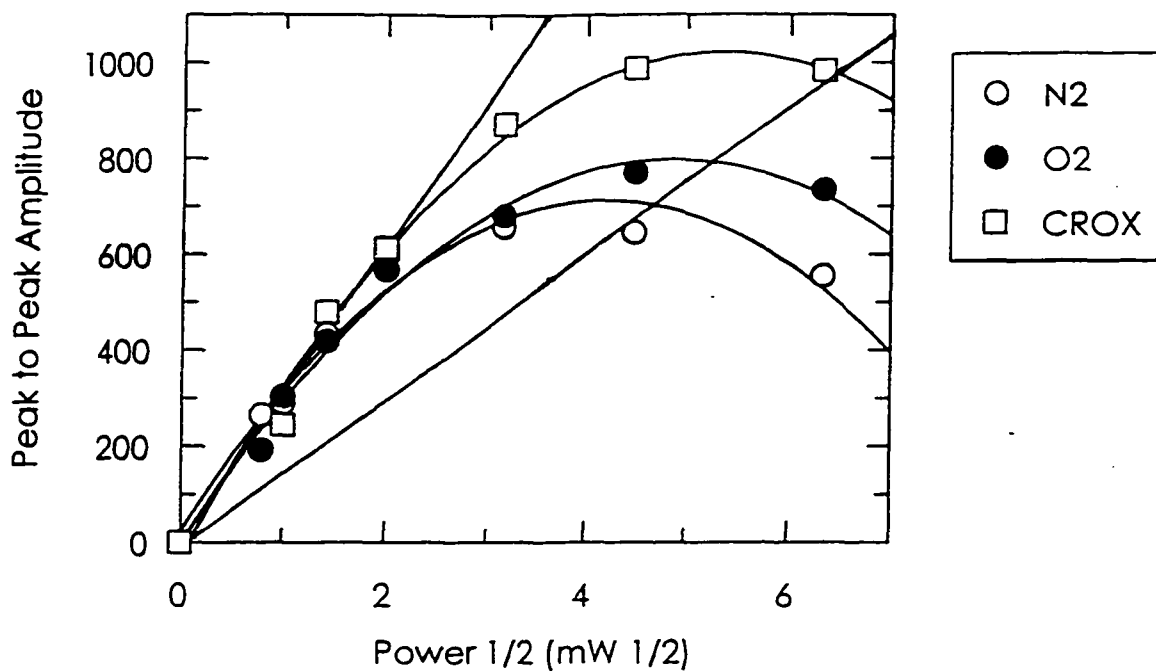


Figure 36. Continuous wave power saturation curves. The peak-to-peak amplitude of the first derivative ESR signal of the center line in arbitrary units is plotted against the square root of the incident microwave power. The straight line which has half of the initial slope of the experimental curves intersects each curve at a value corresponding to the square root of $P_{1/2}$.

box Cys mutants. An example of the effect of 20% O₂ and CROX on the CW saturation curve is shown in Fig. 36. Interaction of the protein-bound spin label with O₂ or CROX makes saturation more difficult to achieve, shifting the curve (and P_{1/2}) to higher powers.

The results obtained from the power saturation experiments are summarized in Table. 5.

Table 5. $\Delta P_{1/2}$ Parameters for MTSL-labeled FepA cysteine mutants in liposomes.

Mutant	$\Delta P_{1/2}$ (20% O₂) (mW)	$\Delta P_{1/2}$ (CROX) (mW)
E280C	1.66	4.57
D12C	1.11	2.95
T13C	1.17	0.25
I14C	0.58	1.82
V15C	2.10	0.80
V16C	0.69	2.72
T17C	1.67	0.87
A18C	0.50	2.44
A19C	0.32	0.94
E20C	0.72	2.81

The variation in both O₂ and CROX accessibilities with label positions from D12C to A18C shows a biphasic periodicity (Fig. 37). For the even-numbered residues, D12C, I14C, V16C, and A18C, the attached MTSL is more accessible to CROX than to O₂, strongly indicating an aqueous environment which would be expected for a location at the inside base of the aqueous channel. For the odd-numbered residues, T13C, V15C, and T17C, the attached MTSL side chain has a higher accessibility to O₂ than to CROX, indicative of the exposure to

The Chromium Oxalate and Oxygen Accessibility of the Nitroxide Side Chains on MTSL-labeled FepA TonB-Box Mutants

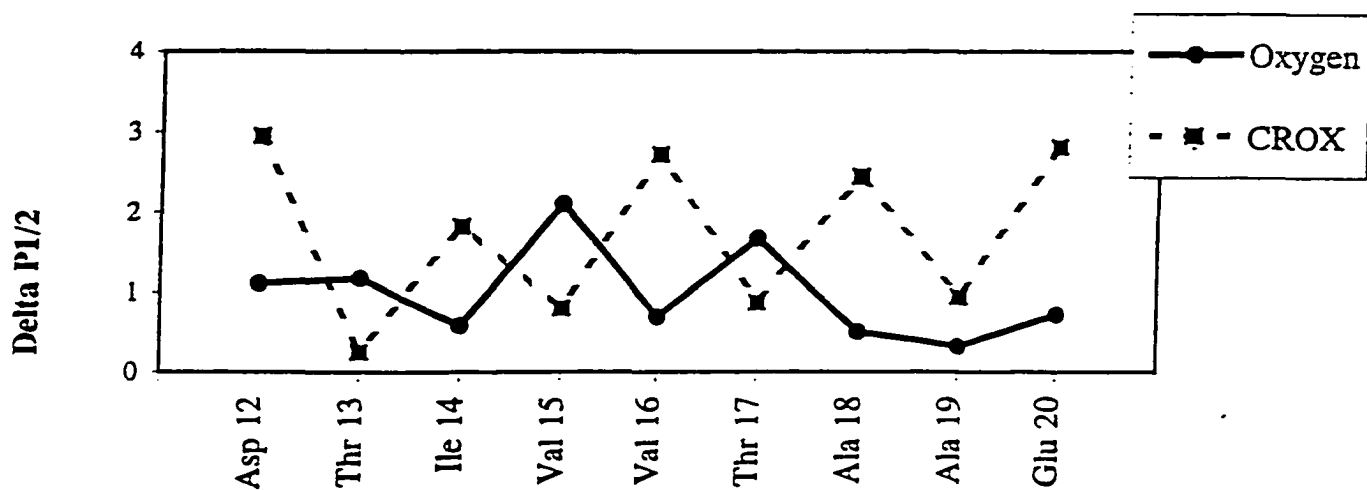


Figure 37. The CROX and O₂ accessibility of the nitroxide side chains on MTSL-labeled FepA TonB-Box mutants.

hydrophobic alkyl chains of lipid bilayer. MTSL attached at E20C shows much more strong interaction with CROX than with O₂, indicating an aqueous surrounding. However, nitroxide side chain of MTSL attached at A19C shows low exposure to both of the relaxation reagents, with more interaction with CROX than with O₂. This restriction is likely due to structure interactions with surface loop.

Chapter IV

Discussion

Part I. ESR Analysis of Conformational Changes of FepA *in vivo*

The Gram-negative bacterial outer membrane is an asymmetric bilayer. The outer leaflet of the OM contacts the external environment. It protects cells from various noxious agents of hostile environment. It also acts as a molecular sieve to allow the passage of nutrients and small molecules. Nutrients interact with OM proteins during the initial stages of transport. FepA is a ligand-specific, high-affinity receptor for ferric enterobactin, that has been postulated as a gated channel (Rutz *et al.*, 1992). Ferric enterobactin binds to the outside of this closed channel in part by ionic interaction (Newton *et al.*, 1997), before it subsequently passes through. So, conformational changes in FepA surface loops are a fundamental part of its suspected transport mechanism.

To investigate the possibility of conformational changes during transport, we reacted nitroxide spin labels with a genetically engineered cysteine, E280C, which resided in a known ligand-binding surface loop (PL5) of FepA. Electron spin resonance (ESR) spectroscopy was used to analyze the labeling bacteria during the transport.

Quartz flat cells were used in our *in vivo* ESR experiments. Our ESR samples contained water. Because of its large dielectric constant, water is highly “lossy”. A large amount of microwave energy is absorbed by water-containing samples, reducing resonator Q value (quality factor) and observed resonator performance. Lossiness is due to the strong interaction of the electric component of the microwave field with the strong dipole of the water molecule. Quartz cells were used because quartz has a high dielectric constant (~3.8), and a low level of paramagnetic impurities that are found in abundance in other glasses. The plane of the flat cell is placed traverse to the length of the cavity so as to locate the whole of the sample in a region of minimum electric field and maximum magnetic field, thus minimizing dielectric absorption and maximizing magnetic absorption.

ESR is used to detect unpaired electrons. The introduction of a stable nitroxide free radical creates a molecular probe that conveys information about its site of attachment. Site-directed spin labeling has been highly successful in providing dynamic and structural information about membrane proteins (Butterfield *et al.*, 1976; Beth *et al.*, 1984; Altenbach *et al.*, 1989a, 1990, 1996; Anthony-Cahill *et al.*, 1992; Millhauser, 1992; Calciano *et al.*, 1993; Miich *et*

al., 1993; Budker *et al.*, 1995; Barranger-Mathys & Cafiso, 1996). Prior SDSL results with purified FepAE280C in detergent or liposomes suggested that FepA could be accessible to chemical modification and analysis *in vivo*. Two findings confirmed that E280C in PL5 was labeled in bacteria by MAL6 or MTSL: First, Bacteria harboring *pfepAE280C* were labeled 30-fold more than the *fepA* host strain KDF541 (*fepA*) or KDF541 expressing the wild-type *fepA*; Second, lysates of KDF541, KDF541/pITS449, and KDF541/E280C cells, previously labeled with MAL6, had been reacted with anti-MAL6 polyclonal serum in western blot. The specificity of the covalent modification was apparent in western blot which indicated nitroxide labels were attached to the engineered Cys residue at residue 280 of FepA PL5 on the surface of bacteria.

At 4°C, the *in vivo* ESR spectra of MTSL at E280C of FepA reproduced its *in vitro* spectra (Liu *et al.*, 1994; Klug *et al.*, 1995, 1997) with the majority of its spins strongly immobilized and a small percentage (3%, peak b in Fig. 14) weakly immobilized. At 37°C, however, a significant proportion of the spin label population (16% in Fig. 14E) of the *in vivo* spectrum was shifted to the weakly immobilized state (Fig. 14, 17). The effects of ferric enterobactin on FepA *in vivo* were distinct from those previously observed *in vitro*: the binding of the siderophore *in vitro* induced a slight immobilization of MTSL at E280C (Liu *et al.*, 1994). This binding stage is TonB- and energy-independent because it occurs in purified FepA.

In order to rule out the possibility that the mobilization of spins *in vivo* was caused by chemical release of MTSL from FepA by ferric enterobactin in the process of experiment, another experiment was carried out and the results refuted this possibility: First, by recooling of the sample to 4°C, the strongly immobilized spins attached to E280C were regenerated in the presence of saturating ferric enterobactin (Fig. 14F); Second, double integration of the X-band spectra showed that spin labels were neither destroyed nor lost during the experiment (Fig. 14, 17).

The effect of ferric enterobactin on the mobility of MTSL attached to FepAE280C in live bacteria at 37°C was showed in Fig 14. This result suggested that during ferric enterobactin transport into living bacteria, PL5 underwent energy-dependent structural changes that relocated PL5, the loop Cys280 resides, away from globular protein structure into the aqueous milieu. These structural changes are distinct from the conformational changes caused by the binding of siderophore on FepA which decreased the weakly immobilized component of ESR spectra and further immobilized the strongly immobilized component. Binding of FeEnt induced a change in FepA structure to a more highly ordered environment in the regions of the bound labels (Liu *et al*, 1994). Our *in vivo* results suggest that after siderophore binding, ferric enterobactin triggered the conformational changes in FepA and project the PL5 into the aqueous milieu.

FepA is also a receptor protein for colicin B (Guterman, 1971; Pugsley & Reeves, 1976; Timmis, 1981; Mende & Braun, 1989). Our experimental data

showed that binding of colicin B to FepA had a little effect on the mobility of MTSL at E280C. Continual incubation of the cells in saturating colicin B (10 μ M) at 4°C did not change the mobility of MTSL at E280C, even over the course of 1 hour. The transport of colicin B, subsequent to binding, is more complicate. The addition of saturating colicin B at 37°C progressively eliminated weakly immobilized spins, enhanced the strongly immobilized peak, and increased the separation between low- and high-field extrema (Fig 15, 17). These results suggested that after the energy-independent stage of binding, colicin B engendered progressive immobilization of MTSL mobility during its transport. The effects of colicin B were opposite to those engendered by the siderophore. Significant proportion of the spin-label population progressively shifted to the strongly immobilization state over 30 min when cells with bound colicin were warmed to 37°C. This result supports the notion that the colicin threads through the surface loops of FepA and into its underlying channel domain, in the process of restricting nitroxide motion by direct contact with the toxin polypeptide. This conversion caused by colicin is irreversible. The irreversibility of the immobilization during recooling supports the idea that the toxin polypeptide remains bound within FepA subsequent to OM transport. And the different steric constraints placed on the spin-labeled site during uptake of colicin B and ferric enterobactin suggested different transport mechanism of FepA for these two structurally diverse ligands.

The intensity of the weakly immobilized peak (at 3472 G) was monitored versus time. The time course ESR results showed that ferric enterobactin stimulated a burst of MTSL motion that peaked and receded over a 5-min period. Two peaks of spin label mobility were observed in about 10 and 20 min after the temperature shift to 37°C. These surges represented the sum of individual, weakly immobilized MTSL spins in the bacterial sample during the uptake. In both peaks, a sigmoidal rise to a maximum is followed by an approximately symmetrical decay to a minimum. The first surge in spin label motion peaked in 140 s and decayed in 140 s. The changing mobility of the MTSL spins in PL5 very likely reflects the opening and closing of the gated FepA channel during siderophore uptake. The integrated areas beneath the two curves were the same, suggesting that the changes in motion arose from an initial, relatively synchronous transport cycle and a second, less synchronous cycle in the same number of cells. In these experiments, ferric enterobactin was supplied in excess, the decrease in motion did not result from its depletion. Thus, the time-resolved fluctuations in PL5 were consistent with an active opening and closing of the channel during the ferric enterobactin transport reaction.

The mobility of MTSL spins attached to E280C induced by both ligands showed conformational changes in FepAE280C are TonB- and energy-dependent. No effects were observed under the conditions of glucose deprivation, low temperatures (4°C), and use of a *tonB* strain (Fig. 18). Experiments using MTSL-

labeled E280C FepA reconstituted in liposomes with colicin B could not induce these effects either (Fig. 16).

In summary, two different kinds of conformational dynamic were observed during FeEnt transport and colicin entry. During the internalization of FeEnt, the conformation of PL5 is more flexible, so the mobility of MTSL attached to FepAE280C in live bacteria increases, probably because of the decreasing contact of spins with nearby amino acid side chains. The internalization of colicin B, on the other hand, immobilizes PL5 by increasing their contact with colicin B or FepA peptide. Our ESR data suggest a prototypic mechanism of how bacterial ligand-gated channels function: After recognition and binding of FeEnt on FepA at least in part through ionic bonds, TonB triggers energy-dependent structural changes in the ligand-binding site that displace PL5 and release the bound siderophore into the underlying FepA channel. These results demonstrate, for the first time, that gated-porin channels open and close during solute transport *in vivo*.

Spin labeled bacteria harboring *pfepAE310C* were also studied by the same method. Because E310C lies close to FepA's ligand binding site at the exterior of the FepA channel, the changes of their w/s ratio during transport also demonstrates a displacement of PL5 that regulates ligand entry into the pore. The results showed that internalization of FeEnt and colicin B affects the mobility of MTSL attached to FepAE310C in live bacteria. The effects of FeEnt and colicin B to relocate spin labels attached to FepAE310C are very similar to their effects to

spin labels attached to FepAE280C in live bacteria. And the remarkable burst of spin label motion accompanying the internalization further confirmed what has been widely hypothesized before and proved by previous experiments with FepAE280C : TonB-dependent gated porins open and close during solute uptake. The TonB- and energy-dependence of the conformational changes show that this loop movement in the OM is also energized by the IM.

The opening and closing of FepA is comparable to other types of gated channels. As mentioned before, the lipid bilayer of biological membranes is intrinsically impermeable to ions and polar molecules. The flow of ions and molecules across biological membranes is controlled by transmembrane proteins. Voltage-gated channels like the sodium channel and the potassium channel mediate action potentials in nerve axon membranes. The transition between the closed and open form is allosterically regulated by voltage. The acetylcholine receptor channel, which mediates synaptic transmission is the best-understood ligand-gated channel. The binding of two acetylcholines opens a channel. The rapid lowering of the acetylcholine concentration in the synaptic cleft by the hydrolytic action of acetylcholinesterase leads to channel closure. A nerve impulse is an electrical signal produced by the flow of ions across the plasma membrane of a neuron. The opening and close of the channel is within about a millisecond. According to our experiments, the opening and closing of ligand-gated iron channel is much slower. The changes in spin label motion peaked and receded in about 5 minutes, a duration of the same order of magnitude as

experimentally measured $^{59}\text{FeEnt}$ turnover number of 1 molecule/FepA monomer/minute. However, the graphic similarity between FepA and acetylcholine receptor channel suggests that the ligand-gated channels like FepA of bacteria are precursors to the more sophisticated, faster channels of higher organisms.

In detergents, liposome, and living bacteria, amino acid E280C resides on the membrane surface, restricted by other element of protein structure. This environment contrasts with the weak spin label immobilization observed during siderophore transport that reflects the relocation of the nitroxide into a more aqueous environment. This conclusion was evaluated by spin label relaximetry. Spin-labeled bacteria harboring *pfepAE280C* were analyzed during siderophore transport in the presence of the hydrophilic spin probe CROX, which diminished the ESR signal because it collided with the nitroxide in the aqueous milieu. This spin label-spin probe relaxation experiment is an important addition to the understanding of the transport reaction, because it confirms by an independent ESR methodology the change in the environment of MTSL at E280C to aqueous, that was inferred from changes in spin label motion.

Our results also suggest that the opening and closing of this TonB-dependent gated porin is a temperature-dependent process. At low temperature, FepA recognizes FeEnt, in part through ionic bonds. The binding reaction between FeEnt and FepA occurs in two or more distinct stages. Low temperatures prevent the effects of FeEnt to relocate spin labels attached to E280C. At 30°C,

the opening and closing of gated FepA channels are slower than at 37°C. This is quite reasonable because at lower temperature, all of the thousands of chemical reactions taking place in cells which are regulated and designed to serve a specific function will be slower. Cells require less ferric ions, so they may regulate the influx of FeEnt to avoid excess by slowing down the opening and closing of FepA channels. This, on the other hand, proves that organisms can economically regulate its biochemical pathways and adjust themselves to a significant change occurs in the environment. Our results also indicates that the gated FepA channels stay at open state and do not close at 42°C. It may indicate bacteria need more ferric ions for their higher metabolic activities at higher temperature. As we all know, an adequate iron supply is critical for many bacterial pathogens to survive in mammalian hosts. FepA is an important iron uptake pathway for these pathogenic species. The molecular understanding of the behavior of FepA at different temperature may be very important to efforts against bacterial pathogenesis and requires further study.

Part II. Location of the TonB-box domain of FepA

All Gram-negative bacteria obtain iron with TonB-dependent systems. TonB-dependent transport systems are high affinity, energy-dependent, multi-protein, multifunctional receptor complexes. Some of their components are unique to specific uptake systems (OM receptors), and some are common to all systems (TonB, ExbB, ExbD). It has been proved that ferric enterobactin

receptor, FepA, is a TonB-dependent gated-porin. Using site-directed substitution mutagenesis, the ligand binding sites in FepA were precisely located (Newton *et al.*, 1997). The time-resolved operation of FepA was observed *in vivo* with electron spin resonance spectroscopy by monitoring the mobility of covalently bound nitroxide spin labels (Jiang *et al.*, 1997). A ligand-binding surface loop of FepA, which normally closes its transmembrane channel, exhibited energy-dependent structural changes during iron and toxin (colicin) transport. These changes were not merely associated with ligand binding, but occurred during ligand uptake through the outer membrane bilayer. The results demonstrate by a physical method that gated-porin channels open and close during membrane transport *in vivo* (Jiang *et al.*, 1997).

FepA, the ferric enterobactin receptor, is prototypic of TonB-dependent siderophore receptor. The initial model of FepA structure was used to predict other TonB-dependent receptor protein structures. In this model, the TonB-box domain of FepA forms the first transmembrane strand of FepA. However, evidence exists that this TonB-box region directly contact with TonB in the periplasm (Tuckman, 1992).

In this study, the localization of the TonB-box domain of FepA was determined. Prior research elucidated the motional parameters and accessibility of nitroxide spin labels in a ligand binding surface loop, PL5, by ESR spectroscopy. Here, we extended SDSL to the FepA TonB-box domain to localize a region of FepA that may contact TonB. We generated single Cys

substitutions within or around the TonB-box of FepA, DTIVVTAAE, at nine sequential sites. These nine mutant proteins that introduce Cys at positions 12-20 were purified, spin-labeled, reconstituted into liposomes, and analyzed by conventional ESR and spin label relaximetry to access their localization in a membrane or aqueous environment.

The phenotypic analysis of these TonB-box Cys single substitution mutants suggested that these nine single Cys substitutions in FepA did not destroy the interaction between the mutant receptors and TonB. They were still functional to transport ferric enterobactin, as well as colicin B, even though they did not function as well as wild-type FepA, E280C, or E310C which have wild-type TonB box. These results indicated these mutations did not have significant effects on FepA conformation. The smaller growth halos and the less sensitivity to colicin B may result from the regional perturbation introduced by Cys mutation. These regional perturbations may alter the protein conformation and impair the ligand binding and transport.

No growth halo and no colicin killing was observed for double mutation, D12C/E20C, on the other hand, suggested the combination of these two substitution may either block the interaction between TonB-box and TonB, or cause the perturbation in globular protein structure of FepA and prevent this FepA mutant from functioning.

The nine engineered receptors were purified by ColB-Sepharose affinity chromatography, and spin labeled with MTSL. Site-directed spin labeling (SDSL) was used to localize the position of FepA TonB-box domain.

To date, SDSL has relied primarily on site-directed mutagenesis to substitute cysteine for the native amino acid at the selective site. The reactive sulfhydryl group is then modified with a sulfhydryl-specific nitroxide spin label. Of all the available spin label probes, MTSL has been extensively utilized because of its specificity, high reactivity, and relatively small molar volume of the group added to the cysteine side chain (Gaffney, 1976; Poole, 1983; Cornish *et al.*, 1994). The introduction of a spin-label side chain in a protein may introduce a local perturbation in structure. However, because SDSL is used to explore secondary structure and topology of the protein backbone, perturbations of side chain positions and minor backbone rearrangement are acceptable. Most spin labels are hydrophobic, they have overall hydrophobicities similar to the valine side chain. However, the nitroxide can participate in hydrogen binding within the protein. Thus the nitroxide is a reasonable compromise for the substitution as well as polar residues. The nitroxide group is not too big. With a molar volume of only about 25% larger than a tryptophan side chain, nitroxide is not expected to be an intolerable steric load (Hyde *et al.*, 1979, 1990; Hubbell & Altenbach, 1994a, b).

The ESR spectrum of each MTSL-labeled FepA mutant in liposomes (Figs. 25-33) shows that nitroxide side chain is fairly strongly immobilized for

each of the MTSL-labeled mutants. All the spectra contain indications of more than one spectral component, reflecting the ability of the side chain to adopt various conformations relative to the protein backbone. These conformations may vary according to site, as defined by interactions with closely neighboring side chains.

Our *in vitro* and *in vivo* SDSL experiment results indicated that most of the FepA TonB-box residues are buried in the bilayer interior phase as postulated by the proposed model of FepA. The data show that the TonB box of FepA does not reside on the inner surface of the OM bilayer, and suggest the proposed physical interaction between FepA in the OM and TonB anchored in the IM may not exist.

Gram-negative bacteria obtain iron with TonB-dependent systems. The mechanism by which TonB catalyzes the movement of ligands through siderophore receptors remains unknown. TonB may transform proton motive force into mechanical or chemical action that changes the conformation of siderophore receptors in the OM, but this has not been demonstrated. According to our results, TonB-box residues do not reside on the inner surface of the OM bilayer, but rather, exist in the OM bilayer. These data suggest that if an interaction occurs between TonB and TonB-box of FepA, then it takes place in the OM bilayer. Knowledge of cell envelope structure and properties has raised conceptual objections to the ability of TonB, an inner membrane-anchored protein to reach across the periplasmic space and physically contact multiple outer

membrane proteins. There are as many as eight (Fiu, FepA, FecA, FhuE, TonA, Cir, IutA, BtuB) TonB-dependent OM receptors. The maximum level of TonB expression maybe as high as 3000 copies/cell., the ratio of receptors/TonB in an iron-deficient environment is at least 10/1 (Klebba *et al.*, 1993). It is very difficult to believe that TonB can rapidly identify siderophore receptors and directly interact with individual receptors to promote OM transport.

Site-directed spin labeling is a powerful tool for studying protein structure and dynamics. It also provides an opportunity to measure distances upon addition of a second paramagnetic center (Greenhalgh *et al.*, 1991; Pali *et al.*, 1992; Raitsimring *et al.*, 1992). Introduction of two nitroxides into the protein and analysis of the static dipolar interaction is an approach for distance determination. A pair of nitroxides was introduced into D12C/E20C FepA protein. By analyzing the spectrum of MTSL-labeled D12C/E20C, the distance between nitroxides at D12 and E20 is calculated in the order of 16 Å in TTE. When this spin labeled protein was reconstituted into liposomes, the dipole-dipole interaction disappeared. Because the maximum interaction distance appears to be on the order of 35 Å, we can estimate that in liposomes the distance this pair of nitroxides is bigger than 35 Å. If TonB-box of FepA form a transmembrane strand which span across the bilayer, the distance between D12 and E20 will be bigger than 35 Å, beyond the detectable range of dipole-dipole interaction for ESR. The absence of dipole-dipole interaction for spin labeled D12C/E20C in

liposomes suggests it is likely that D12 and E20C are located in opposite leaflets of the membrane.

Our CW saturation results indicate the nine residues within and around the FepA TonB box are mostly located within the lipid bilayer. E20C is localized in an extracellular surface domain. The MTSL side chain bound to residue A19C was remarkable inaccessible to CROX and O₂, indicating that A19C may lie near the negatively charged membrane surface with structural interactions with surface loops. In this study, we also used SDSL to map the local secondary structure of a proposed transmembrane β -strand. The accessibilities of two sets of residues (even-numbered residues: D12C, I14C, V16C, and A18C; odd-numbered residues: T13C, V15C and I17C) to oxygen and CROX gave a well-defined alternating periodicity. This periodicity of 2.0 is consistent with β -sheet secondary structure. The even-numbered residues have more accessibility to CROX than O₂, suggesting these residues may locate at the inside base of the aqueous channel. In contrast, the odd-numbered residues did not appear to be exposed to the aqueous phase, because they showed strong interaction with O₂. Unexpectedly, T13C could not be labeled with MTSL without denaturation, which indicates this residue may locate on the opposite side of the channel with strong structural interaction with the surrounding amino acid side chains.

In conclusion, we have studied nine consecutive residues, from 12 to 20, which are located within and around FepA TonB box by CW saturation experiment. Our CW saturation results indicate that residues 19 and 20 are

localized in or near extracellular surface domain, while residues from 12 to 18 form part or whole of a β -strand which span the lipid bilayer. These results rule out any possible physical contact between TonB-box of FepA and TonB protein in periplasmic space.

Chapter V

General Conclusions and Discussion

Since Waring & Werkman documented a microbial requirement for iron in 1944 (Waring & Werkman, 1944), much progress has been made in understanding how microbes assimilate this mundane but biological precious metal. The proteins involved in iron transport can now be grouped functionally across several microbial systems. It is now well known that under iron deficiency bacteria coordinately derepress several iron-uptake systems composed of an outer membrane receptor, a periplasmic protein, and several inner membrane-associated proteins. The function of the receptor is to bring the siderophore to, and through, the cell envelopes. The transport of iron across the outer membrane requires energy. TonB is thought to provide functional link between the inner membrane electrochemical potential to active transport of ferric siderophore complexes through high-affinity outer membrane receptors.

The FeEnt receptor, FepA, is best characterized among TonB-dependent siderophore receptors. Its region of ligand binding has been localized. The model of FepA structure has been established and used to predict other TonB-dependent receptor protein structures. Aside from FepA, little knowledge exists about how these proteins recognize and internalize ligands. Previous work in Dr. Klebba's laboratory, confirmed by others, established that FepA is a TonB-dependent gated porin.

In this dissertation, conformational dynamics and structure of FepA were studied. The major conclusions from these studies are listed below:

1. *In vivo* ESR method was developed to study the conformational changes of FepA during ligand transport. The opening and closing of ligand-gated porin was observed, for the first time, by a physical method.
2. The transport mechanisms of FeEnt and colicin B by FepA are different. These uptake processes require conformational changes in FepA.
3. Our results also proved that the structural changes during iron and colicin transport are TonB- and energy-dependent.
4. Opening and closing of this gated porin is also temperature-dependent.
5. The location of the TonB-box domain of FepA was determined. Most of the TonB-box residues are buried in OM bilayer and form part or entire of a β -strand which spans across the OM.
6. The postulated direct contact between TonB and TonB-box of FepA in periplasmic space does not exist.

To better understand this system, studies can be carried out to further delineate the amino acid residues of FepA responsible for ferric enterobactin binding. *In vivo* SDSL can be extended and refined to identify residues in FepA that are crucial for ligand internalization, and the kinetic characterization of channel dynamic during siderophore and colicin uptake will be studied. Site-directed spin labeling technique which has been highly successful in FepA study will be further used to provide more structural information of FepA. Most importantly, to further study the structure and function of FepA, we need a better understanding of the structure and function of TonB. It will require a great effort to analyze the structure of TonB and further evaluate its interactions with TonB-dependent OM proteins.

REFERENCES

Allen, J. P., Yeates, T. O., Komiya, H., and Rees, D. C. 1987. Structure of the reaction center from *Rhodobacter sphaeroides* R-26: the protein subunits. *Proc. Natl. Acad. Sci. USA* **84**:6162-6166.

Altenbach, C., and Hubbell, W. L. 1988. The Aggregation State of Spin-Labeled Melittin in Solution and Bound to Phospholipid Membranes: Evidence That Membrane-Bound Melittin Is Monomeric. *Proteins: Structure, Function, and Genetics* **3**:230-242.

Altenbach, C., Flitsch, S. L., Khorana, H. G., and Hubbell, W. L. 1989a. Structural Studies on Transmembrane Proteins. 2. Spin Labeling of Bacteriorhodopsin Mutants at Unique Cysteines. *Biochemistry* **28**:7806-7812.

Altenbach, C., Froncisz, W., Hyde, J. S., and Hubbell, W. L., 1989b. Conformation of Spin-Labeled Melittin at Membrane Surfaces Investigated by

Pulse Saturation Recovery and Continuous Wave Power Saturation Electron Paramagnetic Resonance. *Biophys. J.* **56**:1183-1188.

Altenbach, C., Marti, T., Khorana, H. G., and Hubbell, W. L. 1990. Transmembrane Protein Structure: Spin Labeling of Bacteriorhodopsin Mutants. *Science* **248**:1088-1092.

Altenbach, C., Greenhalgh, D. A., Khorana, H. G., and Hubbell, W. L. 1994. A Collision Gradient Method to Determine the Immersion Depth of Nitroxides in Lipid Bilayers: Application to Spin-Labeled Mutants of Bacteriorhodopsin. *Proc. Natl. Acad. Sci. USA* **91**:1667-1671.

Altenbach, C., Yang, K., Farrens, D. L., Farahbakhsh, Z. T., Khorana, H. G., and Hubbell, W. L. 1996. Structural Features and Light-Dependent Changes in the Cytoplasmic Interhelical E-F Loop Region of Rhodopsin: A Site-Directed Spin-Labeling Study. *Biochemistry* **35**:12470-12476.

Anthony-Cahill, S. J., Benfield, P. A., Fairman, R., Wasserman, Z. R., Brenner, S., Stafford, W. F., Altenbach, C., Hubbell, W. L., and DeGrado, W. F. 1992. Molecular Characterization of Helix-Loop-Helix Peptides. *Science* **255**:979-983.

Armstrong, S. K., Francis, C. L., and McIntosh, M. A. 1990. Molecular Analysis of the *Escherichia coli* Ferric Enterobactin Receptor FepA. *J. Biol. Chem.* **265**:14536-14543.

Armstrong, S. K., and McIntosh, M. A. 1995. Epitope Insertions Define Functional and Topological Features of the *Escherichia coli* Ferric Enterobactin Receptor. *J. Biol. Chem.* **270**:2483-2488.

Balakrishnan, K., Hsu, F. J., Hafeman, D. G., and McConnell, H. M. 1982. Monoclonal Antibodies to a Nitroxide Lipid Hapten. *Biochim. Biophys. Acta.* **721**:30-38.

Barranger-Mathys, M. and Cafiso, D. S. 1996. Membrane Structure of Voltage-Gated Channel Forming Peptides by Site-Directed Spin-Labeling. *Biochemistry* **35**:498-503.

Bassford, P. J., Bradbeer, Jr., C., Kadner, R. J., and Schnaitman, C. A. 1976. Transport of vitamin B₁₂ in *tonB* mutants of *Escherichia coli*. *J. Bacteriol.* **128**:242-247.

Benedetti, H., Frenette, M., Baty, D., Lloubes, R., Knibiehler, M., Pattus, F., and Lazdunski, C. 1991. Individual Domains of Colicins Confer Specificity in

Colicin Uptake, in Pore-Properties and in Immunity Requirement. *J. Mol. Biol.* 217:429-434.

Bentley, A. T., and Klebba, P. E. 1988. Effect of Lipopolysaccharide Structure on Reactivity of Antiporin Monoclonal Antibodies with the Bacterial Cell Surface. *J. Biacteriol.* 170:1063-1068.

Berliner, L. J., Ed. 1976. "Spin Labeling Theory and Applications". Academic Press, New York.

Berliner, L. J., Ed. 1979. "Spin Labeling Theory and Applications II". Academic Press, New York.

Berliner, L. J., 1983. The Spin-Label Approach to Labeling Membrane Protein Sulfhydryl Groups. *Ann. N. Y. Acad. Sci.* 414, 153.

Berliner, L. J., and Reuben, J. Eds. 1989. "Biological Magnetic Resonance, Vol. 8". Plenum Press, New York.

Beth, A. H., Robinson, B. H., Cobb, C. E., Dalton, L. R., Trommer, W. E., Birktoft, J. J., and Park, J. H. 1984. Interactions and Spatial Arrangement of

Spin-Labeled NAD⁺ Bound to Glyceraldehyde-3-Phosphate Dehydrogenase. *J. Biol. Chem.* **259**:9717-9723.

Bradbeer, C. 1993. The Proton Motive Force Drives the Outer Membrane Transport of Cobalamin in *Escherichia coli*. *J. Bacteriol.* **175**:3146-3150.

Bradbeer, C., and Woodrow, M. J. 1976. Transport of Vitamin B₁₂ in *Escherichia coli*: Energy Dependence. *J. Bacteriol.* **128**:99-104.

Brewer, S., Tolley, M., Trayer, I. P., Barr, G. C., Dorman, C. J., Hannavy, K., Higgins, C. F., Levine, B. A., and Wormald, M. R. 1990. Structure and Function of X-Pro Dipeptide Repeats in the TonB Proteins of *Salmonella typhimurium* and *Escherichia coli*. *J. Mol. Bio.* **216**:883-895.

Budker, V., Du, J. L., Seiter, M., Eaton, G. R., and Eaton, S. S. 1995. Electron-Electron Spin-Spin Interaction in Spin-Labeled Low-Spin Methemoglobin. *Biophys. J.* **68**:2531-2536.

Bullen, J. J., and Griffiths, E. (Eds) 1987. Iron and Infection, John Wileys Sons, New York.

Butterfield, D. A., Roses, A. D., Appel, S. H., and Chesnut, D. B. 1976. Electron Spin Resonance Studies of Membrane Proteins in Erythrocytes in Myotonic Muscular Dystrophy. *Arch. Biochem. Biophys.* 177:226-232.

Calciano, L. J., Escobar, W. A., Millhause, G. L., Miick, S. M., Rubaloff, J., Todd, A. P., and Fink, A. L. 1993. Side-Chain Mobility of the β -Lactamase A State Probed by Electron Spin Resonance Spectroscopy. *Biochemistry* 32:5644-5649.

Carreras, C. W., Naber, N., Cooke, R., and Santi, D. V. 1994. A C-Terminal Conformational Equilibrium in Thymidylate Synthase Observed by Electron Paramagnetic Resonance Spectroscopy. *Biochemistry* 33:2071-2077.

Castle, J. D., and Hubbell, W. L. 1976. Estimation of Membrane Surface Potential and Charge Density from the Phase Equilibrium of a Paramagnetic Amphiphile. *Biochemistry* 15:4818-4823.

Cornish, V. W., Benson, D. R., Altenbach, C. A., Hideg, K., Hubbell, W. L., and Schultz, P. G. 1994. Site-Specific Incorporation of Biophysical Probes into Proteins. *Proc. Natl. Acad. Sci. USA* 91:2910-2914.

Coughlin, R. T., Haug, A., and McGroarty, E. J. 1983. Electron Spin Resonance Probing of Lipopolysaccharide Domains in the Outer Membrane of *Escherichia coli*. *Bioch. Biophys. Acta* 729:161-168.

Cowan, S. W., Schirmet, T., Rummel, G., Steiert, M., Ghosh, R., Pauptit, R. A., Jansonius, J. N., and Rosenbusch, J. P. 1992. Crystal Structures Explain Functional Properties of Two *E. coli* Porins. *Nature* 358:727-733.

Dalton, L. A., McIntyre, J. O., and Fleischer, S. 1987. Distance Estimate of the Active Center of D- β -Hydroxybutyrate Dehydrogenase from the Membrane Surface. *Biochemistry* 26:2117-2130.

Davies, J. K., and Reeves, P. 1975. Genetics of resistance to colicins in *Escherichia coli* K12: cross resistance among colicins of group A. *J. Bacteriol.* 123:102-106.

Decad, G., and Nikaido, H. 1976. Outer membrane of Gram-negative bacteria. XII. Molecular serving function of cell wall. *J. Bacteriol.* 128:325-328.

Deisenhofer, J., Epp, O., Miki, K., Huber, R., and Michel, H. 1985. Structure of the protein subunits in the photosynthetic reaction center of *Rhodospseudomonas viridis* at 3 Å resolution. *Nature* 318:618-624.

de Lorenzo, V., Giovanuini, F., Herrero, M., and Neilands, J. B. 1988. *J. Mol. Biol.* **203**:875-884.

Goldfine, H. 1982. Lipids of prokaryotes-structure and distribution, In *Current Topics in Membranes and Transport*, Vol 17, pp. 3-41.

Eichler, D. C., Barber, M. J., and Solomonson, L. P. 1985. Anti-Nitroxide Immunoglobulin G: Analysis of Antibody Specificity and Their Application as Probes for Spin-Labeled Proteins. *Biochemistry* **24**:1181-1186.

Ecker, D. J., Lancaster, J. R., and Emery, T. 1982. Siderophore Iron Transport followed by Electron Paramagnetic Resonance Spectroscopy *J. Biol. Chem.* **257**:623-8628.

Elish, E., Pierce, J. R., and Earhart, C. F. 1988. Biochemical Analysis of Spontaneous *fepA* Mutants of *Escherichia coli*. *J. Gen. Microbiol.* **134**:1355-1364.

Evans, J. S., Levine, B. A., Trayer, I. P., Dorman, C. J., and Higgins, C. F. 1986. Sequence-Imposed Structural Constraints in the TonB Protein of *Escherichia coli*. *FEBS Lett.* **208**:211-216.

Farahbakhsh, Z. T., Altenbach, C., and Hubbell, W. L. 1992. Spin Labeled Cysteines As Sensors for Protein-Lipid Interaction and Conformation in rhodopsin. *Photochem. Photobiol.* **56**:1019-1026.

Farahbakhsh, Z. T., Hideg, K., and Hubbell, W. L. 1993. Photoactivated Conformational Changes in Rhodopsin: A Time-Resolved Spin Label Study. *Science* **262**:1416-1419.

Farahbakhsh, Z. T., Huang, Q., Ding, L., Altenbach, C., Steinhoff, H., Horwitz, J., and Hubbell, W. L. 1995a. Interaction of α -Crystallin with Spin-Labeled Peptides. *Biochemistry* **34**:509-516.

Farahbakhsh, Z. T., Ridge, K. D., Khorana, H. G., and Hubbell, W. L. 1995b. Mapping Light-Dependent Structural Changes in the Cytoplasmic Loop Connecting Helices C and D in Rhodopsin: A Site-Directed Spin Labeling Study. *Biochemistry* **34**:8812-8819.

Farrens, D. L., Altenbach, C., Yang, K., Hubbell, W. L., and Khorana, H. G. 1996. Requirement of Rigid-Body Motion of Transmembrane Helices for Light Activation of Rhodopsin. *Science* **274**:268-271.

Feix, J. B., Popp, C. A., Venkataramu, S. D., Beth, A. H., Park, J. H., and Hyde, J. S., 1984. An Electron-Electron Double-Resonance Study of Interactions between ^{14}N - and ^{15}N - Stearic Acid Spin-Label Pairs: Lateral Diffusion and Vertical Fluctuations in Dimyristoylphosphatidylcholine. *Biochemistry* **23**:2293-2296.

Feix, J. B., Yin, J., and Hyde, J. S. 1987. Interactions of ^{14}N : ^{15}N Stearic Acid Spin-Label Pairs: Effects of Host Lipid Alkyl Chain Length and Unsaturation. *Biochemistry* **26**:3850-2856.

Fiss, E. H., Stanley-Samuelson, P., and Neilands, J. B. 1982. Properties and Proteolysis of Ferric Enterobactin Outer Membrane Receptor in *Escherichia coli* K12. *Biochemistry* **21**:4517-4522.

Flitsch, S. L., and Khorana, H. G. 1989. Structural Studies on Transmembrane Proteins. 1. Model Study Using Bacteriorhodopsin Mutants Containing Single Cysteine Residues. *Biochemistry* **28**:7800-7805.

Froncisz, W., and Hyde, J. S. 1982. The Loop-Gap Resonator: A New Microwave Lumped Circuit ESR Sample structure. *J. Magn. Reson.* **47**:515-518.

Gaffney, B. J. 1976. The Chemistry of Spin Labels. In: "Spin Labeling". Berliner, L. J. Ed. Academic Press. New York. 183-238.

Gennis, R., and Ferguson-Miller, S. Structure of cytochrome c oxidase, energy generator of aerobic life. 1995. *Science*. **269**:1063-1064.

Greenhalgh, D. A., Altenbach, C., Hubbell, W. L., and Khorana, H. G. 1991. Locations of Arg82, Asp85, and Asp96 in Helix C of Bacteriorhodopsin Relative to the Aqueous Boundaries. *Proc. Natl. Acad. Sci. USA* **88**:8626-8629.

Guerinot, M. L. 1994. Microbial Iron Transport. *Annu. Rev. Microbiol.* **48**:743-772.

Guterman, S. 1971. Inhibition of Colicin B by Enterochelin. *Biochem. Biophys. Res. Comm.* **44**:1149-1155.

Hannavy, K., Barr, G. C., Dorman, C. J., Adamson, J., Mazengera, L. R., Gallagher, M. P., Evans, J. S., Levine, B. A., Trayer, I. P., and Higgins, C. F. 1990. TonB Protein of *Salmonella typhimurium* A Model for Signal Transduction between Membranes. *J. Mol. Biol.* **216**:897-910.

Harle, C., Kim, I., Angerer, A., and Braun, V. 1995. Signal Transfer through Three Compartments: Transcription Initiation of the *Escherichia coli* Ferric Citrate Transport System from the Cell Surface. *EMBO J.* **14**:1430-1438.

He, M. M., Voss, J., Hubbell, W. L., and Kaback, H. R. 1995a. Use of Designed Metal-Binding Sites to Study Helix Proximity in the Lactose Permease of *Escherichia coli*. 1. Proximity of Helix VII (Asp237 and Asp240) with Helices X (Lys319) and XI (Lys358). *Biochemistry* **34**:15661-15666.

He, M. M., Voss, J., Hubbell, W. L., and Kaback, H. R. 1995b. Use of Designed Metal-Binding Sites to Study Helix Proximity in the Lactose Permease of *Escherichia coli*. 2. Proximity of Helix IX (Arg302) with Helix X (His322 and Glu325). *Biochemistry* **34**:15667-15670.

Hemminga, M. A. 1983. Interpretation of ESR and saturation transfer ESR spectra of spin label lipid and membranes. *Chem. Phys. Lipids* **32**:323-383.

Henderson, R., Baldwin, J. M., Ceska, T. A., Zemlin, F., Beckmann, E., and Downing, K. H. 1990. Model for the structure of bacteriorhodopsin based on high-resolution electron cryo-microscopy. *J. Mol. Biol.* **213**:899-929.

Hollifield, W. C., Fiss, E. H., and Neilands, J. B. 1978. *Biochem. Biophys. Res. Commun.* **83**:739-746.

Hollifield, W. C.. and Neilands, J. B. 1978. Ferric Enterobactin Transport System in Escherichia coli K-12. Extraction, Assay, and Specificity of the Outer Membrane Receptor. *Biochemistry* 17:1922-1928.

Hofnung, M. 1995. An Intelligent Channel (and More). *Science* 267:473-474.

Hubbell, W. L., and Altenbach, C. 1994a. Investigation of Structure and Dynamics in Membrane Proteins Using Site-Directed Spin Labeling. *Curr. Opin. Struct. Biol.* 4:566-572.

Hubbell, W. L., and Altenbach, C. 1994b. Site Directed Spin Labeling of Membrane Proteins. In: "Membrane Protein Structure: Experimental Approaches". White, S. H., Ed. Oxford University Press. 224-248.

Hyde, J. S., Swartz, H. M., and Antholine, W. E. 1979. The Spin-Label Spin-Probe Method. In: "Spin Labeling II". Berliner, L. J. Ed. Academic Press. New York. 71-113.

Hyde, J. S., Yin, J., Feix, J. B., and Hubbell, W. L. 1990. Advances in Spin Label Oximetry. *Pure & Appl. Chem.* 62:255-258.

Jalal, M. A. F., and van der Helm, D. 1989. Purification and Crystallization of Ferric Enterobactin Receptor Protein, FepA, from the Outer Membranes of *Escherichia coli* UT5600/pBB2. *FEBS Lett.* **243**:366-368.

Jap, B. K., Downing, K. H., and Walian, P. J. 1990. Structure of PhoE porin in projection at 3.5 Å resolution. *J. Struct. Biol.* **103**:57-63.

Jap, B. K., Walian, P. J., and Gehring, K. 1991. Structural architecture of an outer membrane channel as determined by electron crystallography. *Nature* **350**:167-170.

Jaskula, J. C., Letain, T. E., Roof, S. K., Skare, J. T., and Postle, K. 1994. Role of the TonB Amino Terminus in Energy Transduction between Membranes. *J. Bacteriol.* **176**:2326-2338.

Jiang, X., Payne, M. A., Cao, Z., Foster, S. B., Feix, J. B., Newton, S. M. C., and Klebba, P. E. 1997. Ligand-Specific Opening of a Gated-Porin Channel in the Outer Membrane of Living Bacteria. *Science* **276**:1261-1264.

Jung, K., Voss, J., He, M., Hubbell, W. L., and Kaback, H. R. 1995. Engineering a Metal Binding Site within a Polytopic Membrane Protein, the Lactose Permease of *Escherichia coli*. *Biochemistry* **34**:6272-6276.

Karlsson, M., Hannavy, K., and Higgins, C. F. 1993. A Sequence-Specific Function for the N-Terminal Signal-Like Sequence of the TonB Protein. *Mol. Microbiol.* **8**:379-388.

Klebba, P. E., McIntosh, M. A., and Neilands, J. B. 1982. Kinetics of biosynthesis of iron-regulated membrane proteins in *Escherichia coli*. *J. Bacteriol.* **149**:880-888.

Klebba, P. E., Rutz, J. M., Liu, J., and Murphy, C. K. 1993. Mechanism of TonB-Mediated Iron Transport through the Bacterial Outer Membrane. *J. Bioenerg. Biochem.* **25**:605-611.

Klebba, P. E., Hofnung, M., and Charbit, A. 1994. A Model of Maltodextrin Transport through the Sugar-Specific Porin, LamB, Based on Deletion Analysis. *EMBO J.* **13**:4670-4675.

Klebba, P. E., Newton, S. M. C., Charbit, A., Michel, V., Perrin, D., and Hofnung, M. 1997. Further Genetic Analysis of the C-Terminal External Loop Region in *Escherichia coli* Maltoporin. *Res. Microbiol.* **148**:375-387.

Klug, C. S., Su, W., Liu, J., Klebba, P. E., and Feix, J. B. 1995. Denaturant Unfolding of the Ferric Enterobactin Receptor and Ligand-Induced Stabilization Studied by Site-Directed Spin labeling. *Biochemistry* 34:14230-14236.

Klug, C. S., Su, W., and Feix, J. B. 1997. Mapping of the Residues Involved in a Proposed β -Strand Located in the Ferric Enterobactin Receptor FepA Using Site-Directed Spin Labeling. *Biochemistry* 36: 13027-13033.

Kreusch, A., Neubuser, A., Schiltz, E., Weckesser, J., and Schulz, G. E. 1994. Structure of the Membrane Channel Porin from *Rhodospseudomonas blastica* at 2.0 Å Resolution. *Protein Sci.* 3:58-63.

Kuhlbrandt, W., Wang, D. N., and Fujiyoshi, Y. 1994. Atomic model of plant light-harvesting complex determined by electron crystallography. *Nature* 350:130-134.

Kunkel, T. A. 1985. Rapid and Efficient Site-Specific Mutagenesis without Phenotypic Selection. *Proc. Natl. Acad. Sci. USA* 82:488-492.

Laemmli, U. K. 1970. *Nature (London)* 227:680-685.

Larsen, R. A., Wood, G. E., and Postle, K. 1993. The Conserved Proline-Rich motif is not Essential for Energy Transduction by *Escherichia coli* TonB Protein. *Mol. Microbiol.* 10:943-953.

Larsen, R. A., Foster-Hartnett, D., McIntosh, M. A., and Postle, K. 1997. Regions of *Escherichia coli* TonB and FepA Proteins Essential for *in vivo* Physical Interactions. *J. Bacteriol.* 179:3213-3221.

Lathrop, J. T., Wei, B., Touchie, G. A., and Kadner. 1995. Sequences of the *Escherichia coli* BtuB Protein Essential for Its Insertion and Function in the Outer Membrane. *J. Bacteriol.* 177:6810-6819.

Letain, T. E., and Postle, K. 1997. TonB Protein Appears to Transduce Energy by Shuttling between the Cytoplasmic Membrane and the Outer Membrane in *Escherichia coli*. *Mol. Microbiol.* 24:271-283.

Likhtenstein, G. I. 1976. "Spin Labeling Methods in Molecular Biology". Wiley (Interscience). New York.

Liu, J., Rutz, J. M., Feix, J. B., and Klebba, P. E. 1993. Permeability Properties of a Large Gated Channel within the Ferric Enterobactin Receptor, FepA. *Proc. Natl. Acad. Sci. USA* 90:10653-10657.

Liu, J., Rutz, J. M., Klebba, P. E., and Feix, J. B. 1997. A Site-Directed Spin-Labeling Study of Ligand-Induced Conformational Change in the Ferric Enterobactin receptor, FepA. *Biochemistry* **33**:13274-13283.

Lou, K., Saint, N., Prilipov, A., Rummel, G., Benson, S. A., Rosenbusch, J. P., and Schirmer, T. 1996. Structural and Functional Characterization of OmpF Porin Mutants Selected for Larger Pore Size. I. Crystallographic Analysis. *J. Biol. Chem.* **271**:20669-20673.

Lowry, O. H., Rosebrough, J. J., Farr, A., Lewis, A., and Randall, R. J. 1951, *J. Biol. Chem.* **193**:265-275

Luckey, M., Ling, R., Dose, A., and Malloy, B. 1991. Role of a Disulfide Bond in the Thermal Stability of the LamB Protein Trimer in *Escherichia coli* Outer Membrane. *J. Biol. Chem.* **266**:1866-1871.

Marsh, D. 1981. In: Membrane spectroscopy, edited by E. Grell. Berlin: springer-Verlag. p.51-137.

Martinez-Yamout, M., and McConnell, H. M. 1994. Site-Directed Mutagenesis and ^1H Nuclear Magnetic Resonance of an Anti-Dinitrophenyl Spin Label Antibody. *J. Mol. Biol.* **244**:301-318.

Mason, R. P., Glavedoni, E. B., and Dalmasso, A. P. 1977. Complement-Induced Decrease in Membrane Mobility: Introducing a More Sensitive Index of Spin-Label Motion. *Biochemistry* **16**:1196-1201.

Mchaourab, H. S., Hyde, J. S., and Feix, J. B. 1993. Aggregation State of Spin-Labeled cecropin AD in Solution. *Biochemistry* **32**:11895-11899.

Mchaourab, H. S., Hyde, J. S., and Feix, J. B. 1994. Binding and State of Aggregation of Spin-Labeled Cecropin AD in Phospholipid Bilayers: Effects of Surface Charge and Fatty Acyl Chain Length. *Biochemistry* **33**:6691-6696.

Mchaourab, H. S., Lietzow, M. A., Hideg, K., and Hubbell, W. L. 1996. Motion of Spin-Labeled Side Chains in T4 Lysozyme. Correlation with Protein Structure and Dynamics. *Biochemistry* **35**:7692-7696.

Mchaourab, H. S., Oh, K. J., Fang, C. J., and Hubbell, W. L. 1997. Conformation of T4 Lysozyme in Solution. Hinge-Bending Motion and the

Substrate-Induced Conformational Transition Studied by Site-Directed Spin Labeling. *Biochemistry* **36**:307-312.

McIntosh, M. A., Earhart, C. F. 1977. *J. Bacteriol.* **131**:331-339.

Mende, J., and Braun, V. 1990. Import-defective colicin B derivatives mutated in the TonB box. *Molec. Microbiol.* **4**:1253-1257.

Messing, J. 1983. New M13 Vectors for Cloning. *Methods Enzymol.* **101**:20-46.

Miick, S. M., Casteel, K. M., and Millhauser, G. L. 1993. Experimental Molecular Dynamics of an Alanine-Based Helical Peptide Determined by Spin Label Electron Spin Resonance. *Biochemistry* **32**:8014-8021.

Millhauser, G. L. 1992. Selective Placement of Electron Spin Resonance Spin Labels: New Structural Methods for Peptides and Proteins. *TIBS* **17**:448-452.

Murphy, C. K., Kalve, V. I., and Klebba, P. E. 1990. Surface Topology of the *Escherichia coli* K-12 Ferric Enterobactin Receptor. *J. Bacteriol.* **172**:2736-2746.

Nakae, T. 1975. Outer membrane of *Salmonella typhimurium*: reconstitution of sucrose-permeable membrane vesicles. *Biophys. Res. Commun.* **64**:1224-1230.

Nakae, T., and Nikaido, H. 1975. Outer membrane as a diffusion barrier in *Salmonella typhimurium*. Penetration of oligo and polysaccharides into isolated outer membrane vesicles and cells with degraded peptidoglycan layer. *J. Biol. Chem.* **250**:7359-7365.

Neilands, J. B. 1981. Microbial Iron Compounds. *Ann. Rev. Biochem.* **50**:715-731.

Neilands, J. B., Erickson, T. J., and Rastetter, W. H. 1981. Stereospecificity of the Ferric Enterobactin Receptor of *Escherichia coli* K-12. *J. Biol. Chem.* **256**:3831-3832.

Neilands, J. B. 1982. Microbial Envelope Proteins Related to Iron. *Ann. Rev. Microbiol.* **36**:285-309.

Neilands, J. B. 1995. Siderophores: Structure and Function of Microbial Iron Transport Compounds. *J. Biol. Chem.* **270**:26723-26726.

Newton, S. M. C., Allen, J. S., Cao, Z., Qi, Z., Jiang, X., Sprencel, C., Igo, J. D., Foster, S. B., Payne, M. A., and Klebba, P. E. 1997. Double Mutagenesis of a Positive Charge Cluster in the Ligand-Binding Site of the Ferric Enterobactin Receptor, FepA. *Proc. Natl. Acad. Sci. USA* **94**:4560-4565.

Nikaido, H. 1973. Biosynthesis and Assembly of Lipopolysaccharide and the Outer Membrane Layer of Gram-Negative Cell Wall. Leive, L. Ed. *Bacterial Membrane and Walls*. Marcel Dekker. New York. 131-208.

Nikaido, H., and Nakae, T. 1979. The Outer Membrane of Gram-Negative Bacteria. *Adv. Microb. Physiol.* **20**:163-250.

Nikaido, H., and Rosenberg. 1981. Effects of Solute Size on Diffusion Rates through the Transmembrane Pores of the Outer Membrane of *Escherichia coli*. *J. Gen. Physiol.* **77**:121-135.

Nikaido, H. 1983a. Proteins Forming Large Channels from Bacterial and Mitochondrial Outer Membranes: Proins and Phage Lambda Receptor Protein. *Methods Enzymol.* **98**:85-100.

Nikaido, H., and Rosenberg, E. Y. 1983b. Porin Channels in *Escherichia coli*: Studies with Liposomes Reconstituted from Purified Proteins. *J. Bacteriol.* **153**:241-252.

Nikaido, H., and Vaara, M. 1985. Molecular basis of outer membrane permeability. *Microbiol. Rev.* **49**:1-32.

Nikaido, H., Nikaido, K., and Harayama, S. 1991. Identification and Characterization of Porins in *Pseudomonas aeruginosa*. *J. Biol. Chem.* **266**:770-779.

Oh, K. J., Zhan, Q., Cui, C., Hideg, K., Collier, R. J., and Hubbell, W. L. 1996. Organization of Diphtheria Toxin T Domain in Bilayers: a Site-Directed Spin Labeling Study. *Science* **273**:810-813.

Pali, T., Bartucci, R., Horvath, L. I., and Marsh, D. 1992. Distance Measurements Using Paramagnetic Ion-Induced Relaxation in the Saturation Transfer Electron Spin Resonance of Spin-Labeled Biomolecules. *Biophys. J.* **61**:1595-1598.

Payne, M. A., Igo, J. D., Cao, Z., Foster, S. B., Newton, S. M. C., and Klebba, P. E. 1997. Biphasic Binding Kinetics between FepA and Its Ligands. *J. Biol. Chem.* **35**:21950-21955.

Perozo, E., and Hubbell, W. L. 1993. Voltage Activation of Reconstituted Sodium Channels: Use of Bacteriorhodopsin as a Light-Driven Current Source. *Biochemistry* **32**:10471-10478.

Pierce, J. R., and Earhart, C. T. 1988. *J. Bacteriol.* **166**:930-936.

Plastow, G. S., and Holland, I. B. 1979. Identification of an *Escherichia coli* inner membrane polypeptide specified by a λ -tonB transducing bacteriophage. *Biochem. Biophys. Res. Commun.* **90**:1007-1014.

Poole, C. P. 1983. "Electron Spin Resonance". Wiley (Interscience), New York.

Popp, C. A., and Hyde, J. S. 1981. Effects of Oxygen on EPR Spectra of Nitroxide Spin-Label Probes of Model Membranes. *J. Magn. Reson.* **43**:249-254.

Postle, K. 1990. TonB and the Gram-negative Dilemma. *Mol. Microbiol.* **4**: 2019-2025.

Pugsly, A. P., and Reeves, P. 1976. Characterization of group B colicin-resistant mutants of *Escherichia coli* K-12: colicin resistance and the role of enterochelin. *J. Bacteriol.* 127:218-228.

Pugsly, A. P., and Reeves, P. 1977. Uptake of Ferrienterochelin by *Escherichia coli*: Energy-Dependent Stage of Uptake. *J. Bacteriol.* 130:26-36.

Rabenstein, M. D., and Shin, Y. 1995. Determination of the Distance between Two Spin Labels Attached to a Macromolecule. *Proc. Natl. Acad. Sci. USA* 92: 8239-8242.

Raitsimring, A., Peisach, J., Lee, H. C., and Chem, X. 1992. Measurement of Distance Distribution between Spin Labels in Spin-Labeled Hemoglobin Using an Electron Spin Echo Method. *J. Phys. Chem.* 96:3526-3532.

Rakowsky, M. H., More, K. M., Kulikov, A. V., Eaton, G. R., and Eaton, S. S. 1995. Time-Domain Electron Paramagnetic Resonance as a Probe of Electron-Electron Spin-Spin Interaction in Spin-Labeled Low-Spin Iron Porphyrins. *J. Am. Chem. Soc.* 117:2049-2054.

Randall-Hazelbauer, L., and Schwartz, M. 1973. *J. Bacteriol.* 116:1436-1439.

Rees, D. C., DeAntonio, L., and Eisenberg, D. 1989. Hydrophobic Organization of Membrane Proteins. *Science* **245**:510-512.

Resek, J. F., Farahbakhsh, Z. T., Hubbell, W. L., and Khorana, H. G. 1993. Formation of the Meta II Photointermediate Is Accompanied by Conformational Changes in the Cytoplasmic Surface of Rhodopsin. *Biochemistry* **32**:12025-12032.

Rutz, J. M., Abdullah, T., Singh, S. P., Kalve, V. I., and Klebba, P. E. 1991. Evolution of the Ferric Enterobactin Receptor in Gram-Negative Bacteria. *J. Bacteriol.* **173**:5964-5973.

Rutz, J. M., Liu, J., Lyons, J. A., Goranson, J., Armstrong, S. K., McIntosh, M. A., Feix, J. B., and Klebba, P. E. 1992. Formation of a Gated Channel by a Ligand-Specific Transport Protein in the Bacterial Outer Membrane. *Science* **258**:471-475.

Schmid B, Kromer, M., Schulz, G. E. 1996. Expression of porin from *Rhodospseudomonas blastica* in *Escherichia coli* inclusion bodies and folding into exact native structure. *FEBS Lett* **381**(1-2):111-114.

Schirmer, T., Keller, T. A., Wang, Y., and Rosenbusch, J. P. 1995. Structural Basis for Sugar Translocation Through Maltoporin Channels at 3.1 Å Resolution. *Science* **267**:512-514.

Schnaitman, C. A. 1971. *J. Bacteriol.* **108**:553-563.

Sharff, A. J., Rodseth, L. E., and Quioco, F. A. 1993. Refined 1.8 Å Structure Reveals the Mode of Binding of Beta-Cyclodextrin to the Maltodextrin Binding Protein. *Biochemistry* **32**:10553-10559.

Shea, C. M., and McIntosh, M. A. 1991. *Mol. Microbiol.* **5**:1415-1428.

Shin, Y., and Hubbell, W. L. 1992. Determination of electrostatic potential at biological interfaces using electron-electron double resonance. *Biophys. J.* **61**:1441-1453.

Shin, Y., Levinthal, C., Levinthal, F., and Hubbell, W. L. 1993. Colicin E1 Binding to Membranes: Time-Resolved Studies of Spin-Labeled Mutants. *Science* **259**:960-963.

Skare, J. T., Ahmer, B. M. M., Seachord, C. L., Darveau, R. P., and Postle, K. 1993. Energy Transduction between Membranes. *J. Biol. Chem.* **268**:16302-16308.

Stokes, D. L., and Green, N. M. 1990. Three-dimensional crystals of CaATPase from sarcoplasmic reticulum. Symmetry and molecular packing. *Biophys. J.* **57**:1-14.

Subczynski, W. K., and Hyde, J. S. 1981. The diffusion-concentration product of oxygen in lipid bilayers using the spin label T₁ method. *Biochim. Biophys. Acta* **643**:282-291.

Swamy, M. J., and Marsh, D. 1994. Spin-Label Electron Spin Resonance Studies on the Dynamics of the Different Phases of N-Biotinylphosphatidylethanolamines. *Biochemistry* **33**:11656-11663.

Tatsumi, Y., Maejima, T., and Mitsuhashi, S. 1995. Mechanism of *tonB*-Dependent Transport of KP-736, a 1, 5-Dihydroxy-4-Pyridone-Substituted Cephalosporin, into *Escherichia coli* K-12 Cells. *Antimicrobial Agents and Chemotherapy* **39**:613-619.

Timmis, K. 1972. Purification and characterization of colicin D. *J. Bacteriol.* **109**:12-20.

Todd, A. P., Cong, J., Levinthal, F., Levinthal, C., and Hubbell, W. L. 1989. Site-Directed Mutagenesis of Colicin E1 Provides Specific Attachment Sites for Spin Labels Whose Spectra are Sensitive to Local Conformation. *Proteins: Structure, Function, and Genetics* **6**:294-298.

Tsukihara, T., Aoyama, H., Yamashita, E., Tomizaki, T., Shinzawa-Itoh, K., Nakashima, R., Yaono, R., and Yoshikawa, S. Structures of metal sites of oxidized bovine heart cytochrome c oxidase at 2.8 Å. *Science* **269**:1069-1074.

Tsukihara, T., Aoyama, H., Yamashita, E., Tomizaki, T., Shinzawa-Itoh, K., Nakashima, R., Yaono, R., and Yoshikawa, S. 1996. The Whole Structure of the 13-subunit oxidized cytochrome c oxidase at 2.8 Å. *Science* **272**:1136-1144.

Tuckman, M., and Osburne, M. S. 1992. In Vivo Inhibition of TonB-Dependent Processes by a TonB Box Consensus Pentapeptide. *J. Bacteriol.* **174**:320-323.

Uemura, J., and Mizushima, S. 1975. *Biochim. Biophys. Acta* **413**:163-176.

Unger, V. M., and Schertler, G. F. 1995. Low-Resolution Structure of Bovine Rhodopsin Determined by Cryo-Electron Microscopy. *Biophys. J.* **68**:1776-1782.

van der Ley, P., Kuipers, O., Tommasen, J., and Lugtenberg, B. 1986. O-antigenic Chains of Lipopolysaccharide Prevent Binding of Antibody Molecules to An Outer Membrane Pore Protein in *Enterobacteriaceae*. *Microb. Pathol.* **1**: 43-49.

Volwerk, J. J., and Griffith, O. H. 1988. In: *Magnetic Resonance Review*. London: Gordon and Breach, vol. 13, p. 135-178.

Voss, J., Hubbell, W. L., and Kaback, H. R. 1995. Distance Determination in Proteins Using Designed Metal Ion Binding Sites and Site-Directed Spin Labeling: Application to the Lactose Permease of *Escherichia coli*. *Proc. Natl. Acad. Sci. USA* **92**:12300-12303.

Wang, C. C., and Newton, A. 1969a. Iron Transport in *Escherichia coli*: Relationship between Chromium Sensitivity and High Iron Requirement in Mutants of *Escherichia coli*. *J. Bacteriol.* **98**:1135-1141.

Wang, C. C., and Newton, A. 1969b. Iron Transport in *Escherichia coli*: Roles of Energy-Dependent Uptake and 2,3-Dihydroxybenzoylserine. *J. Bacteriol.* **98**: 1142-1150.

Waring, W. S., and Werkman, C. H. 1944. Iron deficiency in bacterial metabolism. *Arch. Biochem.* **4**:75-87.

Weiss, M. S., Wacker, T., Weckesser, J., Welte, W., and Schulz, G. E. 1990. Three Dimensional Structure of Porin from *Rhodobacter capsulatus* at 3 Å Resolution. *FEBS Letters* **267**:268-271.

Weiss, M. S., Abele, U., Weckesser, J., Welte, W., Schiltz, E., and Schulz, G. E. 1991. Molecular Architecture and Electrostatic Properties of a Bacterial Porin. *Science* **254**:1627-1630.

Wiener, M., Freymann, D., Ghosh, P., and Stroud, R. M. 1997. Crystal Structure of Colicin Ia. *Nature* **385**:461-464.

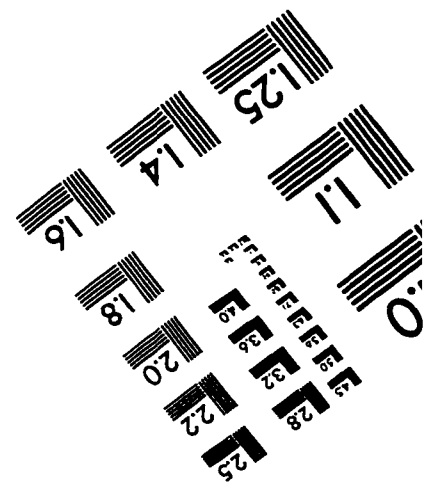
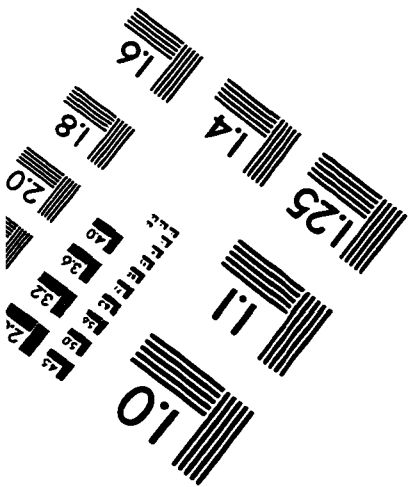
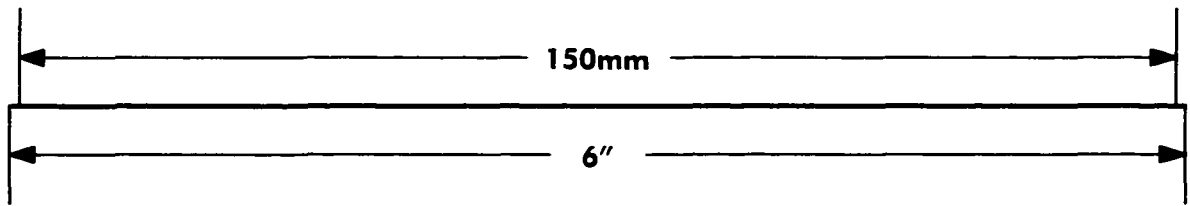
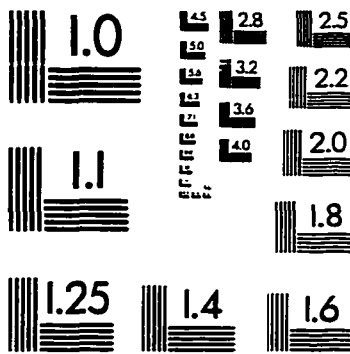
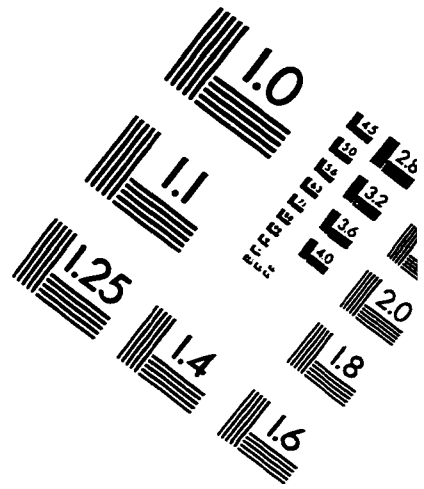
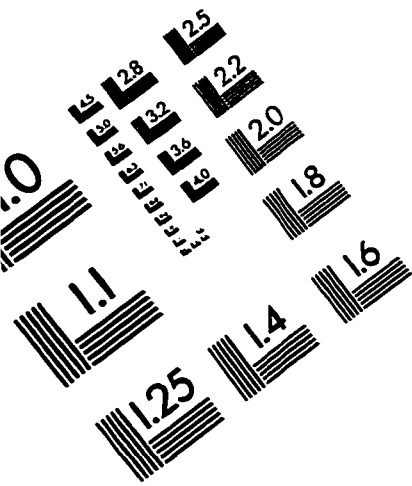
Wookey, P. 1982. *FEBS Lett.* **139**:145-154.

Wu, G., and Hubbell, W. L. 1993. Phospholipid Asymmetry and Transmembrane Diffusion in Photoreceptor Disc Membranes. *Biochemistry* 32:879-888.

Zhan, H., Oh, K. J., Shin, Y., Hubbell, W. L., and Collier, R. J. 1995. Interaction of the Isolated Transmembrane Domain of Diphtheria Toxin with Membranes. *Biochemistry* 34:4856-4863.

Zimmermann, L., Hantke, K., and Braun, V. 1984. Exogenous Induction of the Iron Dicitrate Transport System of *Escherichia coli* K-12. *J. Bacteriol.* 159:271-277.

IMAGE EVALUATION TEST TARGET (QA-3)



APPLIED IMAGE, Inc
1653 East Main Street
Rochester, NY 14609 USA
Phone: 716/482-0300
Fax: 716/288-5989

© 1993, Applied Image, Inc., All Rights Reserved